This is to certify that the
dissertation entitled

ROLE OF RECEPTOR ACTIVITY MODIFYING PROTEIN-3 IN ERK-MEDIATED PROLIFERATION OF MESANGIAL CELLS

presented by

Carolyn S. Hall

has been accepted towards fulfillment
of the requirements for the

Doctoral degree in Physiology

Major Professor's Signature

12.XII.07

Date

ROLE OF RECEPTOR ACTIVITY-MODIFYING PROTEIN-3 IN ERK-MEDIATED PROLIFERATION OF MESANGIAL CELLS

By

Carolyn S. Hall

A DISSERTATION

Submitted to
Michigan State University
In partial fulfillment of the requirements
For the degree of

DOCTOR OF PHILOSOPHY

Department of Physiology

2007

ROLE

Recep
protei
and re
comp
(CR1
R2 o
AM2
dem
inte
the
und
hav
ger
exp
(P
th
cH

ABSTRACT

ROLE OF RECEPTOR ACTIVITY-MODIFYING PROTEIN-3 IN ERK-MEDIATED PROLIFERATION OF MESANGIAL CELLS

By

Carolyn S. Hall

Receptor activity-modifying proteins (RAMPs) are single transmembrane accessory proteins critical to various G-protein coupled receptors for plasma membrane expression and receptor phenotype. A functional receptor for the ligand, adrenomedullin (AM), is comprised of RAMP2 (R2) or RAMP3 (R3) and calcitonin receptor-like receptor (CRLR). Although R2 and R3 share only 30% homology, when CRLR is expressed with R2 or R3 virtually identical (pharmacologically and biologically) AM receptors (AM-1R, AM2-R, respectively) are produced. Recent studies from our laboratory have demonstrated that R3 regulates the recycling of the AM2 receptor through protein interactions involving a PSD-95/Discs-large/ZO-1 homology (PDZ) domain located at the extreme C-terminus of R3. Differential RAMP gene expression has been studied under many disease models, physiological changes, and drug treatments. Several reports have indicated that growth associated conditions can result in specific upregulation of R3 gene expression, including a study from our laboratory that demonstrated increased R3 expression in rat mesangial cells following platelet-derived growth factor beta (PDGFββ) treatment. The mechanisms of R3 involvement in proliferation have not been thoroughly investigated. Uncontrolled mesangial cell proliferation is a general characteristic of a variety of progressive glomerular diseases. PDGFββ and basic

fibroblast growth factor (FGF-2) are potent mesangial cell mitogens that play critical roles in the progression of renal disease. Both exert proliferative responses by activation of a mitogen-activated protein kinase (MAPK) signal transduction cascade, namely extracellular signal-regulated kinase -1/2 (ERK). The major aim of this study was to determine the role of R3:ERK interaction in PDGFββ and FGF-2 stimulated mesangial cell proliferation. Employing GST fusion protein overlay assays; we discovered that R3 could physically interact with ERK protein. We also observed that R3 gene knockdown resulted in a complete inhibition of PDGFββ and FGF-2 stimulated proliferation in mesangial cells. Accordingly, R3 introduction into a normal rat fibroblast cell line, NRK, resulted in an increased proliferative response following FGF-2 treatment. Mutating specific amino acid residues within a putative N-terminal ERK docking domain of R3 identified residues mediating the R3:ERK interaction. These mutations also resulted in decreased FGF-2 proliferation of NRK following FGF-2 treatment. Subcellular fractionation and confocal microscopy revealed that R3:ERK interaction occurs at the endoplasmic reticulum. Finally, Co-immunoprecipitation experiments identified interaction between R3 and pERK in a supernatant fraction from a 100,000G spin, which probably represents a cytosolic cellular fraction. This interaction was increased following PDGF-ββ treatment. R3 was detected only in the 100,000G pellet fraction (representing membrane) when co-immunoprecipitated with the N-terminal Flag epitope. Further experiments are warranted to determine the fate of R3's signal peptide. Taken together, these results suggest a novel role for R3 in ERK-mediated proliferation in NRK and RMC.

To my sons and my parents for their unwavering love,
and
To the Department of Physiology for providing the opportunity to pursue my dream.

ACKNOWLEDGEMENTS

I would like to express my gratitude to my committee members: Dr. Julia Busik, Dr. Gregory Fink, Dr. Kathy Gallo, Dr. Laura McCabe, and Dr. William Spielman for their guidance and assistance throughout my graduate career. I would like to thank Drs. Busik, Gallo, and McCabe for their continual encouragement as well as the time they devoted in reviewing this dissertation and helping me prepare my thesis defense seminar. I would like to thank Dr. Fink for his guidance regarding statistics, and for sharing his advice regarding my findings. I would especially like to thank my major advisor, Dr. William Spielman, for providing unwavering support and friendship for so many years. I would not have been able to accomplish my dream without your help. I would also like to extend my thanks to Dr. Harvey Sparks, for hiring me as his technician twenty years ago. The scientific skills I learned in your laboratory remain with me today.

My laboratory life was greatly enriched on countless occasions by my good friends in the Physiology Department. I'm particularly thankful to the immeasurable kindness and friendship offered to me by Dr. Narayanan Parameswaran. Nara was always there for me, in good times and bad.

I would also like to thank my good friends in the Physiology Department office, Barbara Burnett, Michelle Duchene, and Tanja Brady, for their love and support.

THE

TABLE OF CONTENTS

LIST OF TABLES

THE

LIST OF FIGURES

THES

KEY TO ABBREVIATIONS:

AM, adrenomedullin
AM1R, adrenomedullin-1 receptor (composed of CRLR and RAMP2)
AM2, intermedin
AM2R, adrenomedullin-2 receptor (composed of CRLR and RAMP3)
AMPAR, α-amino-3-hydroxy-5-methylisoxazolepropionate receptor
AngII, angiotensin-II
CaSR, calcium-sensing receptor
CCl4, carbon tetrachloride
CGRP, calcitonin gene-related peptide
CRLR, calcitonin receptor-like receptor
CRT, calreticulum
CT, calcitonin
CTR, calcitonin receptor
DAG, diacylglycerol
d-siRNA, diced small interfering RNA.
ECM, extracellular matrix
EGF, epidermal growth factor
ER, endoplasmic reticulum
ERK1/2, extracellular signal-regulated kinase -1/2
ERKDD, extracellular signal-regulated kinase docking domain
ET-1, endothelin-1
FGF-2, basic fibroblast growth factor
GDP, guanosine diphosphate
GEF, guanine nucleotide exchange factor
GH, growth hormone
GPCR, G protein-coupled receptor
GST, glutathione *S*-transferase
HGF, hepatocyte growth factor
HSPGs, heparan sulfate proteoglycans
IL-1β, interleuken-1β
ITSN, intersectin
JNK, c-Jun amino-terminal kinase
KSR, Kinase Suppressor of Ras
MAPK, mitogen-activated protein kinase
MC, mesangial cell
MC, mesangial cell
MEK, MAP kinase kinase
MERM, merlin/ezrin/radixin/myosin
MP-1, MEK-1 Partner 1
NGF, nerve growth factor
NHERF-1, Na+/H+ exchanger regulatory factor-1
NRK, normal rat kidney interstitial fibroblasts

THE

NSF, *N*-ethylmaleimide-sensitive factor
PDGF, platelet-derived growth factor
PDGF-αα, platelet-derived growth factor-alpha alpha
PDGF-αβ, platelet-derived growth factor-alpha beta
PDGF-ββ, platelet-derived growth factor-beta beta
PDZ, PSD-95/Discs-large/ZO-1 homology domain type-I
PH, pleckstin homology
PI, phosphatidylinositol
PI, phosphoinositide
PLCγ, phospholipase Cγ
PNS, post-nuclear supernatant
PNS, post-nuclear supernatant
PTB, phosphotyrosine binding
PTH-R, parathyroid hormone receptor
PTK, protein tyrosine kinase
RAMP, receptor activity-modifying protein
R2, RAMP2, receptor activity-modifying protein-2
R3, RAMP3, receptor activity-modifying protein-3
RKIP, Raf-1 kinase inhibitor protein
RMC, rat mesangial cell
RTK, receptor tyrosine kinase
Sef, similar expression to FGF
SH2, Src homology 2
SOS, son of sevenless
SP, signal peptidase
SPP, signal peptide peptidase
SRP, sequence recognition particle
TGF-α, transforming growth factor type α
TNF-α, tumor necrosis factor type α
VEGF, vascular endothelial growth factor
VPACR, vasoactive intestinal peptide/pituitary adenylate cyclase-activating peptide
β2-AR, β2-adrenergic receptor

THE

1. INTRODUCTION:

The discovery of receptor activity modifying proteins (RAMPs) has broadened our understanding of G protein-coupled receptor (GPCR) signaling. RAMPs 2 and 3 (R2 and R3) when expressed with the calcitonin receptor-like receptor (CRLR) generate adrenomedullin (AM) receptors. In addition to their documented roles in the trafficking and internalization of CRLR, RAMPs have been shown to interact with other class B and C GPCRs. In addition, studies from our laboratory have demonstrated that R3 interacts with Na^+/H^+ exchange regulatory factor-1 (NHERF-1) and N-ethylmaleimide sensitive factor (NSF) to mediate R3:CRLR internalization and recycling to the plasma membrane. These protein interactions occur through a PSD-95/Discs Large/Zona occulens-1 (PDZ-1) domain located at the extreme C-terminus of R3. R3 mRNA and protein are up-regulated in several proliferative diseases, and in several cell lines and animal models of growth. In particular, R3 expression is increased in rat mesangial cells (RMC) following PDGFββ treatment even though RMC express abundant basal levels of R3. In addition, R3 harbors a putative extracellular regulated kinase docking domain (ERK-DD). ERK-DD's are important in regulating the specificity and efficiency of ERK activation in the cell. The research within this thesis investigates the role of the R3 ERK-DD in ERK-mediated proliferation utilizing RMC, normal rat kidney (NRK), and human embryonic kidney (HEK)293 cells. It identifies the critical amino acid residues within the ERK-DD that mediate R3:ERK interaction and subsequent ERK activation. It reveals the cellular location of R3:ERK interaction following growth factor treatment.

This introductory chapter is followed by a comprehensive review of the literature as it pertains to this thesis work. Subsequent chapters are organized according to the

THES

proposed specific aims. Each of these chapters are comprised of an introduction, materials and methods, experimental results, and a brief discussion of these results. Chapter three identifies a putative ERK D-Domain within R3's amino acid sequence, and demonstrates R3:ERK interaction *in vitro.* Subsequent chapters investigate R3's role in ERK activation and proliferation following PDGFββ or basic fibroblast growth factor (FGF-2) treatment, and the cellular location of R3:ERK interaction. Finally, it assesses R3 protein expression following FGF-2 treatment of NRK. The concluding chapter describes the major hypotheses tested and a summary of the results. It discusses the positive outcomes, the limitations of the work, and future directions to be undertaken.

2. LITERATURE REVIEW:

2.1. Mesangial cells.

2.1.1. Mesangial cell functions

The glomerulus, a network of capillaries originating in the afferent arteriole, is the filtration unit of the kidney. Mesangial cells are located primarily in the glomerular tuft. The contractile properties of mesangial cells allow for an important role in the regulation of glomerular hemodynamics. By contracting, mesangial cells can reduce the blood flow to specific capillary loops, thus reducing glomerular filtration area. Unlike other renal cell: cell interactions, mesangial cells are in direct contact with the endothelial lining of the glomerular capillaries. There is no basement membrane separating them from the capillaries. As a result, mesangial cells are in free contact with plasma and various macromolecules such as lipids, immune complexes, growth factors and advanced glycosylated end products [1, 2].

By regulating the amount and composition of the surrounding extracellular matrix (ECM), mesangial cells provide the essential structural support for the glomerular capillary tuft. The normal mesangial extracellular matrix consists of collagens IV, V, VI, glycoproteins (laminin and fibronectin), heparan sulfate (syndecan) and chondroitin sulfate proteoglycans [3, 4]. Loss of coordinated regulation, associated with altered composition and increased mesangial ECM deposition, often leads to progressive glomerulosclerosis, loss of filtration function, and end-stage renal disease [5].

2.1.2. Mesangial cells in disease

The primary locus of renal dysfunction is the glomerulus, and the mesangial cell (MC) appears to be a central site of the microscopically observable renal damage. By regulating the amount and composition of the surrounding extracellular matrix (ECM), mesangial cells provide the essential structural support for the glomerular capillary tuft. MC proliferation is a general characteristic of a variety of progressive glomerular diseases. Loss of coordinated regulation, associated with altered composition and increased mesangial ECM deposition, often leads to progressive glomerulosclerosis, loss of filtration function, and end-stage renal disease [5]. It follows, therefore, that an understanding of the regulatory mechanisms for MC proliferation is important for our understanding of glomerular disease and its eventual treatment.

The turnover rate of mesangial cells in the normal adult human kidney is low; the renewal rate is less than 1% [6]. Under normal conditions, quiescent mesangial cells either face few mitogenic signals, or are unable to respond to them. In several models of progressive glomerular disease (immunoglobulin A nephropathy, lupus nephritis, hemolytic uremic syndrome, and diabetic nephropathy), mesangial cell proliferation, phenotypic change and increased growth factor expression precede up-regulation of genes for ECM and mesangial expansion [7, 8]. Ultimately, mesangial cell hypercellularity and deregulation of ECM production and are hallmarks of many glomerular diseases.

2.1.3. Animal Models of Glomerulonephritis

Several animal models have been developed to investigate the effects of mesangial proliferation in glomerulonephritis [9-13]. Of these models, the IgA

THE

nephropathy and anti-Thy1.1 models have been the most extensively studied. In the rat anti-Thy1.1 model, glomerulonephritis is induced by injection of an anti-mesangial cell antibody (anti-Thy1.1) which leads to an acute phase of complement-dependent mesangial cell lysis with disruption of the mesangial matrix, followed by a phase of robust mesangial cell proliferation [14]. A similar pathology occurs, namely mesangial cell degeneration (necrosis or lysis), and subsequent mesangial proliferation, in several human renal diseases including diabetic nephropathy, IgA nephropathy, diffuse lupus nephritis, renal transplant rejection, and acute glomerulonephritis [15].

2.2. PDGFββ.

2.2.1. PDGFββ Introduction

Platelet-derived growth factor (PDGF) is a potent simulator of growth and motility of connective tissue cells, such as fibroblasts, smooth muscle cells, and cardiac myocytes [16], but also acts on other cell types, including capillary endothelial cells and neurons. PDGF has important roles during the embryonic development, as revealed by recent studies on mice with PDGF or PDGF receptor genes ablated. Inactivation of the β-chain [17] or the β receptor [18] results in defective kidney development with a total absence of mesangial cells in the glomeruli, as well as defective development of blood vessels with an inability to attract pericytes to the vessel wall[19]; these mice die around the time of birth. In the adult, PDGF stimulates wound healing[20] and has an important role in the maintenance of the interstitial fluid pressure[21]. PDGF is implicated in the development of certain disorders involving excess cell proliferation, including certain malignancies, atherosclerosis and fibrotic conditions.

THE

2.2.2. Interaction between PDGF isoforms and PDGF receptors

The level and types of PDGF receptors expressed by a target cell determines its response to PDGF. PDGF is a dimeric molecule consisting of 30-kDa disulfide-bonded A- and B-polypeptide chains. Homodimeric (PDGF-αα, PDGF-ββ) as well as heterodimeric (PDGF-αβ) isoforms exert their effects on target cells by binding with different specificities to two structurally related protein tyrosine kinase receptors, denoted α- and β receptors. The A- and B-chains of PDGF are both synthesized as precursor molecules that undergo proteolytic processing. The mature A- and B-polypeptide molecules, which consist of about 100 amino acid residues each and are about 60% identical in their sequences, are encoded by separate genes located on chromosomes 7 and 22, respectively [22-24]. The three-dimensional structure of PDGF [25] is similar to that of the related vascular endothelial growth factor (VEGF)[26], and show some distant resemblance to those of nerve growth factor and transforming growth factor-β [27], although the latter factors show no sequence similarities to PDGF. Since the PDGF isoforms are dimeric molecules, they have two separate receptor binding epitopes each. Thus, one PDGF molecule binds two receptor molecules simultaneously[28-30]. The α-receptor binds both A- and B-chains. Thus, PDGF-α receptor binds all three isoforms, whereas PDGF-β receptors bind with high affinity to the BB homodimer [31-33]. The α– and β–receptors for PDGF each contains five extracellular immunoglobulin domains and an intracellular tyrosine kinase domain with a characteristic inserted sequence [34-39]. PDGF thus forms a bridge between two receptor molecules. The ligand-receptor

THE

complex is further stabilized by a direct interaction between domain 4 of the two receptors [40-42].

Binding of PDGF dimmers to the extracellular portion of the receptor induces receptor dimerization. Dimerization of the receptors is the key event in PDGF receptor activation. It juxtaposes the intracellular parts of the receptors which then allows phosphorylation in trans (autophosphorylation) between the two receptors in the complex [43]. Autophosphorylation provides attachment sites for direct interaction between substrate proteins of the different signaling pathways and the activated receptor [44]. Such interactions are exerted by specific domains, e.g. Src homology 2 (SH2) domains and phosphotyrosine binding (PTB) domains which recognize phosphorylated tyrosine residues in specific environments, SH3 domains which recognize proline-rich regions, pleckstin homology (PH) domains which recognize membrane phospholipids and PDZ domains which recognize a C-terminal valine residue and specific upstream sequences. More than 10 different SH2-domain-containing molecules have been shown to bind to different autophosphorylation sites in the PDGF α- and β-receptors.

2.2.3. PDGFββ and renal disease

Platelet-derived growth factor beta (PDGFββ) is a potent *in vitro* and *in vivo* mesangial cell mitogen [14, 45, 46], and is involved in the regulation of mesangial cell matrix synthesis [47]. The normal adult kidney expresses only low amounts of PDGF protein and receptors, primarily by mesangial cells [44, 48]. In renal disease states, infiltrating inflammatory cells (monocytes/macrophages) and platelets are a major source of PDGF [49]. Exposure of mesangial cells *in vitro* to growth factors, such as epidermal growth factor (EGF), growth hormone (GH), transforming growth factor type α (TGF-a),

basic fibroblast growth factor (FGF-2), and tumor necrosis factor type α (TNF-α) induce expression of PDGF mRNAs. EGF, TNF-α, and FGF-2 also stimulate MCs to secrete PDGF [50] Inflammatory agents such as interleuken-1β (IL-1β) and IL-6, as well as vasoactive mediators such as vasopressin, endothelin-1 (ET-1), and angiotensin-II (AngII) [51]. Expression of PDGF$\beta\beta$ and its receptor are also significantly increased in mesangial cells of animal models of glomerulonephritis [52, 53] and in human glomerulonephritis in which mesangial proliferation occurs [52, 54, 55]. The importance of PDGF$\beta\beta$ in glomerulonephritis was first demonstrated experimentally by the administration of anti-PDGF$\beta\beta$ antibodies in the anti-Thy1.1 model. Anti- PDGF$\beta\beta$ antibody treatment did not affect the initial mesangiolysis that occurs, but did result in a 50% reduction in mesangial cell proliferation and a corresponding reduction in ECM accumulation [53, 56]. More recent studies using the non-specific PDGF$\beta\beta$ inhibitors trapidil [57], dipyridimole [58], and TNP-470 [59] as well as the selective PDGF$\beta\beta$ inhibitor STI 571 [60], have confirmed the importance of PDGF$\beta\beta$ in both animal models and human glomerulonephritis.

2.3. FGF-2.

2.3.1. FGF-2 Introduction

The first fibroblast growth factor (FGF) was discovered as a mitogen for cultured fibroblasts at least 30 distinct FGFs have been identified thus far. Basic fibroblast growth factor (FGF-2) is a member that affects the growth, differentiation, migration and survival of a wide variety of cell types [61]. FGF-2 and other members of the FGF family bind to heparin and heparin sulfate. Binding of FGF-2 to heparin sulfate has been demonstrated to reflect a complex biochemical regulatory mechanism for this growth

factor. FGF-2 is a proteolytic product of the primary 18 kDa form [61]. Larger forms of FGF-2 (22, 22.5 and 24 kDa) have also been identified resulting from alternate CUG-translation start sites. Sequence homology for FGF-2 is very high (>90%). FGF-2 contains four cysteine residues with no intramolecular disulfide bonds, a large number of basic residues, two sites (Ser 64 and Thr 112) that can be phosphorylated by protein kinases A and C, respectively[61]. FGF-2 consists of 12 anti-parallel β-sheets organized into a trigonal pyramidal structure. Heparan sulfate proteoglycans (HSPGs) are membrane-bound (e.g., syndecans and glypicans) or extracellular matrix (e.g., perlecan) macromolecules that consist of a core protein and one or more heparan/heparin sulfate glycosaminoglycan chains. Heparin is only synthesized by connective tissue mast cells, heparin sulfate is widely distributed throughout all mammalian tissues and organs attached to core proteins as HSPGs [62]. Heparan sulfate proteoglycans are potent, specific regulators of cell–matrix interaction, cell adhesion, migration, proliferation, angiogenesis, and development. The binding of HSPGs facilitates the self-association of FGF-2 molecules into dimmer and higher-order oligomers [63]. HSPGs are found on cell surfaces and in the extracellular matrix where they have been demonstrated to interact with FGF-2 and modulate its distribution and function [64].

FGF-2 lacks a consensus signal sequence for secretion, however significant amounts of the 18 kDa form of FGF-2 are found outside the cell, the higher molecular weight forms are predominantly localized to the nucleus [61]. The mechanism of secretion of the 18-kDa FGF-2 remains unclear. FGF-2 does not progress through the endoplasmic reticulum and the Golgi via the regular secretory pathway. It has been suggested that FGF-2 is released from cells as the result of cell damage, death and non-

lethal membrane disruptions [4]. Released FGF-2 is found stored in the extracellular matrix and basement membranes bound to HSPG [65]. Extracellular FGF-2 binds to cell surface receptors and HSPGs and is subject to internalization and lysosomal degradation. However, a considerable amount of FGF-2 can translocate into the nuclear fraction of various cell types [66]. Nuclear translocation is cycle dependent, occurring in the G1-S transition. This results in an overall decrease in FGF-2 degradation and correlates with enhanced mitogenic activity [61, 66] . FGF-2 plays key roles in development, remodeling and disease states in almost every organ system [61]. One of the best-characterized activities of FGF-2 is its ability to regulate the growth and function of vascular cells such as endothelial and smooth muscle cells. A role of HSPG in modulating FGF-2 activity is its ability to modulate the binding of FGF-2 to its receptor. Cells that do not express HSPG show reduced receptor binding affinity and reduced biological response [63].

2.3.2. FGF-2 Signaling

FGF-2 interacts with specific cell surface receptor proteins derived from four separate genes (FGFR1-4). Splice variants confer specificity in signaling in response to the 23 identified FGF family members. FGF-2 has been proposed to have two separate receptor binding sites which might allow a single FGF-2 to bind to two receptors or to interact with a single receptor in two separate positions [67]. HSPGs can increase the affinity of FGF-2 for its receptors [68] and act as a bridge to facilitate the dimerization of receptors.

Like all receptor tyrosine kinases, the FGFR2 is composed of an extracellular ligand-binding domain, a single transmembrane domain and a cytoplasmic domain. The

extracellular domain of FGFRs is composed of three Ig-like domains (D_1, D_2, and D_3) in which D_2 and D_3 function as FGF-and heparin-binding regions. Formation of a ternary FGF/heparin/FGFR complex results in FGFR dimerization and activation. The cytoplasmic domain of FGFR contains in addition to the catalytic protein tyrosine kinase (PTK) core, several regulatory sequences. The juxtamembrane domains of FGFRs are considerably longer than that of other receptor tyrosine kinases. There are seven tyrosine residues in the cytoplasmic tail of FGFR-1 that can be substrates for phosphorylation: Tyr463, Tyr583, Tyr585, Tyr653, Tyr654, Tyr730 and Tyr766. Tyr766 is necessary for FGFR activation of phospholipase Cγ (PLCγ) through SH2 domain binding [69]. Mutational analysis of Tyr766 has shown that the phosphorylation of this tyrosine residue is essential for complex formation with and tyrosine phosphorylation of PLCγ, resulting in PLCγ activation, stimulation of phosphatidylinositol (PI) hydrolysis and the generation of the two second messengers, diacylglycerol (DAG) and Ins (1,4,5) P3 [69]. This region contains a highly conserved sequence that serves as a binding site for the PTB domains of the two members of the FGFR signaling adaptor (FRS2) docking proteins, FRS2α and FRS2β [70, 71]. FGF-stimulation leads to tyrosine phosphorylation of FRS2α and FRS2β, followed by recruitment of multiple Grb2/Sos complexes resulting in activation of the Ras/MAP kinase signaling pathway [72]. FRS2α contains four binding sites for the adaptor protein Grb2 and two binding sites for the protein tyrosine phosphatase Shp2. FGF-stimulation leads to tyrosine phosphorylation of Shp2 resulting in complex formation with additional Grb2 molecules. Grb2/Sos complexes are thus recruited directly and indirectly via Shp2 upon tyrosine phosphorylation of FRS2α in response to FGF-stimulation [72]. In addition to enhancement of tyrosine phosphorylation, FGF-

THES

stimulation induces MAPK-dependent phosphorylation of FRS2α on at least eight threonine residues. Threonine phosphorylation of FRS2α is accompanied by reduced tyrosine phosphorylation of FRS2α, decreased recruitment of Grb2 and attenuation of the MAP kinase response [73].

2.3.3. FGF-2 in renal disease

FGF-2 is expressed by a variety of cells, including endothelial cells, smooth muscle cells, macrophages, fibroblasts, and mesangial cells [74]. In addition to FGF-2 receptors, heparan sulfate proteoglycans, especially syndecan, are essential for the binding of FGF-2 to its cellular receptor [75, 76]. Since mesangial cells express FGF-2 and its receptor components, its not surprising that FGF-2 is a potent mitogen for mesangial cells [74]. However, FGF-2 lacks a signal peptide for secretion and is not normally released into the circulation [77]. FGF-2 is released from adult mesangial cells only following an injury and may lead to further mesangial cell injury by stimulating nitric oxide production [78]. Nitric oxide can be toxic to cells by causing nitrosylation of Fe-S groups on non-heme enzymes, resulting in respiratory inhibition. This feed-forward progression of FGF-2-induced mesangiolysis is an important feature of the early phase of anti-Thy1.1 nephritis. After the initial mesangiolysis, the marked proliferation of mesangial cells that occurs in the anti-Thy1.1 model is associated with an increased glomerulosynthesis of FGF-2 [74]. Further evidence of the importance of FGF-2 in this model are the observations that injection of FGF-2 following anti-Thy1.1 antibody administration resulted in increased mesangiolysis [74], while treatment with anti-FGF-2 blocked the initial mesangiolysis, resulting in less mesangial proliferation and less ECM deposition [79].

THE

2.4. RAMPs and the AM signaling system.

2.4.1. The AM signaling system

AM belongs to a large regulatory peptide family that includes calcitonin gene-related peptide (CGRP), amylin, calcitonin (CT), and a recently discovered member, intermedin (AM2). These peptides bind to and act via selective receptors derived from the calcitonin receptor-like receptor (CRLR). CRLR is a seven-transmembrane-spanning G-protein coupled receptor (GPCR) belonging to the class B GPCR family (secretin family of GPCRs). Human CRLR is comprised of 464 amino acids and is 54% homologous to the human calcitonin receptor (CTR). CRLR acts as either a CGRP or an AM receptor depending on its interaction with receptor activity modifying proteins (RAMPs). RAMP1 (R1), RAMP2 (R2), and RAMP3 (R3) are distinct gene products and have been characterized as single-transmembrane domain proteins capable of direct interaction with CRLR. An important study was published in 1998 by McLatchie et al. that clarified the elusiveness of the AM and CGRP receptors, and provided a novel paradigm of GPCR regulation. When CRLR was expressed with R1, a CGRP receptor was produced. In HEK293 cells when CRLR was expressed with R2 or R3 virtually identical (pharmacologically and biologically) AM receptors (AM-1R, AM2-R, respectively) were produced [80], even though R2 and R3 share only approximately 30% sequence identity.. RAMPs and their receptor partners form stable complexes that originate in the endoplasmic reticulum (ER) and Golgi apparatus. These complexes are maintained during the processes of translocation to the cell surface, agonist activation, internalization and trafficking to lysosomes [81-83].

THE

2.4.2. RAMP gene and protein structure

RAMPs are a family of three type I transmembrane proteins. R1 and R2 were initially cloned from human neuroblastoma cell (SKN-MC) DNA library, whereas R3 was isolated from the human spleen. A scan of the human genome revealed no more sequences similar to the RAMPs [84]. R1 and -3 share some similarities in their gene composition, being comprised of three exons divided by large introns. The R1 and -3 genes are large in comparison to that of R2 (approximately 24 Kb vs. 5 Kb, respectively). Despite the relatively low amino acid sequence identity between the RAMP isoforms (approximately 30%), the hydrophobicity plot analysis suggests similar protein structures. The sequence similarity of the RAMP isoforms between species is quite well conserved, at approximately 90% between mouse and rat. Sequence identity between the rodent and human sequences is 70, 65, and 85% for R1, R2, and R3, respectively [85, 86]. RAMP proteins have a molecular weight of only approximately 14-17 kilo-Daltons. R1 and R3 are 148 amino acid proteins, while R2 is composed of 175 amino acids. All isoforms are made up of a large extracellular domain, an approximately 20 amino acid transmembrane domain, and a 10 amino acid intracellular domain [87]. While some key amino acid residues are conserved across all RAMP isoforms, their sequence heterogeneity is the basis for their ligand binding, receptor trafficking, and cell signaling diversity (Figure 1).

THE

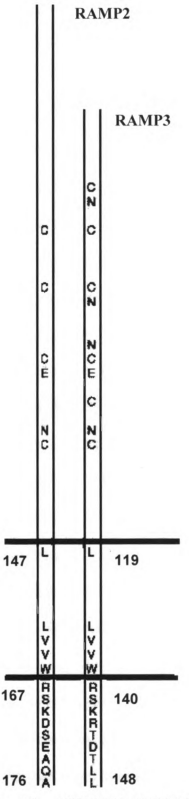

Adapted from: **TIBS 31**(11): 631-38 ref [88]

Figure 1. Amino acid sequences of RAMPs. R1, R2, and R3 share approximately 30% sequence homology. The sequences are most diverse within the long, extracellular N-terminal regions of RAMPs. The N-terminal region of R1 and 3 are the most conserved among the isoforms, R2 is 26 amino acids longer. Conserved cysteine (C) residues and N-terminal glycosylation sites (N) are shown. The transmembrane domain is highly conserved between isoforms. All three RAMPs harbor conserved serine (S) and lysine (K) residues within their short, cytoplasmic tails. R3 contains a PDZ domain at the extreme C-terminus.

THE

2.4.3. Role of RAMP N-terminal and transmembrane domains

The N-terminal sequences of RAMPs are poorly conserved (less than 20% of amino acid identity) but share in common a significant number of consensus sites for cotranslational modifications including cysteine residues (potentially involved in disulfide bond formation) and N-glycosylation consensus sites (Asn-X-Ser/Thr). The N-terminus is comprised of amino acids1-119 for R1 and 3, 1-147 for R2, and the transmembrane domains are composed of 20 amino acids thereafter. The N-terminal sequences have been reported to be important for ligand binding specificity, while the transmembrane domain stabilizes the CRLR-RAMP heterodimer complex [80].
The structural domain(s) involved in selective AM binding have been studied using various RAMP chimeras and deletion mutants. Co-expression of chimeric RAMPs and CRLR in HEK293 cells revealed that residues 77-101, situated in the extracellular N-terminal domain of human R2, were crucial for selective AM-evoked cAMP production. In addition, deletion of hR2 residues 86-92 significantly attenuated high-affinity ^{125}I-AM binding and AM-evoked cAMP production despite cell surface expression of CRLR-R2. Deletion of hR3 residues 59-65 had a similar effect.

Disulfide bonds are also critical for CRLR-RAMP activation. Four cysteine residues are conserved in all RAMP isoforms, and R1 and 3 harbor two additional conserved cysteine residues. While similar studies have not been completed using R1, mutation of each of the six cysteines results in a significant loss of R3 cell-surface expression and ligand binding [88]. Several consensus sites for N-glycosylation (Asn-X-Ser/Thr) have also been identified on R2 and R3. Four N-glycosylation sites identified

THE

on human, mouse and rat R3 are conserved in the mouse R2, R1 has no consensus sites for N-glycosylation [89]. In a recent study, it was demonstrated that N-glycosylated R2 and R3 are expressed at the cell surface, and their transport to the plasma membrane requires N-glycans. R1 is not N-glycosylated and is transported to the cell surface only upon formation of heterodimers with CRLR [90].

2.4.4. Role of RAMP C-terminal domains

While many studies have investigated the functional roles of both RAMP extracellular and transmembrane domains, recent work has implicated the importance of short C-terminal domains in receptor function and cellular signaling. Deletion of the cytoplasmic tail of either R1 or R3 does not alter trafficking of CRLR to the plasma membrane, but its deletion from R2 inhibits CRLR transport to the cell surface.[91]. The C-termini of all three RAMP isoforms contain highly conserved serine and lysine residues. While these residues do not effect internalization of either R1-CRLR or R2-CRLR, they negatively regulate internalization of R3-CRLR [92]. A PSD-95/Discs-large/ZO-1 homology domain type-I (PDZ) recognition motif (Asp-The-Leu-Leu) on the extreme C-terminus of R3, but not R1 or R2, that is responsible for protein-protein interactions important in the regulation of trafficking of the R3-CRLR complex [93, 94]. N-ethylmalemide-sensitive factor (NSF) is a hexameric ATPase that targets both β2-adrenergic receptor (β2-AR) and the α-amino-3-hydroxy-5-methylisoxazolepropionate receptor (AMPAR) for recycling by a PDZ-binding domain interaction [95, 96]. Recent reports from our laboratory have also demonstrated the importance of a R3 C-terminal PDZ-binding domain in R3-CRLR trafficking. R3 interaction with NSF results in the recycling of the R3-CRLR complex following agonist stimulation, while the absence of

THE

NSF, or deletion of the R3 PDZ domain, results in receptor degradation [97] (Figure 2). In addition, the R3 PDZ-binding motif plays a role in CRLR internalization via novel R3 protein: protein interactions. Na^+/H^+ exchanger regulatory factor-1 (NHERF-1) tethers membrane receptors to the cytoskeleton via PDZ interactions with the merlin/ezrin/radixin/myosin (MERM) family of proteins [98]. Recent evidence has revealed important associations between the NHERF-1 and several G protein-coupled receptors such as the β2AR, the kappa-opioid receptor, and the PTHR, as well as growth factor tyrosine kinase receptors such as the platelet-derived growth factor receptor and the epidermal growth factor receptor [98-101]. In HEK293 cells, overexpression of NHERF-1, together with CRLR-R3 (but not CRLR-R1 or CRLR-R2) abolishes agonist-mediated internalization [102]. These results were confirmed in a primary human proximal tubule cell line that expresses abundant amounts of NHERF-1. In these cells AM treatment results in no internalization of CRLR, and knockdown of NHERF-1 by RNA interference allows internalization to occur following AM treatment. Protein kinase A and C phosphorylation consensus sites also are present on the C-terminal intracellular domains of R1 and R3, but not R2 [85, 103]. The role of these phosphorylation sites has not been fully elucidated.

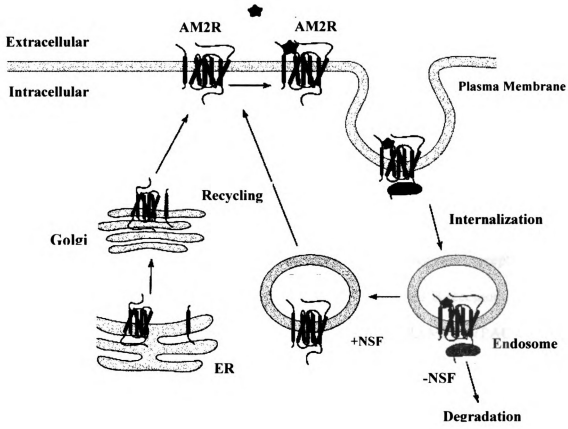

Adapted from: **TIBS 31**(11): 631-38 ref [104]

Figure 2. Recycling of the AM-1R. Co-expression of CLR and R3 in HEK293 cells enables the receptor complex to form a stable dimer that originates at the ER and Golgi. The dimer is maintained during translocation to the cell surface, receptor activation, internalization and degradation. Activation of the receptor complex by AM results in cAMP generation with subsequent desensitization (not shown). The receptor complex is then internalized and targeted for degradation. Over-expression of NSF prevents the CLR–R3 complex from undergoing degradation.

THE

2.4.5. RAMP interaction with other class B and C receptors

In addition to CRLR, other members of the class B GPCR family include receptors for secretin, glucagon, glucagons-like peptide, amylin, gastric inhibiting peptide, vasoactive intestinal peptide/pituitary adenylate cyclase-activating peptide (VPACR), growth-hormone-releasing-hormone, parathyroid hormone (PTHR), and CTR. In a recent RAMP binding study, when co-expressed with RAMPS, 6 out of 10 class B receptors demonstrated RAMP interaction [105]. VPAC2 receptor (VPAC2R), glucagon-like peptide receptors, and growth-hormone-releasing-hormone receptor did not interact with any of the co-expressed RAMP isoforms. Three class B receptors, namely VPAC, glucagon, and PTH, have been shown to associate with RAMPs. VPAC1 receptor (VPAC1R) interacts with all three RAMP isoforms, parathyroid hormone-1 receptor (PTH1R) and glucagon receptor with R2, and parathyroid hormone-2 receptor (PTH2R) with R3. Unlike the interaction of RAMPs with CRLR, VPAC1R is expressed at the plasma membrane independently of RAMP presence. The classic coupling pathway associated with VPAC1R is a significant accumulation of cAMP with little phosphoinositide (PI) hydrolysis. However, the VPAC1R:R2 heterodimer exhibits enhanced PI hydrolysis with no significant change in cAMP stimulation. These intriguing results suggest RAMPs may modulate GPCR coupling efficiency through diverse cell signaling pathways. Similar to the ability of R2 to alter VPAC1R:R2-mediated signaling, it is conceivable that R3 may play a diverse role in cellular signaling

Several published reports have concentrated on the regulation of class B GPCRs by RAMP interactions. However, a recent study has demonstrated that a class C GPCR, a

THE

calcium-sensing receptor (CaSR), interacts with RAMPs [106]. In a paradigm similar to CRLR, recombinant CaSR expressed in COS7 cells does not translocate to the plasma membrane unless R1 or R3 (but not R2) is also co-expressed. In the same study, R3 was shown to mediate both the glycosylation and trafficking of CaSR from the ER to Golgi. In the absence of R3, CaSR was retained in an intracellular compartment that confocal microscopy identified to be the ER. Further studies are needed to determine if and how RAMPs interact/modulate other class C GPCR functions.

2.4.6. RAMPs are a regulated component of the AM signaling system

RAMP mRNA distribution has been analyzed in several species including mouse, rat, and human. R1 has shown predominant expression in human heart, brain, skeletal muscle, pancreas, thymus, spleen, fat, and kidney; R2 expression is abundant in the heart, aorta, kidney, spleen, fat, skeletal muscle, and lung. R3 is the most widely distributed; its expression is greatest in the kidney, heart, brain, and lung [86, 87, 107-110]. Changes in RAMP gene expression have been studied under many disease models, physiological changes, and drug treatments. Variable RAMP gene expression has been reported in several human/animal disease states including carbon tetrachloride (CCl4)-induced liver cirrhosis [111], cancer[112-115], cardiac hypertrophy [116] , chronic heart failure [186] pregnancy-induced hypertension [112-115] and hypoxia [reviewed in [117]] (Table 1). In several of the disease models described above, RAMP expression did not correlate with CRLR expression. These findings suggest specific, receptor-independent RAMP cellular activities might contribute to disease prevention/progression.

Model	Tissue	R1	R2	R3	Ref.
LV Hypertrophy	Rat L ventricle	ND	↑↑	↑↑↑	[116]
Chronic Heart Failure	Rat Atria	↑	-	↑↑↑	[118]
	Rat Ventricles	↑↑	-	↑↑	
Hypertensive Rat	Renal Cortex	ND	↓↓↓	↑↑	[119]
DOCA Salt Loaded	Renal Medulla	ND	↓↓	↑↑	[120]
Hypoxia	Rat Lung	↑↑↑	-	↑	[121]
LPS Sepsis	Mouse Lung/Spleen	↓↓	↓↓↓	↑↑↑	[107]
LPS Sepsis	AM+/-Mouse Lung	ND	↓↓↓	↓↓↓	[122]
Pregnancy	Rat Mammary Gland	↓↓	-	↓↓	[112]
Liver Cirrhosis (CCl_4)	Rat Liver	↑↑	↑	↑↑↑	[111]
Prostate Cancer	Biopsy	-	-	↑↑	[123]

Adapted from: **Semin Cell Dev Biol 15**(3): 299-308 ref [117]

Table 1. Variable RAMP gene expression in disease models. Level of expression is shown as increase (↑), decrease (↓), or no change (-). Single, double and triple arrows indicate weak, moderate, and strong increase/decrease. ND: not determined.

2.4.7. Growth related mediators of R3 expression

Using both animal and cell culture models, several reports have indicated that growth associated conditions can result in alterations of R3 gene expression. However the mechanisms of R3 involvement in proliferation have not been thoroughly investigated. Published reports from our lab demonstrate that R3, but not R2, is dose-dependently upregulated in RMC following PDGF-BB treatment [124]. The growth-stimulating parathyroid hormone also increases R3 expression in primary mouse osteoblasts [125] in a dose and time-dependent manner. R3 is expressed in the rapidly growing thymus of newborn rats, but not in quiescent thymus of adult animals [126]. R3 is expressed in the prostate cancer cell line, DU145 [123]; in prostate carcinoma biopsies the levels of R3 were significantly elevated (compared to prostate hyperplasia biopsies) while expression levels of R2 were unchanged in these samples [123]. Estrogen and phytoestrogen are important mediators of uterine growth and differentiation. In rats, administration of either of these mitogens preferentially increases uterine R3 expression levels, and actually significantly deceases CRLR levels [114, 127]. R3 is also exclusively upregulated in cultured rat neonatal cardiac fibroblasts with IL-1beta [128], and in a rat model volume overload-induced cardiac hypertrophy R3 was significantly increased, while other AM signaling components were only modestly or not increased at all [128, 129]. Angiotensin II induces hypertrophy of cultured rat neonatal cardiomyocytes. mRNA levels of R1 and R3 are significantly elevated following 24-h treatment with Ang II (without a change of those of R2 and CRLR), and the effects of Ang II on R1 and R3 expression were abolished by an Ang II type 1 (AT1) receptor antagonist [130]. It is

evident from the reports described above that R3 is differentially regulated compared to other AM2R components, namely CRLR and R2. Further studies are warranted to assess R3's involvement in these conditions (Table 2).

Treatment	Cell Line/ Animal Model	R1	R2	R3	Ref.
Ang II	Rat Cardiomyocytes	↑↑	-	↑↑	[130]
PDGF-ββ	RMC	ND	-	↑↑	[124]
Estrogen	Rat Uterus following injection	-	↑	↑↑↑	[114]
PTH	Primary mouse osteoblasts	-	-	↑↑	[131]
Prostate Cancer	DU 145 cells	-	-	↑↑	[123]
IL-1β	Rat neonatal fibroblasts	ND	-	↑↑	[128]

Table 2. Growth-mediators that influence R3 expression. Level of expression is shown as increase (↑), decrease (↓), or no change (-). Single, double and triple arrows indicate weak, moderate, and strong increase/decrease. ND: not determined.

TH

2.5. MAPK Cell Signaling.

2.5.1. MAPK Introduction

Cells recognize and respond to extracellular stimuli by engaging specific intracellular programs, such as the signaling cascade that leads to activation of the mitogen-activated protein kinases (MAPKs). All eukaryotic cells possess multiple MAPK pathways, which coordinately regulate diverse cellular activities from gene expression, mitosis, and metabolism to motility, survival and apoptosis, and differentiation. Five distinct groups of MAPKs have been characterized in mammals: ERKs 1 and 2 ERK1/2, c-Jun amino-terminal kinases (JNKs 1, 2, and 3), p38 isoforms α, β, γ, and δ, ERKs 3 and 4, and 5. MAPKs can be activated by a wide variety of different stimuli, but in general, ERK1, and ERK2 are preferentially activated in response to growth factors and phorbol esters, while the JNK and p38 kinases are more responsive to stress stimuli ranging from osmotic shock and ionizing radiation to cytokine stimulation.

Each family of MAPKs is composed of a set of three evolutionarily conserved, sequentially acting kinases: a MAPK, a MAPK kinase (MAPKK), and a MAPKK kinase (MAPKKK). The MAPKKKs, which are serine/threonine kinases, are often activated through phosphorylation and/or as a result of their interaction with a small GTP-binding protein of the Ras/Rho family in response to extracellular stimuli [36,98]. MAPKKK activation leads to the phosphorylation and activation of a MAPKK, which then stimulates MAPK activity through dual phosphorylation on threonine and tyrosine

residues located in the activation loop of kinase sub domain VIII. Once activated, MAPKs phosphorylate target substrates on serine or threonine residues followed by a proline; however, substrates selectivity is often conferred by specific interaction motifs located on physiological substrates. MAPK cascade specificity is also mediated through interaction with scaffolding proteins that organize pathways in specific modules through simultaneous binding of several components. Since it is widely believed that the ERK cascade is a primary mediator in many proliferative responses, inhibition of the ERK signaling cascade has been targeted extensively in diseases such as cancer and vascular remodeling [132, 133].

2.5.2. ERK1/2 Properties

The ERK1/2 module, also known as the classical mitogen kinase cascade, consists of the MAPKKKS A-Raf, B-Raf, and Raf-1, the MAPKKs MEK1 and MEK2, and the MAPKs ERK1 and ERK2. ERK1/2 are serine/threonine kinases that mediate proliferation by transmitting signals from the cell surface to the nucleus to regulate the activity of transcription factors. ERK1 and ERK2 have 83% amino acid identity and are expressed to various extents in all tissue. They are strongly activated by growth factors, serum, and phorbol esters and to a lesser extent by ligands of the heterotrimeric G protein-coupled receptors, cytokines, osmotic stress, and microtubule disorganization [134]. Cell surface receptors such as tyrosine kinases, (RTK) and G protein-coupled receptors transmit activation signals to the Raf/MEK/ERK cascade through different isoforms (H-Ras, N-Ras, and K-Ras 4B/4A) of the small GTPase protein Ras [135, 136]. Activation of only 5% of Ras molecules is sufficient to induce full activation of ERK1/2 [137]. Ras proteins must associate with the cytosolic leaflet of cellular membranes to be

fully activated [138, 139]. Post-translational modifications of a conserved C-terminal CAAX sequence (C=cysteine, A=aliphatic amino acid, X=any amino acid) in Ras mediates this membrane association [140]. Membrane-association of Ras is also achieved through recruitment of SOS (son of sevenless), a Ras-activation guanine nucleotide exchange factor (GEF). SOS stimulates Ras to change GDP to GTP, allowing it to interact with a wide range of downstream effector proteins, including isoforms of the serine/threonine kinase Raf [141]. Activated Raf binds to and phosphorylates the dual specificity tyrosine/threonine kinases MEK1 and -2, which in turn phosphorylate ERK1/2 within a conserved Thr-Glu-Tyr (TEY) motif in their activation loop. Phospho-Erk forms dimers that are transported into the nucleus, where they phosphorylate the Ets family of transcription factors, including Elk-1. Regulation of both Ras and Raf is crucial for the proper maintenance of cell proliferation, as activating mutations in these genes lead to oncogenesis [142]. Ras has been shown to be mutated in 30% of all human cancers, while B-Raf is mutated in 60% of malignant melanomas [143, 144].

All signal transduction cascades transmit signals from the cell surface into the cytoplasm and nucleus to elicit a cellular response. These cascades contain multiple components, and classical cascades act by a sequential series of phosphorylation steps. Since MAP kinases phosphorylate very similar motifs (consensus sequence Ser/Thr-Pro (S/TP)), and several potential substrates contain this motif, it is important to provide specificity to direct individual kinases towards the correct substrates. Multiple mechanisms exist for generating signaling specificity within these cascades to ensure specific cellular responses, including the association of the cascade components with

their activating kinases, inactivating phosphatases, and scaffold proteins that facilitate distinct signaling complexes.

2.5.3. Scaffolding proteins are ERK-activity modulators

Scaffolding protein interaction is one means of ensuring efficiency and specificity in MAPK signaling cascades [145]. Several proteins have been shown to interact with members of the ERK cascade, including the scaffold proteins MEK-1 Partner 1 (MP-1), and Kinase Suppressor of Ras (KSR) and the modulators Connector Enhancer of KSR (CNK) and Raf-1 Kinase Inhibitor Protein (RKIP), resulting in stimulation or inhibition of the ERK1/2 cascade [146]. MP1 was isolated in a yeast two-hybrid screen using MEK-1 as bait [147]. This small protein displays no sequence homology with known proteins and does not contain any recognizable motif. MP1 selectively interacts with ERK-1 and MEK-1 but fails to bind to ERK-2 and MEK-2. In vitro, MP1 enhances the activation of MEK by Raf, and when overexpressed in cells, MP1 can selectively induce the activation of ERK-1 but not that of ERK-2, suggesting that MP1 could help to discriminate between two closely related MAPKs in the same module. MP1 MAPK scaffolding activity is localized to the cytoplasmic surface of late endosomes/lysosomes, thereby combining catalytic scaffolding and subcellular compartmentalization as means to modulate MAPK signaling within a cell [148]. KSR is a protein kinase identified by genetic screens in *Caenorhabditis elegans* and *Drosophila*. A database search revealed that Raf family kinases are the closest relatives to KSR, however KSR lacks the necessary Ras binding domain so it is unable to bind to activated Ras [149]. Biochemical studies using mouse KSR-1 revealed that the kinase domain of KSR interacts strongly

with MEK-1 and MEK-2, ERK via the CA4 domain, and to Raf-1 via the CA5 kinase domain [150]. While the interaction with MEK appears constitutive, the ability of KSR to interact with Raf-1 and ERK is induced by cell treatment with growth factors [151]. In addition, KSR is cytosolic in resting cells but a fraction is translocated to the membrane upon cell treatment with growth factors [152]. A physiological substrate for KSR has not been identified therefore the exact mechanism by which this kinase regulates the Raf/MEK/ERK pathway has not been elucidated. RKIP was isolated in a two-hybrid screen using the kinase domain of Raf-1 as a bait and belongs to the family of phosphatidylethanol-binding proteins, which are widely expressed and highly conserved. In vitro, RKIP was found to bind MEK, Raf-1, and ERK, but not to Ras. This interaction is exclusive since the binding sites for Raf and MEK in RKIP overlap [153]. Consequently, overexpression of RKIP can disrupt the physical interaction between Raf-1 and MEK, thereby impairing MEK phosphorylation by Raf, without affecting that of ERK by MEK. Cell treatment with growth factors provokes the release of RKIP from Raf-1, allowing phosphorylation and activation of MEK. RKIP co-immunoprecipitates with Raf-1 and MEK from cell lysates and colocalizes with Raf-1 at the plasma membrane when examined by confocal microscopy. RKIP represents a new class of protein-kinase-inhibitor protein that regulates the activity of the Raf/MEK/ERK module.

2.5.4. ERK Docking Domains are ERK-activity modulators

The first description of docking domain function arose from the observation that the transcription factor c-Jun differs in several respects from its oncogenic counterpart v-Jun. Namely, the δ-domain present in c-Jun is absent in v-Jun, suggesting an important function for this motif. Mutational analysis revealed that the c-Jun δ-domain acts as a

binding site for the c-Jun N-terminal kinase (JNK) and this function is lost in v-Jun [154-156]. The δ-domain was subsequently defined as a JNK MAP kinase-docking domain. Binding of JNK to this docking site was shown to be important for efficient phosphorylation of c-Jun by JNK and for the activity of its transcriptional activation domain. The δ-domain has also been implicated in directing the site-specific phosphorylation of c-Jun. *In vitro*, c-Jun is normally phosphorylated on Ser63 and Ser73, but, upon deletion of the δ-domain, alternative phosphorylation sites in c-Jun become preferentially phosphorylated decreasing the overall efficiency of c-Jun activation [157].

Subsequently, other transcription factor–MAP kinase combinations were studied, and an important theme that emerged was that many MAP kinase substrates possess docking sites that serve to recruit MAP kinases and increase the efficiency of their phosphorylation. In fact, each of the three major classes of MAP kinases (ERK, JNK and p38) has been shown to bind to transcription factors, and, in each case, the docking site serves to enhance substrate phosphorylation.

It is clear from the discussion above that one of the major functions of docking sites is to promote the specificity, efficiency and accuracy of substrate phosphorylation by MAP kinases. However, some scaffolding proteins contain docking domains; their primary function is to bring several MAPK molecules in close proximity at a precise subcellular location. For example, the scaffolding protein JIP-1 binds specifically to JNK MAP kinases via its docking domain and brings together several JNK MAP kinase cascade molecules resulting in the cytoplasmic retention of JNK and its inhibition [158,

159]. Another example is JunB, which, like c-Jun, contains a docking site but lacks phosphoacceptor motifs. In this case, JunB acts to recruit JNK MAP kinases, which can then act *in trans* to phosphorylate other proteins such as its heterodimerization partner JunD, which contains a phosphoacceptor site but lacks a functional docking site [157]. Thus, docking domains can serve to recruit MAP kinases either into signaling complexes to enhance their regulation or onto promoters where they can phosphorylate other transcription proteins. ERK, p38 and JNK all have conserved domains that are used for docking to their specific activators (MAPKKs/MEKs), their inactivators (MKPs), their substrates (MAPKAPKs), chaperones, and scaffolding molecules [160, 161].

Although there is no clear overall consensus, docking domains contain an LxL motif located 3–5 amino acids downstream from a region containing several basic residues. Differences in the spacing and composition of these motifs are apparent for substrates that are recognized by different classes of MAP kinases. These specific sequences within MAP kinase docking domains impose both the specificity and efficiency of protein partner interaction. For example, the ERKDD of MEK allows it to interact with ERK only, not other MAPK family members, such as JNK or p38. Similarly, the docking sites of MEF2A and MEF2C only direct phosphorylation by a subset of p38 isoforms [162]. However, some docking domains are recognized by two different classes of MAP kinases, as observed with Elk-1, where the docking site directs both ERK and JNK MAP kinases to this substrate [163], permitting responses to a wider variety of stimuli.

The consensus sequences of MEK1/2 D-domains are located at their N-terminal region and consist of two residues of the basic amino acids arginine or lysine, followed immediately by the helix breaking amino acid proline, followed two to six amino acids later by the hydrophobic amino acids leucine or isoleucine [160, 164] (Consensus: -$(R/K)_2$-(P)-$(X)_{2-6}$-(L/I-X-L/I)-). Experiments utilizing a blocking peptide consisting of the MEK1 ERK D-domain resulted in a complete, specific blockade of MEK1:ERK1 interaction suggesting that MEK D-domains are necessary to direct the specific recognition, binding, and phosphorylation of ERK [160, 161, 165].

2.5.5. Plasma membrane and ERK signaling

Protein tyrosine kinase receptors (PTKR) located on the plasma membrane are known to activate the Ras/MAPK signaling cascade. Regulation of ERK signaling can be achieved through spatial regulation, utilizing scaffolding proteins that recruit ERK cascade components to specific subcellular compartments. One such scaffolding protein is kinase suppressor of Ras (KSR). Following EGF stimulation, KSR1 colocalizes with activated Ras and Raf-1 at the plasma membrane, facilitating the phosphorylation reactions required for the activation of MEK and MAPK [166]. Although the importance of plasma membrane MAPK signaling has been studied extensively, a role for endosomal, ER, and golgi targeting in MAPK mediated cellular events has recently been suggested (Table3).

Cellular Locations of ERK Signaling

Plasma Membrane:
KSR-mediates raf:MEK:ERK interaction/activation
CNK and SUR8-mediate ras:raf interaction/activation

Endosomes: (HGF,EGF,PDGF,NGF)
MP1-facilitates MEK1:ERK1 interaction/activation
β–arrestin- targets ERK activity to cytoplasm

ER and Golgi:
RKTG-negative modulator of raf
RasGRP1-activates Ras on the Golgi
Sef-recruits MEK and ERK and directs activated ERK towards cytosolic targets instead of nuclear

Table 3. ERK signaling in specific cellular compartments.

2.5.6. Endosomes and ERK signaling

PTKRs are internalized via clathrin-dependent and independent pathways. This ligand-induced endocytosis was originally thought to be a mechanism of receptor inactivation. Recent studies, however, suggest that receptors remain active on the cytoplasmic face of endosomes [167, 168] and that signaling can occur from these sites [169, 170]. In EpH4 (murine mammary epithelial cells), Caco-2 cells, and HeLa cells, MAPK scaffolding activity localizes to the cytoplasmic surface of late endosomes/lysosomes, thereby combining scaffolding and subcellular compartmentalization as means to modulate MAPK signaling within a cell [148]. Kermorgant et al. have recently demonstrated that traffic to endosomes is essential for hepatocyte growth factor (HGF/c-Met) to trigger an ERK response [171]. In addition, normal endocytic trafficking of EGFR is important for the full activation of MAPK. Inhibition of clathrin-mediated endocytosis by dominant-negative dynamin in EGF-activated cells revealed that internalization of EGFR is needed for maximal MAPK activation [172]. Burke et al. have also reported that the EGF receptor (EGFR) activates its targets Ras, Raf, and MAPKK (MEK) at the plasma membrane, but endocytosis had to occur to activate ERK [167, 173]. Like EGFR, nerve growth factor (NGF) activation of TrkA receptors results in internalization of phosphorylated TrkA via endocytosis. Howe et al. demonstrated that upon NGF stimulation, PC12 derived endosomes contained phosphorylated TrkA, Shc, Raf, ERK, as well as activated Ras [174].

In similar fashion, following EGF stimulation, the scaffolding protein MEK1 partner 1 (MP1) is recruited to late endosomes where it binds MEK1, phosphorylates ERK then releases the activated ERK to prolong its activation [175]. This turnover could

provide an amplification mechanism that translates low MEK activity into sustained ERK/MAPK activation, in which MP1 continues to supply MEK1 with inactive ERK for phosphorylation. MAPK organizer-1 (MORG1), a recently isolated MP1-interaction partner, also associates with Raf-1, B-Raf, MEK and ERK/MAPK on endosomal vesicles. MORG1 shows the typical properties of a scaffold, enhancing ERK/MAPK activation at low concentrations and inhibiting it at higher levels. MORG1 function seems to be stimulus-specific — it affects ERK/MAPK activation by serum, lysophosphatidic acid and phorbol esters, but not by EGF or PDGF [176]. β-arrestin also localizes to endosomes and serves as a Raf-1/MEK/ERK scaffold downstream of GPCRs. Originally characterized as a mediator of GPCR desensitization, β-arrestin is now recognized as a multifunctional protein that regulates internalization of GPCRs into clathrin-coated vesicles and serves as a scaffold for both the ERK and JNK MAPK modules [177]. Several lines of evidence implicate β-arrestin functionally in the transmission of signals from Raf-1 to MEK and ERK on endosomes. Raf-1 overexpression increased MEK and ERK binding to β-arrestin [177], and a dominant-negative form of β-arrestin blocked ERK activation downstream of GPCR activation [168]. Thus, endosomes serve as an organelle that supports both PTKR and GPCR signaling to ERK, and each system uses its own scaffold.

2.5.7. Golgi membrane associated ERK signaling

As mentioned above, Ras proteins undergo post-translational modifications of their CAAX motif that render them membrane-associated. One of these modifications, namely farnesylation of the CAAX motif, targets Ras to ER and golgi membranes[178]. The motif is then processed by enzymes found exclusively in the ER and golgi [179,

180]. The CAAX motif alone targets Ras proteins to the endomembrane system where they are methylated. Thus, rather than promoting nonspecific membrane association, prenylation mediates specific Ras association with the ER and Golgi membranes, and further processing there allows for its trafficking to the plasma membrane. Recently, it was demonstrated that the information required for accurate membrane localization is contained within the CAAX region [181], which also dictates how Ras proteins traffic to their destinations. Whereas H- and N-Ras traffic to the PM along the secretory pathway through the ER then Golgi complex, K-Ras4B is directly routed from the ER to the plasma membrane [178, 182]. The presence of H-Ras in these intracellular locations seems not to be a transient event associated with the transport and/or recycling of H-Ras proteins to and from the PM; instead, a pool of H-Ras appears to permanently reside in these organelles. These observations have led investigators to ask whether ER/golgi associated H-Ras undergoes GTP-GDP exchange and subsequent MAPK pathway signaling. Using live cell imaging utilizing a probe consisting of Raf-1's Ras binding domain fused to green fluorescent protein (RBD-GFP), Chiu et al. demonstrated that following EGF stimulation activated Ras is present at the plasma membrane, ER and the Golgi [183]. Although the Golgi-associated Ras was initially conceived of as a pool that does not traffic to the plasma membrane, recent studies have elucidated a plasma membrane/Golgi cycle that functions as a consequence of palmitoylation/depalmitoylation [184, 185]. Using transfected COS-1 cells, prenylated but depalmitoylated Ras appears to traffic between membrane compartments though the cytosol, probably bound to a chaperone. In this model, Ras could be activated at the plasma membrane, and then traffic in a GTP-bound state to another compartment such as

the Golgi. Rocks et al. [184] investigated this palmitoylation/depalmitoylation cycle by applying the palmitoyltransferase inhibitor 2-bromopalmitate and observed a decrease in Ras activation on the Golgi, suggesting that the acylation/deacylation cycle is required for Ras activation on this organelle. In addition, recent work in glutamate-stimulated hippocampal neurons has revealed that GFP-tagged Ras dissociates from the plasma membrane and associates with intracellular membranes (including Golgi) in a calcium/calmodulin-dependent fashion [186].

Golgi membrane regulation of ERK signaling is also mediated through protein:protein interactions. Sef (similar expression to FGF) is a transmembrane protein that was identified as the product of an FGF-induced gene and feedback inhibitor of the ERK/MAPK pathway in zebrafish [187]. The exact mechanism of inhibition is unclear, but seems to involve interference at the level of phosphorylation of FGF receptor substrates and at the level of MEK-mediated ERK/MAPK phosphorylation. A recent study demonstrated that Sef captures activated MEK–ERK/MAPK complexes at the Golgi apparatus [188]. Sef selectively bound to activated MEK and permitted ERK/MAPK activation. However, Sef retained activated ERK/MAPK in the complex, preventing its nuclear translocation and restricting ERK/MAPK signaling to cytosolic substrates. Golgi-associated Ras proteins are activated by a pathway that is different from the canonical one (through Grb2 and the GEF son-of-sevenless (SOS)) that is used by RTKs to activate Ras at the cell membrane [189]. Localization at the Golgi could therefore dedicate the ERK/MAPK module to selectively connecting a distinct set of inputs with specific signaling outputs.

2.5.8. ERK signaling at the ER

In addition to evidence of signaling on the Golgi, recent evidence has been presented for Ras signaling on the ER. When palmitoylation-deficient forms of Ras are expressed in COS-1 cells, they accumulate on the ER and in the cytosol [178]. When these palmitoylation-deficient forms of Ras are expressed along with the GFP-RBD Ras activation reporter mentioned above, GTP-bound H-Ras accumulates on the ER. EGF stimulation activates H-Ras at the ER in less than one minute [183], and this ER-restricted H-Ras selectively engages the ERK pathway resulting in fibroblast transformation. One interpretation for this result is that GEFs can rapidly activate ER-associated Ras. This idea has been supported by Arozarena et al. who showed that endogenous Ras GEFs are highly expressed in neurons and rapidly translocate to the ER to activate H-Ras on this compartment [190]. Ras GEFs, both endogenous and over-expressed, were present in the endoplasmic reticulum but not in the Golgi complex. Utilizing H-Ras constructs specifically tethered to the plasma membrane, endoplasmic reticulum, and Golgi complex, they demonstrated that RasGRF1 and RasGRF2 can activate plasma membrane and reticular, but not Golgi-associated, H-Ras. Further evidence for Ras signaling from the ER comes from the discovery of a Ras inhibitor that is restricted to the ER compartment. Sobering et al. described a protein in *Saccharomyces cerevisiae* designated ER-associated Ras inhibitor (Eri1) that behaved genetically like an inhibitor of Ras, bound preferentially to GTP-bound Ras via its effector domain, and was localized to the ER [191].

2.5.9. Potential roles of compartment-specific ERK signaling

Compartmentalized signaling is a relatively new paradigm in signal transduction. One hypothesis is that greater specificity in Ras/MAPK signaling might be achieved through spatial regulation. In this fashion, compartmentalized signaling could increase the signaling specificity by altering kinetic outputs down a single pathway and/or by allowing for activation of distinct downstream pathways. This increase in complexity may help explain how a single regulatory molecule such as Ras can control such a plethora of cellular responses such as cell proliferation, differentiation, transformation, and apoptosis. To test whether or not compartmentalized signaling mediates specific signaling cascades, Chiu et al. designed experiments in which transmembrane tethers were used to artificially and stringently target Ras proteins to various membrane compartments [183]. When oncogenic Ras was targeted to the ER or Golgi with a transmembrane tether, it retained full transforming activity, indicating that all the signaling events required for the complex cellular phenotype of transformation can be set into motion from internal membranes [183, 192]. This might suggest that Ras signaling from internal membranes is no different than from the plasma membrane. However, quantitative differences in signal output could be detected. In transfected COS-1 cells, Golgi-associated Ras activated ERK and PI3K with potency equal to that of natively targeted Ras, the JNK pathway was poorly activated. Conversely, ER-tethered Ras was a potent activator of JNK but a relatively poor activator of ERK and PI3K. In addition, this compartmentalization altered the signaling kinetics. Using the same COS-1 system, Chiu demonstrated that activated Ras accumulation at the plasma membrane was rapid following EGF stimulation (1-3 minute onset), activation of Ras at the golgi was delayed

(10 minute onset) and sustained [183]. The compartment-associated effects of Ras signaling seem to be cell specific. In antigen receptor stimulated Jurkat T cells, as well as in primary T cells, Ras activation on the golgi is rapid, and no Ras activation is detected at the plasma membrane [138]. Evidence for compartmentalized Ras signaling has also emerged from the study of fission yeast. In *Schizosaccharomyces pombe*, Ras1 controls both the mating pathway via a MAPK cascade and elongated cellular morphology through an exchange factor for Cdc42 [193]. ER-restricted Ras1 can support morphology but not mating and the converse is true for Ras1 restricted to the plasma membrane. ERK/MAPK activation at the ER could provide mechanisms for altering the quality, quantity or kinetics of ERK/MAPK signaling.

3. *In Vitro* identification and characterization of the ERKDD amino acid sequence in R3

3.1 Introduction

PDGF-ββ and FGF-2 stimulate mesangial cell proliferation by transmitting signals from the cell surface to the nucleus to regulate the activity of transcription factors. The binding of growth factors to their tyrosine kinase receptors facilitates the exchange of guanosine diphosphates (GDP) for guanosine triphopsphates (GTP). GTP bound Ras, a small GTP binding protein, then initiates the activation of a linear cascade of protein kinases defined sequentially as mitogen activated protein (MAP) kinase kinase kinase, referred to as MEKK, and MAP kinase kinase (MEK1 and MEK2), which in turn activate MAP kinase (ERK1/2). Activated (phosphorylated) ERK then translocates to the nucleus to exert effects on transcription. Since MAP kinases phosphorylate very similar motifs (consensus sequence Ser/Thr-Pro (S/TP)), and several potential substrates contain this motif, it is important to provide specificity to direct individual kinases towards the correct substrates. Multiple mechanisms exist for generating signaling specificity within these cascades to ensure specific cellular responses, including the association of the cascade components with their activating kinases, inactivating phosphatases, and scaffold proteins that facilitate distinct signaling complexes.

ERK-DDs are sites in which members of the ERK family bind to interacting protein partners. These protein partners can be upstream ERK regulators such as the MAPKKs MEK1 and 2; which activate (phosphorylate) ERK following docking, ERK phosphatases such as PTP-Sl, STEP, and MKPs; which inactivate (dephosphorylate) ERK following docking, ERK chaperones; which translocate ERK to a specific subcellular location

following docking, or ERK scaffolding proteins such as KSR; which bring several ERK signaling molecules together in close proximity [160]. Although docking domains can sometimes be recognized by more than one class of MAPK, they are generally thought to increase signaling specificity by directing the level of MAPK activation, the phosphorylation of their substrates, and in some instances their subcellular localization.

The characterization of receptor activity modifying proteins (RAMPs) has enhanced our understanding of mechanisms involved in the regulation of G protein-coupled receptors (GPCRs). R1, R2, and R3 are distinct gene products and have been characterized as single-transmembrane domain proteins capable of direct interaction with the class B (secretin family) G-protein coupled receptors, calcitonin receptor (CTR) and CR-like receptor (CRLR) [87, 105, 194]. When CRLR is expressed with R1 in HEK293 cells, a CGRP receptor is produced. Even though R2 and R3 share only approximately 30% sequence identity, when CRLR is expressed with R2 or R3 in HEK293 cells virtually identical (pharmacologically and biologically) AM receptors (AM-1R, AM2-R, respectively) are produced [80]. Upon activation, the CRLR-RAMP receptor complex causes cyclic AMP activation in most systems, irrespective of whether the ligand is AM or CGRP. For many years, RAMP interactions were thought to occur only between a few select class B receptors. However, in a recently published RAMP binding study, when co-expressed with RAMPs, 6 out of 10 class B receptors demonstrated select RAMP interaction [105]. VPAC1 receptor (VPAC1R) interacts with all three RAMP isoforms, parathyroid hormone-1 receptor (PTH1R) and glucagon receptor with R2, and parathyroid hormone-2 receptor (PTH2R) with R3. Another study has demonstrated that a class C GPCR, a calcium-sensing receptor (CaSR), interacts with RAMPs [106]. In a

paradigm similar to CRLR, recombinant CaSR expressed in COS7 cells does not translocate to the plasma membrane unless R1 or R3 (but not R2) is also co-expressed. In the same study, R3 was shown to mediate both the glycosylation and trafficking of CaSR from the ER to Golgi. In the absence of R3, CaSR was retained in an intracellular compartment that confocal microscopy identified to be the ER. It is evident that diverse amino acid sequences within the three RAMP isoforms allow them to play a much broader role in GPCR regulation than what was initially proposed.

All three RAMP isoforms harbor short, intracellular C-terminal tails. RAMPs contain a conserved Ser-Lys (S, K; brown) sequence in the intracellular domains. While the Ser-Lys motif does not effect internalization of either R1-CRLR or R2-CRLR, they negatively regulate internalization of R3-CRLR [92]. The R3 cytoplasmic tail also contains a conserved Leu-Leu motif. This motif is known to mediate internalization of the human vasopressin V2 receptor through interactions with proteins involved in endocytosis (clathrin, adaptins and arrestins) [195]. CRLR, R1 and arrestins do exist as a ternary complex in HEK-293 cells, resulting in dynamin- and β-arrestin-dependent internalization following CGPR exposure [196]. No such interaction has been identified thus far for R2 or 3. All three RAMP isoforms also contain putative phosphorylation sites (threonine in R1 and 3; serine in R2), however the potential roles of these residues in GPCR internalization/endocytosis have not been studied. A unique PSD-95/Discs-large/ZO-1 homology domain type-I (PDZ) recognition motif (Asp-The-Leu-Leu) on the extreme C-terminus of R3 mediates protein-protein interactions involved in the regulation and trafficking of the R3-CRLR complex. Recent reports from our laboratory have demonstrated that in HEK293 cells, overexpression of the Na^+/H^+ exchanger regulatory

factor-1 adaptor protein (NHERF) together with CLR and R3 abolished agonist-induced receptor internalization without affecting desensitization[102]. R3 PDZ motif interaction with the *N*-ethylmaleimide-sensitive factor (NSF) also mediates the recycling of CRLR in HEK293 cells [97]. In these experiments, the absence of NSF overexpression resulted in CRLR degradation following agonist stimulation. In RMCs, CRLR is normally recycled following agonist-induced desensitization [197]. R3 knockdown, as well as pharmacological inhibition of NSF abolishes RMC CRLR recycling [97].

The N-terminal sequences of RAMPs share less than 20% of amino acid homology but share in common a significant number of consensus sites for cotranslational modifications including cysteine residues (potentially involved in disulfide bond formation) and N-glycosylation consensus sites (Asn-X-Ser/Thr). The N-terminal sequences have been reported to be important for ligand binding specificity and efficient receptor transport to the membrane The structural domain(s) involved in selective AM binding have been studied using various RAMP chimeras and deletion mutants. Co-expression of chimeric RAMPs and CRLR in HEK293 cells revealed that residues 77-101, situated in the extracellular N-terminal domain of human R2, were crucial for selective AM-evoked cAMP production. In addition, deletion of hR2 residues 86-92 significantly attenuated high-affinity ^{125}I-AM binding and AM-evoked cAMP production despite cell surface expression of CRLR-R2. Deletion of hR3 residues 59-65 had a similar effect. Disulfide bonds are also critical for CRLR-RAMP activation. Four cysteine residues are conserved in all RAMP isoforms, and R1 and 3 harbor two additional conserved cysteine residues. While similar studies have not been completed using R1, mutation of each of the six cysteines results in a significant loss of R3 cell-

surface expression and ligand binding [88]. Several consensus sites for N-glycosylation (Asn-X-Ser/Thr) have also been identified on R2 and R3. Four N-glycosylation sites identified on human, mouse and rat R3 are conserved in the mouse R2, R1 has no consensus sites for N-glycosylation [89]. In a recent study, it was demonstrated that N-glycosylated R2 and R3 are expressed at the cell surface, and their transport to the plasma membrane requires N-glycans. R1 is not N-glycosylated and is transported to the cell surface only upon formation of heterodimers with CRLR [90].

Published reports from our laboratory have demonstrated that RMCs endogenously express both the AM1R (CRLR + R2) and the AM2R (CRLR + R3) [197]. Furthermore, Nowak, et al. demonstrated that R3 is differentially upregulated following PDGFββ treatment in cultured RMCs [124]. The emphasis of this paper was to investigate the mechanisms of R3 upregulation and the subsequent increases in AM-mediated (antiproliferative) RMC responses. The possibility that R3 may play a role in addition to (or instead of) its known contribution in CRLR activation was not addressed. RAMP isoforms vary greatly in their amino acid sequences. Given the recent characterizations of novel, R3 protein:protein interactions, it seems plausible that R3 may independently mediate some aspect of growth. The major aim of this study was to identify and characterize amino acid regions within R3's sequence that could potentially mediate PDGFββ mediated growth responses in RMC.

3.2 Materials and Methods

3.2.1. Materials

pGEX5X-2 vector was purchased from Amersham (Piscataway, NJ). Activated ERK2 and MEK1 were obtained from Sigma Aldrich (St.Louis, MO) and inactive ERK2

from Calbiochem (San Diego, CA). R2, R3, and ERK2 antibodies were from Santa Cruz (Santa Cruz, CA). Anti-MEK1/2 antibody was from Cell Signaling (Beverly, MA). BL competent cells were from Stratagene (La Jolla, CA). All other reagents were of the highest quality available.

3.2.2. *Scansite* analysis of putative human R3 protein interaction amino acid sequences

The human R3 (NP_005847) and human R2 (NP_005845) amino acid sequences were entered into the database *Scansite* (Massachusetts Institute of Technology) to search for putative protein interaction sequences [198]. This database compares the amino acid sequences of more than 35,000 proteins. Images in this thesis/dissertation are presented in color.

3.2.3. GST Protein Overlays

Full-length human R2 and R3 cDNA were sub cloned into a pGEX5X-2 vector and induced as described previously [97, 102]. 10uG of R2 and R3 GST fusion proteins were resolved on a 10%SDS-polyacrylamide gel and transferred to a PVDF membrane. Filters were blocked with 5% w/v fat-free milk powder in Tris-buffered saline with Tween 20 (TTBS: 20 mM Tris, pH 7.4, 500 mM NaCl, 0.1% v/v Tween 20) for 1 hour at room temperature then incubated overnight at 4 degrees in a solution containing either 25nM purified active or inactive ERK. The following day the blots were washed three times with TTBS, probed with antibodies to ERK-2 (1:500), washed three times with TTBS, and incubated with a horseradish peroxidase-conjugated secondary antibody to detect ERK interaction. Protein bands were visualized by soaking the blots in Supersignal West Pico chemiluminescent substrate (Pierce), and exposing to x-ray film.

The blots were then stripped using a solution of .5% sodium dodecyl sulfate and .1X sodium chloride/sodium citrate (SSC) heated to 95 degrees Celsius and then re-probed as described above with antibodies to either R2 or R3 (1:300) to confirm their presence on the membrane. To test GSTR3:MEK interaction, 10uG GSTR3 and 5uG activated ERK protein (positive control) were resolved on gels and probed with a solution containing purified His-tagged MEK1 protein. HRP-anti MEK1/2 antibody was used to detect MEK interaction. Blots were then stripped as described above, and re-probed with R3 and ERK-2 antibodies to confirm R3 and ERK presence on the blots.

3.3.Results

3.3.1. *In Vitro* identification and characterization of ERKDD amino acid sequences in human R3

The *Scansite* database search revealed that the amino acid sequence of R3 contains a putative ERKDD motif at amino acids 6 through 18. In fact, the search indicated a 100% match between R3 and the established ERK docking domains of MEK. The consensus sequence of this domain consists of the basic amino acids arginine or lysine, followed immediately by the helix breaking amino acid proline, followed two to six amino acids later by the hydrophobic amino acids leucine or isoleucine [160, 164]. The N-terminal amino acid sequence of R2 harbors some similarity to an ERK D-Domain, however, some critical residues were not present. (Figure 3).

3.3.2. GST Overlays to identify R3:ERK and R3:MEK interaction

GST overlay experiments demonstrated that R2 protein does not interact with neither inactive nor active forms of ERK-2 protein. GSTR3, however, showed a robust

interaction with both inactive and active forms of the purified ERK-2 protein. No detectable bands were observed when GST-R3 blots were incubated with purified, activated MEK1 protein and probed with anti-MEK1/2 antibody. (Figure 4A and B)

Docking Domain Sequences of human MAPKK (MEK)

Human MEK1 ^{3}KKK<u>P</u>TPIQLNPAPDGS^{18}

Human MEK2 ^{4}RRK<u>P</u>VLPALTINPTIAEG^{21}

Human R3 ^{5}LRR<u>P</u>QLLPLLLLLCGGCP^{24}

Human R2 ^{19}VGR<u>P</u>AALRLLLL^{31}

Consensus: -(R/K)$_2$-(<u>P</u>)-(X)$_{2-6}$-(L/I-X-L/I)-

Figure 3. *Scansite* analysis of putative human R3 protein interaction amino acid sequences. Human R3 (NP_005847) and R2 (NP_005845) amino acid sequences were entered into the database *Scansite* (Massachusetts Institute of Technology) to search for putative protein interaction sequences [198]. This database compares the amino acid sequences of more than 35,000 proteins. The search revealed that the amino acid sequence of R3 contains a putative ERKDD motif similar to that of human MEK1 and 2.

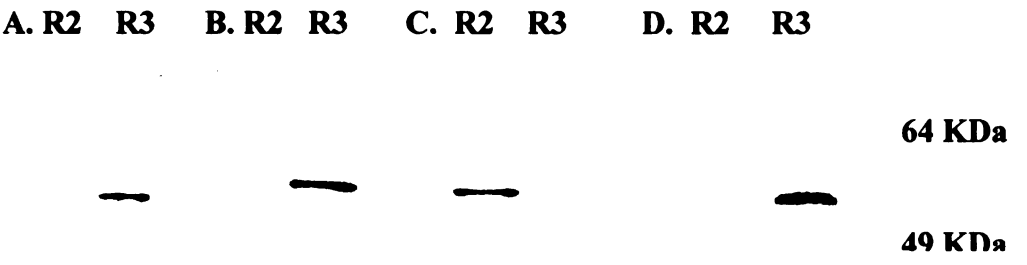

Figure 4A. GST protein overlays illustrating R3 interaction with ERK. 10uG of human R2 and R3 GST fusion proteins were resolved on a 10%SDS-polyacrylamide gel and transferred to a PVDF membrane. Filters were incubated with solutions containing either 25nM purified active or inactive human ERK. The following day the blots were probed with antibodies to ERK-2 (A. and B.) then HRP-secondary antibody to detect ERK interaction. Protein bands were visualized by soaking the blots in Supersignal West Pico chemiluminescent substrate (Pierce), and exposing to x-ray film. The blots incubated with active ERK were then stripped and then re-probed as described above with antibodies to either R2 (C) or R3 (D) to confirm RAMP presence on the membrane. n=3.

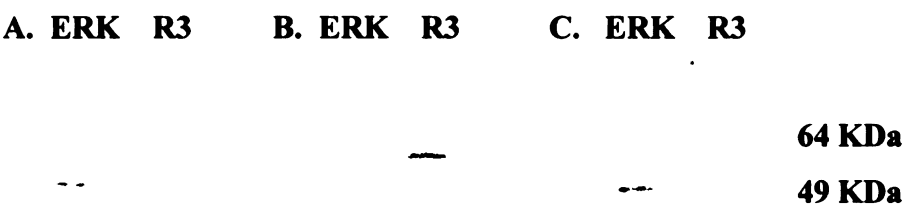

Active MEK1 **R3** **ERK-2**

Figure 4B. GST protein overlays illustrating R3 interaction with activated human MEK1. 10uG human R3 GST fusion protein and 5ug purified active ERK protein were resolved on a 10%SDS-polyacrylamide gel and transferred to a PVDF membrane. Filters were incubated with a solution containing 50 units activated MEK1 protein. The following day the blots were probed with antibodies to MEK1/2 (A) then HRP-secondary antibody to detect MEK1 interaction. Protein bands were visualized by soaking the blots in Supersignal West Pico chemiluminescent substrate (Pierce), and exposing to x-ray film. The blots incubated with active MEK1 were then stripped and then re-probed as described above with antibodies to either R3 (C) or ERK (D) to confirm their presence on the membrane. n=3.

3.4. Discussion

Although RAMPs share only ~30% sequence identity, the hydrophobicity plots of the three RAMPs suggesting the typical structure of class I transmembrane proteins. R2 is the least conserved, being 26 amino acids longer than R1 and R3 [87] The N-terminal extracellular domain of R3 is composed of amino acids 1-119. As expected, a significant number of consensus sites for co-translational modifications including cysteine residues (potentially involved in disulfide bond formation) and N-glycosylation consensus sites (Asn-X-Ser/Thr) are located within this region. These sites are known to mediate membrane expression and ligand-binding activity of the CRLR:R3 complex. In addition to these established motifs, a *Scansite* database search of putative protein interaction domains within the R3 N-terminal (aa1-119) sequence revealed several interaction domains within this region of R3 that could potentially be involved in growth signaling. Using high-stringency parameters, *Scansite* predicted putative interaction motifs for human SH2 and SH3 proteins, as well as an ERK D-Domain, similar to that of human MEK1/2 within the extreme N-terminus of R3. Using the same parameters, no such motifs were identified for R2. In addition, R3, but not R2, protein was capable of human ERK2 interaction. R3 did not demonstrate interaction with purified activated human MEK protein. From the preliminary results obtained thus far, we derived the following "working hypothesis":

R3 is a critical regulator of PDGF-ββ -stimulated *RMC proliferation through direct interaction with the MAPK cascade within specific subcellular compartments.* (Figure 6).

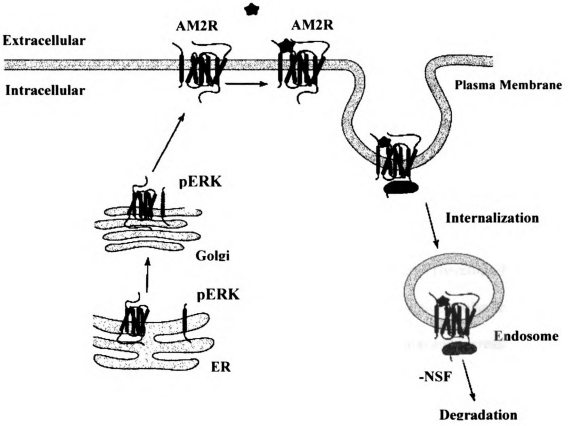

Adapted from: **TIBS 31**(11): 631-38 ref [104]

Figure 5. Potential Subcellular locations for R3:ERK interaction. Potential R3:ERK membrane interaction sites include the ER, golgi, caveolae, and endosomes.

4. The role of R3 in ERK phosphorylation and cellular proliferation following growth factor stimulation

4.1. Introduction

The primary locus of renal dysfunction is the glomerulus, and the mesangial cell (MC) appears to be a central site of the microscopically observable renal damage. By regulating the amount and composition of the surrounding extracellular matrix (ECM), mesangial cells provide the essential structural support for the glomerular capillary tuft. . The turnover rate of mesangial cells in the normal adult human kidney is low; the renewal rate is less than 1% [6]. Under normal conditions, quiescent mesangial cells either face few mitogenic signals, or are unable to respond to them. Therefore, MC proliferation is a general characteristic of a variety of progressive glomerular diseases. Loss of coordinated regulation, associated with altered composition and increased mesangial ECM deposition, often leads to progressive glomerulosclerosis, loss of filtration function, and end-stage renal disease [5]. It follows, therefore, that an understanding of the regulatory mechanisms for MC proliferation is important for our understanding of glomerular disease and its eventual treatment.

Platelet-derived growth factor beta (PDGFββ). is a potent *in vitro* and *in vivo* mesangial cell mitogen [14, 45, 46], and is involved in the regulation of mesangial cell matrix synthesis [47]. The normal adult kidney expresses only low amounts of PDGF protein and receptors, primarily by mesangial cells [44, 48]. In renal disease states, infiltrating inflammatory cells (monocytes/macrophages) and platelets are a major source of PDGF [49]. Exposure of mesangial cells *in vitro* to growth factors, such as epidermal growth factor (EGF), growth hormone (GH), transforming growth factor type α (TGF-a),

basic fibroblast growth factor (FGF-2), and tumor necrosis factor type α (TNF-α) induce expression of PDGF mRNAs. EGF, TNF-α , and FGF-2 also stimulate MCs to secrete PDGF [50] Inflammatory agents such as interleuken-1β (IL-1β) and IL-6, as well as vasoactive mediators such as vasopressin, endothelin-1 (ET-1), and angiotensin-II (AngII) [51]. Expression of PDGFββ and its receptor are also significantly increased in mesangial cells of animal models of glomerulonephritis [52, 53] and in human glomerulonephritis in which mesangial proliferation occurs [52, 54, 55]. The importance of PDGFββ in glomerulonephritis was first demonstrated experimentally by the administration of anti-PDGFββ antibodies in the anti-Thy1.1 model. Anti- PDGFββ antibody treatment did not affect the initial mesangiolysis that occurs, but did result in a 50% reduction in mesangial cell proliferation and a corresponding reduction in ECM accumulation [53, 56]. More recent studies using the non-specific PDGFββ inhibitors trapidil [57], dipyridimole [58], and TNP-470 [59] as well as the selective PDGFββ inhibitor STI 571 [60], have confirmed the importance of PDGFββ in both animal models and human glomerulonephritis.

Basic fibroblast growth factor (FGF-2) is expressed by a variety of cells, including endothelial cells, smooth muscle cells, macrophages, fibroblasts, and mesangial cells [74]. In addition to FGF-2 receptors, heparan sulfate proteoglycans, especially syndecan, are essential for the binding of FGF-2 to its cellular receptor [75, 76]. Since mesangial cells express FGF-2 and its receptor components, its not surprising that FGF-2 is a potent mitogen for mesangial cells [74]. However, FGF-2 lacks a signal peptide for secretion and is not normally released into the circulation [77]. FGF-2 is released from adult mesangial cells only following an injury and may lead to further mesangial cell

injury by stimulating nitric oxide production [78]. This feed-forward progression of FGF-2-induced mesangiolysis is an important feature of the early phase of anti-Thy1.1 nephritis. After the initial mesangiolysis, the marked proliferation of mesangial cells that occurs in the anti-Thy1.1 model is associated with an increased glomerular synthesis of FGF-2 [74]. Further evidence of the importance of FGF-2 in this model are the observations that injection of FGF-2 following anti-Thy1.1 antibody administration resulted in increased mesangiolysis [74], while treatment with anti-FGF-2 blocked the initial mesangiolysis, resulting in less mesangial proliferation and less ECM deposition [79].

RAMP mRNA distribution has been analyzed in several species including mouse, rat, and human. In fact, Ramps are expressed in some cell lines that do not express CRLR receptors [87]. R3 is the most widely distributed RAMP isoform; its expression is greatest in the kidney, heart, brain, and lung [86, 87, 107-110] Using both animal and cell culture models, several reports have indicated that growth associated conditions can result in alterations of R3 gene expression. However the mechanisms of R3 involvement in proliferation have not been thoroughly investigated. R3, but not R2, is upregulated in mesangial cells following PDGF-ββ treatment [124]. The growth-stimulating parathyroid hormone also increases R3 expression in primary mouse osteoblasts [125]. R3 is expressed in the rapidly growing thymus of newborn rats, but not in quiescent thymus of adult animals [126]. R3 is expressed in the prostate cancer cell line, DU145 [123]; in prostate carcinoma biopsies the levels of R3 were significantly elevated (compared to prostate hyperplasia biopsies) while expression levels of R2 were unchanged in these samples [123]. R3 is also exclusively upregulated in cultured rat

neonatal cardiac fibroblasts with IL-1β [128], and in a rat model volume overload-induced cardiac hypertrophy R3 was significantly increased, while other AM signaling components were only modestly or not increased at all [128, 129]. Angiotensin II induces hypertrophy of cultured rat neonatal cardiomyocytes. mRNA levels of R1 and R3 are significantly elevated following 24-h treatment with Ang II (without a change of those of R2 and CRLR), and the effects of Ang II on R1 and R3 expression were abolished by an Ang II type 1 (AT1) receptor antagonist [130]. It is plausible from the reports described above that R3 plays a role in growth-mediated events. The purpose of this study is to identify the role of R3 in ERK phosphorylation and cell proliferation in RMCs following PDGF-ββand FGF-2 stimulation

4.2. Materials and Methods

4.2.1. Materials

Rat mesangial cells (RMC) and Normal rat kidney interstitial fibroblasts (NRK-49F) were obtained from ATCC. RPMI1640, DMEM, penicillin/streptomycin, fetal bovine serum, non-essential amino acids, BLOCK-iT Dicer RNA interference kit, and Lipofectamine 2000 were purchased from Invitrogen (Carlsbad, CA). PDGF-ββ was obtained from Sigma Aldrich (St.Louis,MO) and FGF-2 from Oncogene (Cambridge, MA). MTS assay kits were from Promega (Madison, WI). The MEK inhibitors, PD98059 and U0126, were obtained from Calbiochem (San Diego, CA).
Gene-specific RNA oligonucleotides were purchased from Dharmacon (Lafayette, CO) and were transfected into RMC using Mirus TKO transfection reagent (Madison, WI). Antibodies were from Santa Cruz Biotechnology (Santa Cruz, CA) and chemiluminescence reagents from Pierce (Rockford, IL). PfuTurbo DNA polymerase,

pCMVTag2 vector, and BL-21, DH5α competent cells were from Stratagene (La Jolla, CA) and Fugene 6 transfection reagent was obtained from Roche (Nutley, NJ). ^{3}H methylthymidine was purchased from Perkin Elmer (Waltham, MA). All other reagents were of the highest quality available.

4.2.2. Cell Culture

NRK were maintained in Dulbecco's modified Eagle's medium supplemented with 4 mM L-glutamine, 1.5 g/L sodium bicarbonate and 4.5 g/L glucose, 5% bovine calf serum, 5% Non-Essential Amino Acids, and 1% Penicillin/Strepomycin. RMC were maintained in RMPI 1640 media containing 15% FBS and 1% penicillin-streptomycin.

4.2.3. MTS assay for RMC proliferation following PDGF-ββ treatment

RMC were plated at a concentration of 2000 cells/well in a 96-well tissue culture plate. The following day, the cells were serum-starved overnight, then treated for 16 hours with 0, 1, 5, 10, 50, and 100ng/mL PDGFββ. An MTS assay was used to measure the RMC proliferative response.

4.2.4. MTS assay for RMC proliferation following MEK inhibition

RMC were serum-starved overnight, pre-treated with MEK inhibitor, either 10uM PD98059 or 1uM U0126 for fifteen minutes prior to 50mg/mLPDGFββ treatment. 16 hours later, proliferation of the cells was measured by MTS assay following manufacturer's directions.

4.2.5. MTS assay for RMC proliferation following gene-specific knockdown

Gene-specific knockdown was performed two ways. In the initial RMC knockdown experiments, gene-specific d-siRNA for lacZ (control), R2, and R3 were generated and purified using the BLOCK-iT Dicer RNA interference kit (Invitrogen).

RMC's were transfected with d-siRNAs using Lipofectamine 2000 as per the manufacturer's instructions (Invitrogen). 24 hours following transfection, cells were plated on 96-well plates at a concentration of 200 cells/well. The following day the cells were serum-starved overnight and treated with 50ng/mL PDGFββ. 16 hours later, proliferation of the cells was measured by MTS assay as per manufacturer's instructions. To confirm the BLOCK-iT Dicer RNA interference results, gene-specific d-siRNA for mismatched RNA (NS) and R3 (Dharmacon) was transfected into RMC's using Mirus TKO transfection reagent as per manufacturer's instructions and proliferation was measured by MTS assay.

4.2.6. Confocal Microscopy

5 days after gene-specific knockdown using d-siRNAs for lacZ (control), R2, and R3 (Invitrogen), or mismatched (NS) and R3 (Dharmacon), RMC were plated on coverslips. Cells were fixed with 4% paraformaldehyde then permeablized with 0.1% v/v Triton X-100 in PBS. Coverslips were blocked overnight in 0.1% v/v Triton X-100 in PBS + 10% goat serum. Samples were incubated in primary antibody in blocking buffer for 2h at room temperature (R2 or R3 at 1:200). Appropriate secondary antibodies were applied for 1h at room temperature (Goat anti-rabbit Cy5 at 1:400). Coverslips were mounted in Shandon mounting medium. Cells were visualized on a Zeiss 210 laser confocal microscope. Images presented are representative single optical sections and are representative of at least 20 fields imaged from at least three experiments.

4.2.7. Membrane-associated ERK phosphorylation following PDGF-ββ treatment and R3 knockdown in RMC

A PDGFββ-induced ERK phosphorylation time course was established by serum starving RMC overnight, then treating the cells with 50ng/mL PDGFββ for 0 (control),5, 10, 15, 30, and 60 minutes. The media was removed and the plates were snap-frozen to preserve the phosphorylation status of the cells. The cells were then scraped from the plates in homogenization buffer (10mMHepes, 0.15MnaCl, 1mM EDTA, 1mM PMSF, 0.2mM sodium orthovanadate, 100nM NaF, 5ug/mL leupeptin, and 10ug/mL aprotinin). This lysate was dounce-homogenized for 20 strokes. The homogenates were centrifuged at 1300xg for 20 minutes at 4°C to pellet nuclear and cell debris. The supernatant was centrifuged at 100,000xg at 4°C for 1 hour to isolate the membrane (pellet) fraction. Protein concentration was determined by the Bradford assay. For each time point, 40ug membrane fraction protein was separated on a 10% SDS-polyacrylamide gel. Western blotting was performed with anti-pERK antibody at 1: 500 to assess ERK phosphorylation status. Bands were visualized using chemiluminescence (Pierce Supersignal West Pico) on XO-Mat film. Blots were stripped by immersion in a 95°C solution of.5% SDS/.1XSSC and then re-probed for ERK-2 at 1:500. The PDGFββ-induced ERK phosphorylation time course described above was repeated in RMC following gene-specific R3 knockdown using Dharmacon si-RNA as described above.

4.2.8. Membrane-associated ERK phosphorylation following FGF-2 treatment in NRK

An FGF mediated, membrane-associated ERK phosphorylation time course was established in NRK by serum-starving NRK overnight, then treating the cells with 5ng/mL FGF-2 for 0, 5, 10, 15, 30, and 60 minutes. The media was removed and the plates were snap-frozen to preserve the phosphorylation status of the cells. The cells were then scraped from the plates in homogenization buffer (10mMHepes, 0.15MnaCl,

1mM EDTA, 1mM PMSF, 0.2mM sodium orthovanadate, 100nM NaF, 5ug/mL leupeptin, and 10ug/mL aprotinin). This lysate was dounce-homogenized for 20 strokes. The homogenates were centrifuged at 1300xg for 20 minutes at 4°C to pellet nuclear and cell debris. The supernatant was centrifuged at 100,000xg at 4°C for 1 hour to isolate the membrane fraction. NRK cells were transfected with 5ug of pCMVTag2-R3 DNA per 100mm tissue culture dish using Fugene 6 transfection reagent (Roche) following manufacturer's instructions. Control samples were transfected with pCMV vector. 24 hours following transfection, cells were plated on 150mm tissue culture dishes, then serum-starved overnight and the ERK phosphorylation time courses were repeated with FGF-2. Protein concentration was determined by the Bradford assay. For each time point, 40ug membrane fraction protein was separated on a 10% SDS-polyacrylamide gel. Western blotting was performed with anti-pERK antibody (Santa Cruz) to assess ERK phosphorylation status. Bands were visualized using chemiluminescence (Pierce Supersignal West Pico) on XO-Mat film. Blots were stripped by immersion in a 95°C solution of.5% SDS/.1XSSC and then re-probed for ERK-2 (Santa Cruz).

4.2.9. R3 Cloning and Mutagenesis Procedure

Full-length cDNA of human R3 was cloned into a pCMV-Tag2 (Flag epitope tag at N-terminus) vector using the restriction cut sites EcoR1/Xho1 as described previously. Site-directed mutagenesis was performed using a pair of complementary oligonucleotides (Michigan State University Macromolecular Structure Facility) containing the appropriate point mutations in the sequence of the R3 ERK DD (Figure 6). The PCR for the mutation was introduced in a pCMV-Tag2 as follows: 94 °C for 2 min; 25 cycles of 94 °C for 30 s, 50 °C for 30 s, 68 °C for 4 min; final cycle of 68 °C for 7 min using PfuTurbo DNA

polymerase, then Dpn1 digested for 2 hours. The mutated DNA sequences were confirmed by automated sequencing (Michigan State University Genomic Technology Support Facility). NRK cells were transfected with 3ug of pCMVTag2-R3, R3EE, or R3EEG DNA using Fugene 6 transfection reagent following manufacturer's instructions Mutations were confirmed by automated sequencing (Michigan State University Genomic Technology Support Facility).

4.2.10. ^{3}H Thymidine Incorporation Assay for proliferation of NRKs

A dose-response curve for NRK proliferation following FGF-2 treatment was established using ^{3}H methylthymidine incorporation . Briefly, cells were plated at a concentration of 3000 cells/well on a 24-well plate. The following day the cells were serum starved overnight, then treated for 16 hours with 0,1,5, and 10ng/mL FGF-2. 0.5υCi ^{3}H methylthymidine was added to each well. Four hours later, cells were washed with PBS, and 10% TCA was added to the wells to stop the incorporation. The TCA was aspirated; the cells were lysed with0.2N NaOH. ^{3}H methylthymidine incorporation was assessed by counting the samples on a β–counter. To measure the effect of MEK inhibition on FGF-2-mediated NRK proliferation, cells were pre-treated with1uM U0126 for fifteen minutes prior to 5mg/mL FGF-2 treatment and subsequent 3H methylthymidine incorporation. For proliferation assessment following R3 introduction, R3 was sub-cloned into the pCMV-Tag2 expression vector and 5 micrograms per 100mm dish were transfected into the NRKs using Fugene 6 following the manufacturer's protocol. 24 hours after transfection, cells were plated at a concentration of 3000 cells/well on a 24-well plate. The following day the cells were serum starved overnight,

and proliferation following 5ng/mL FGF-2 was assessed using ^{3}H methylthymidine incorporation.

4.2.11. GST Overlay with R3 Mutations

Site-directed mutagenesis was performed using a pair of complementary oligonucleotides (Michigan State University Macromolecular Structure Facility) containing the appropriate point mutations in the sequence of the R3 ERK DD. (Figure 7) The mutation was introduced into a pGEX5X-2 vector using PCR as follows: 94 °C for 2 min; 25 cycles of 94 °C for 30 s, 50 °C for 30 s, 68 °C for 4 min; final cycle of 68 °C for 7 min using PfuTurbo DNA polymerase (Stratagene), then Dpn1 digested for 2 hours. The mutated DNA sequences were confirmed by automated sequencing (Michigan State University Genomic Technology Support Facility). 10uG of R3, R3Q, R3EE, and R3EEG GST fusion proteins were resolved on a 10%SDS-polyacrylamide gel and transferred to a PVDF membrane. Filters were blocked with 5% w/v fat-free milk powder in Tris-buffered saline with Tween 20 (TTBS: 20 mM Tris, pH 7.4, 500 mM NaCl, 0.1% v/v Tween 20) for 1 hour at room temperature then incubated overnight at 4 degrees in a solution containing either 25nM purified inactive or active ERK (Sigma and Calbiochem). The following day the blots were washed three times with TTBS, probed with antibodies to ERK-2 (1:500 Santa Cruz), washed three times with TTBS, and incubated with a horseradish peroxidase-conjugated secondary antibody to detect R3:ERK interaction. Protein bands were visualized by soaking the blots in Supersignal West Pico chemiluminescent substrate (Pierce), and exposing to x-ray film.

4.2.12. Statistics

Data are presented as mean ± S.E.M. Multiple group comparisons were made using analysis of variance (ANOVA), followed by Bonferoni's multiple comparison between treatments. Two treatment comparisons were compared using Student's t-test method. Statistical significance was set at $P<0.05$.

4.3. Results

4.3.1. MTS assay for RMC proliferation following MEK inhibition

First, a PDGF-ββ stimulated dose-response curve was established in RMC to determine the PDGF-ββ concentration to be used for future experiments (Figure 7). A dose of 50ng/mL PDGF-ββ was chosen. The MEK inhibitor, U0126, significantly decreased PDGF-ββ- proliferation of RMC (25%±4.7 vs. 3.2%± .7) (Figure8).

4.3.2. ^{3}H Thymidine Incorporation Assay for proliferation of NRKs following MEK inhibition

An FGF-2 stimulated dose-response curve was established in NRK to determine the FGF-2 concentration to be used for future experiments (Figure 9). A dose of 5ng/mL FGF-2 was chosen. The MEK inhibitor, U0126, significantly decreased and FGF-2-induced proliferation of NRK (4.80fold±0.7 vs. 1.2fold±0.3) (Figure10).

4.3.3. MTS assay for proliferation following gene-specific knockdown

Confocal microscopy was utilized to assess expression levels of RAMPs in RMC 5 days after gene-specific knockdown using BLOCK-iT Dicer RNA interference (Figure11). Dicer RNA R3 knockdown in RMC resulted in a significant decrease in PDGF-ββ -stimulated proliferation compared to non-specific (Lac-Z) knockdown (Figure12). Confocal microscopy also illustrated R3 knockdown in RMC following treatment with gene-specific d-siRNA (Figure13). Using the Dharmacon si-RNA

technique, R3 knockdown significantly decreased PDGF-ββ -stimulated proliferation (33.9%±6.6vs.3.1%±2.8) (Figure14).

4.3.4. Membrane-associated ERK phosphorylation following PDGF-ββ treatment and R3 knockdown

A membrane-associated ERK1/2 phosphorylation time course was established in RMC by serum-starving them overnight, then treating the cells with 50ng/mL PDGF-ββ for 0 (basal), 5, 10, 15, 30 and 60 minutes. Phosphorylated ERK was normalized to ERK protein levels to determine maximal ERK activation. Following PDFGF-ββ stimulation, ERK activation peaked at 10 minutes and returned to basal levels by 30 minutes. R3 knockdown, using gene-specific RNA interference technology, resulted in significantly decreased maximal ERK activation at the 10 (91%±5 vs. 50.7%±6.9) and 15-minute time points (56%±12.7 vs. 16.3%±1.3) (Figures 15 and 16).

4.3.5. Proliferative effects of R3 introduction into NRK cells

^{3}H thymidine incorporation assays demonstrated that introduction of R3 into NRK cells resulted in a significant increase of both basal (584cpm±43 vs.1483cpm±110) and 5ng/mL FGF-2 stimulated (2403cpm±202 vs. 5461cpm±437) proliferation (Figure 17).

4.3.6. Effect of R3 on membrane-associated ERK phosphorylation in NRKs following FGF-2 treatment

A membrane-associated ERK1/2 phosphorylation time course was established in NRK by serum-starving them overnight, then treating the cells with 5ng/mL FGF-2 for 0 (basal), 5, 10, 15, 30 and 60 minutes. Phosphorylated ERK was normalized to ERK protein levels to determine maximal ERK activation. Following FGF-2 stimulation, ERK activation peaked at 5 minutes and returned to basal levels by 10 minutes. R3

introduction resulted in significantly increased membrane-associated ERK activation at the 10-minute time point compared to control (pCMV) (90.1%maximal.response±0.5 vs. 45.2%±.08) (Figure 18).

4.3.7. Expression of R3 and R3 D-Domain mutants

Mutating the putative D-Domain of R3: R_6R_7 to E_6E_7 (ΔEE), $R_6R_7P_8$ to $E_6E_7G_8$(ΔEEG), and L_{11} to Q_{11}(ΔQ) did not effect the membrane fraction expression of R3 (Figure 19).

4.3.8. Effect of R3 ERKD-Domain mutation on membrane-associated ERK phosphorylation in NRKs following FGF-2 treatment

R3 significantly increased membrane-associated ERK activation levels at 5 (2.72±.3 fold) and 10 minutes (2.8±..24 fold) following FGF-2 stimulation, compared to respective basal (0 time point) levels of ERK activation. R3Q also significantly increased membrane-associated ERK activation at these time points (3.4±.62 and 3.5±.66 fold, respectively) (Figure 20).

4.3.9. The role of R3 ERK-DD in FGF-2-stimulated proliferation of NRK

Proliferation of NRKs following transfection of R3, R3ΔEE, R3ΔEEG, RΔQ, and subsequent FGF-2 treatment was assessed using ^{3}H Thymidine incorporation. R3 introduction in NRK resulted in a significantly increased proliferative responses compared to control (pCMV) levels (3.98fold±1.2 vs. 2.0±.62). Introducing R3-ΔEE and R3-ΔEEG mutations in NRK resulted in a significantly decreased the FGF-2 proliferative response compared to R3 (2.5fold ±.7 and 1.6fold±.8 vs. 3.98fold±1.2) The proliferation response of R3ΔEEG mutation introduction was also significantly different

from R3ΔQ (1.6fold±.8 vs. 3.31.6fold±.81.2). The proliferative responses following R3-ΔEE, R3ΔEEG, and R3ΔQ introduction and FGF-2 stimulation were not significantly different from control (pCMV) levels (Figure 21).

4.3.10. R3 Mutation:ERK interactions using GST Overlay

All of the GST-R3 ERK docking domain mutant proteins are capable of *in vitro* ERK-interaction. However, using overlay experiments, R3ΔEE and R3ΔEEG mutants demonstrated less ERK-2 binding than wild type R3 and the R3ΔQ mutant (Figure 22).

Putative ERK D-Domain Sequence:

^{5}LRR<u>P</u>QLLPLLLLLCGGCP^{24}

Primer Sequences Used to Generate ERKD-Domain Mutations:

ΔR_7 to E:
$^{5'}$GAG ACT GGA GCG CTG GAG CGC CCG CAA CTT$^{3'}$
$^{5'}$AAG TTG CGG GCG CTC CAG CGC TCC AGT CTC$^{3'}$

ΔR_7R_8 to EE:
$^{5'}$GAG ACT GGA GCG CTG GAG GAG CCG CAA CTT CTC$^{3'}$
$^{5'}$GAG AAG TTG CGG CTC CTC CAG CGC TCC AGT CTC$^{3'}$

ΔR_7R_8<u>P$_9$</u> to EEG:
$^{5'}$GAG ACT GGA GCG CTG GAG GAG GGG CAA CTT$^{3'}$
$^{5'}$AAG TTG CCC CTC CTC CAG CGC TCC AGT CTC$^{3'}$

ΔL_{12} to Q:
$^{5'}$GGA GCG CTG CGG CGC CCG CAA CAG CTC CCG TTG CTG$^{3'}$
$^{5'}$CAG CAA CGG GAG CTG TTG CGG GCG CCG CAG CGC TCC$^{3'}$

Figure 6. Sequences of oligonucleotide primers used to generate ERKDD mutations in human R3.

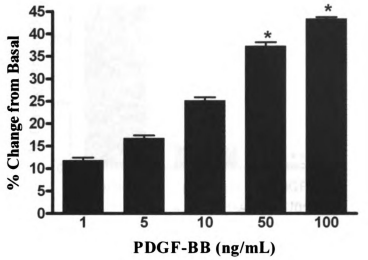

Figure 7. PDGFββ-Induced Proliferation of RMC Cells using MTS Assay. RMC were plated at a concentration of 2000 cells/well on 96-well plates and serum-starved overnight, and then treated with 1, 5, 10, 50, or 100mg/mL PDGFββ for 16 hours. Proliferation of the cells was measured by MTS assay (Promega) following manufacturer's directions. * $p \leq 0.05$; n=3.

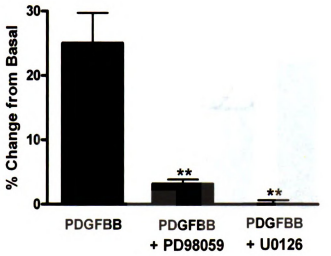

Figure 8. ERK Inhibition of PDGFββ-Induced Proliferation of RMC Cells using MTS Assay. RMC were plated at a concentration of 2000 cells/well on 96-well plates and serum-starved overnight, pre-treated with either 10uM PD98059 or 1uM U0126 (Calbiochem) for fifteen minutes prior to 50mg/mL PDGFββ treatment. Proliferation of the cells was measured by MTS assay (Promega) following manufacturer's directions.

** $p \leq 0.001$ (U0126 and PD98059 vs. PDGF); n=3.

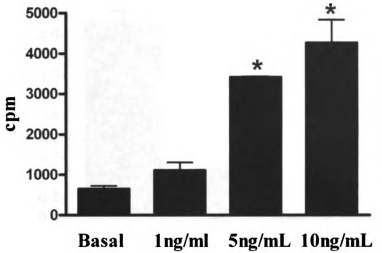

Figure 9. Dose-response curve for NRK proliferation following FGF-2 treatment. NRK were plated at a concentration of 3000 cells/well on a 24-well plate. The following day the cells were serum starved overnight then treated with FGF-2 for 16 hours. NRK proliferation was assessed using ^{3}H methylthymidine incorporation. $^{*}p \leq 0.05$ (5, 10 ng/mL FGF-2 vs. Basal); n=4.

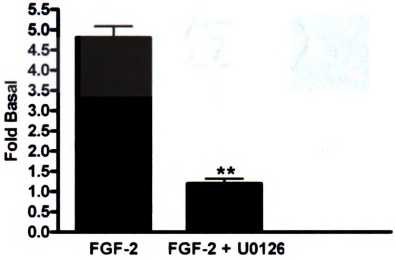

Figure 10. ERK Inhibition of FGF-2-Induced Proliferation of NRK Cells using ^{3}H methylthymidine incorporation as described above.**$p \leq 0.001$ (U0126 vs. FGF-2); n=3.

R3 Control **LacZ (NS) Knockdown** **R3 Knockdown** **R2 Control** **R2 Knockdown**

Figure 11. Confocal Microscopy depicting expression levels of RAMPs. 5 days after gene-specific knockdown using d-siRNAs for lacZ, R2, and R3 (Invitrogen). RMC were cultured on coverslips, fixed, and then permeablized with 0.1% v/v Triton X-100 in PBS. Coverslips were blocked overnight in 0.1% v/v Triton X-100 in PBS + 10% goat serum. Samples were incubated in primary antibody in blocking buffer for 2h at room temperature (R2 or R3 at 1:200). Appropriate secondary antibodies were applied for 1h at room temperature (Goat anti-rabbit Cy5 at 1:400). Coverslips were mounted in Shandon mounting medium. Cells were visualized on a Zeiss 210 laser confocal microscope. Images presented are representative single optical sections and are representative of at least 20 fields imaged from at least three experiments.

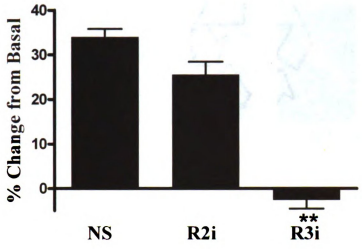

Figure 12. MTS Assay for RMC Proliferation following gene-specific knockdown. Gene-specific d-siRNA for lacZ (NS), R2, and R3 were generated and purified using the BLOCK-iT Dicer RNA interference kit. RMC's were transfected with d-siRNAs using Lipofectamine 2000 as per the manufacturer's instructions (Invitrogen). 48 h after transfection, cells were serum-starved overnight and treated with 50ng/mL PDGFββ. 24 hours later, proliferation of the cells was measured by MTS assay. R3 knockdown significantly inhibited PDGFββ-induced proliferation. **$p \leq 0.001$ (vs. control and R2 knockdown); n=5.

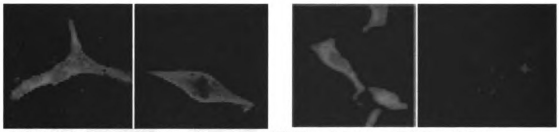

Figure 13. Confocal Microscopy depicting Gene-Specific R3 knockdown using Dharmacon d-siRNA for mismatched RNA (NS) and R3. R3 knockdown was performed as described in Methods section. Confocal microscopy was performed as in figure 12. Cells were visualized on a Zeiss 210 laser confocal microscope. Images presented are representative single optical sections from at least 20 fields imaged from at least three experiments.

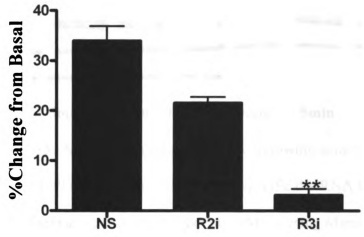

Figure 14. MTS Assay for RMC proliferation using Dharmacon gene-specific knockdown. Gene-specific d-siRNA for mismatched RNA (NS control), R2, and R3 (Dharmacon) was transfected into RMC's using Mirus TKO transfection reagent as per manufacturer's instructions. 24 hours following transfection, cells were plated on 96-well plates at a concentration of 2000 cells/well. The following day the cells were serum-starved overnight and treated with 50ng/mL PDGFββ. 16 hours later, proliferation of the cells was measured by MTS assay (Promega) as per manufacturer's instructions. **$p \leq 0.001$ (R3 vs. NS); n=5.

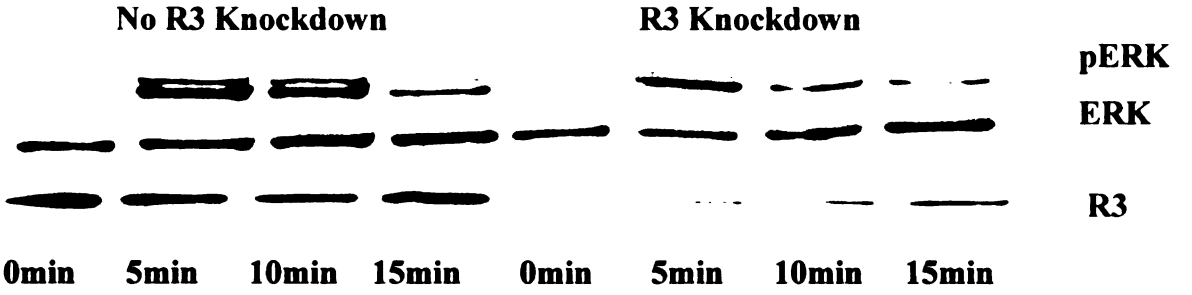

Figure 15. Membrane-associated pERK following gene-specific R3 knockdown and 50ng/mL PDGFββ stimulation. Gene-specific d-siRNA for mismatched RNA (NS) and R3 (Dharmacon) was transfected into RMC's using Mirus was transfected into RMC's using Mirus TKO transfection reagent as per manufacturer's instructions. Following 50ng/mL PDGFββ treatment, a membrane fraction was prepared as described above. Western blotting was preformed with anti-R3 antibody at 1:300 (Santa Cruz) and visualized using chemiluminescence. Blot represents one of six experiments.

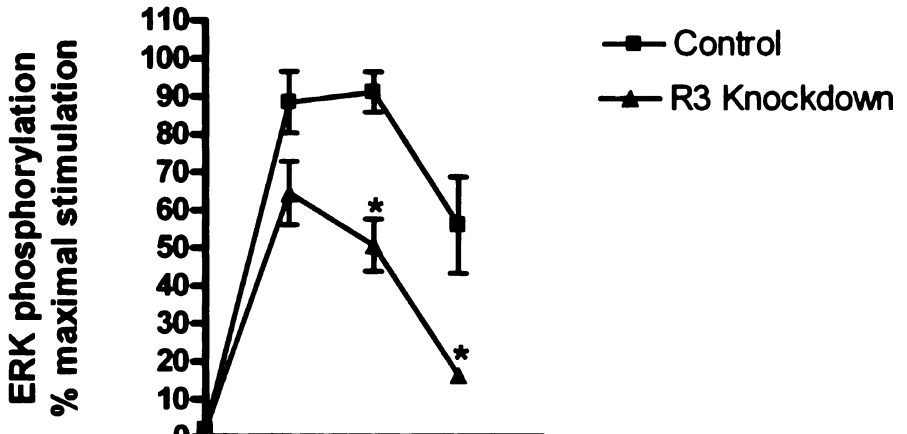

Figure 16. The effect of R3 knockdown on maximal membrane-associated ERK phosphorylation following PDGFββ treatment. Graph represents pERK/ERK ratios observed following experimental conditions described in Figure 18. *p≤0.05 (R3i Vs. control at 10,15 min); n=6.

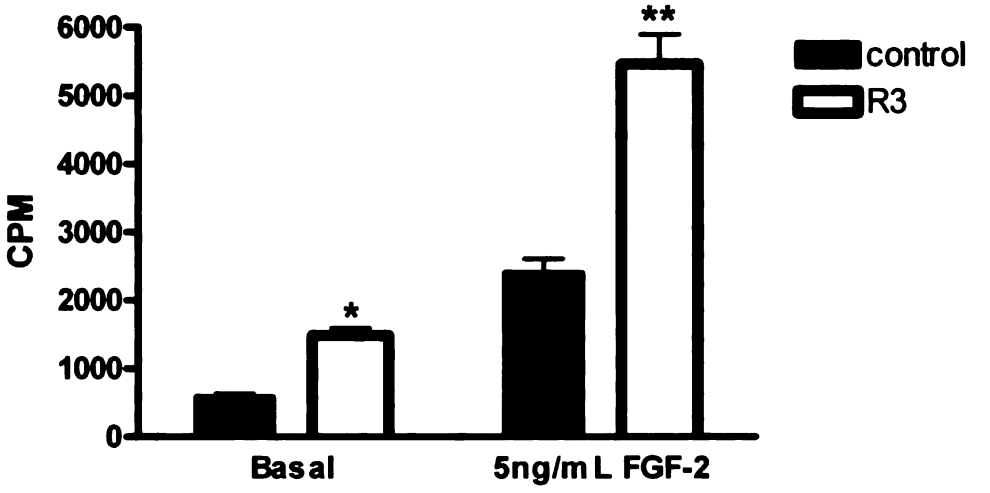

Figure 17. ^{3}H Thymidine Incorporation Assay for proliferation of NRK following R3 transfection. R3 was sub-cloned into the pCMV-Tag2A expression vector and 5 micrograms per 100mm dish were transfected into NRK using Fugene 6 (Roche) following the manufacturer's protocol. 24 hours after transfection, cells were plated at a concentration of 3000 cells/well on a 24-well plate. The following day the cells were serum starved overnight then treated with 5ng/mL FGF-2 for 16 hours. NRK proliferation was assessed using ^{3}H methylthymidine incorporation. Control represents pCMV transfected NRK. *$p \leq 0.05$ (R3 basal vs. control basal) **$p \leq 0.001$ (R3 FGF-2 treated vs. control FGF-2 treated); n=5.

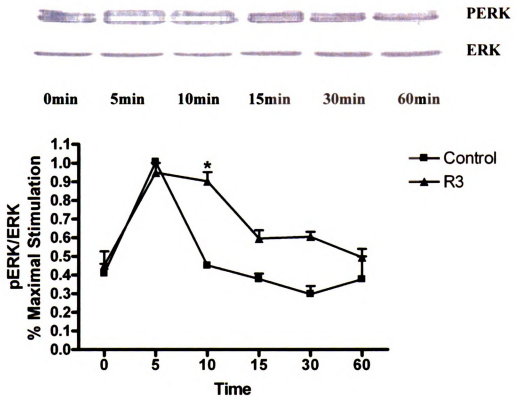

Figure 18. Effect of R3 on membrane-associated ERK phosphorylation in NRK following FGF-2 treatment. An FGF-2-induced, membrane-associated ERK phosphorylation time course was established in NRK as in Methods section for control (pCMV) and pCMVTag2(Flag)-R3 transfected cells. Protein concentration was determined by the Bradford assay. For each time point, 40ug membrane fraction protein was separated on a 10% SDS-polyacrylamide gel. Western blotting was performed with anti-pERK antibody (Santa Cruz) to assess ERK phosphorylation status. Bands were visualized using chemiluminescence (Pierce Supersignal West Pico) on XO-Mat film. Blots were stripped by immersion in a 95°C solution of.5% SDS/.1XSSC and then re-probed for ERK-2 (Santa Cruz). Graph represents pERK/ERK ratios. *$p \leq 0.05$; n=5

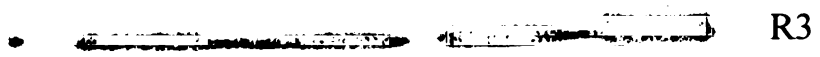

Control **R3** **R3ΔEE** **R3ΔEEG** **R3ΔQ**

Figure 19. Membrane expression of R3 and R3 mutants. NRK cells were transfected with 5ug of pCMV vector (control), pCMVTag2-R3, R3ΔEE, R3ΔEEG, or R3ΔQ DNA. Membrane protein fractions were obtained as described in Methods section. Protein concentration was determined by the Bradford assay. 40ug membrane fraction protein was separated on a 10% SDS-polyacrylamide gel. Western blotting was performed with anti-R3 antibody (1:300 Santa Cruz). Bands were visualized using chemiluminescence (Pierce Supersignal West Pico) on XO-Mat film. Blot is representative of four experiments.

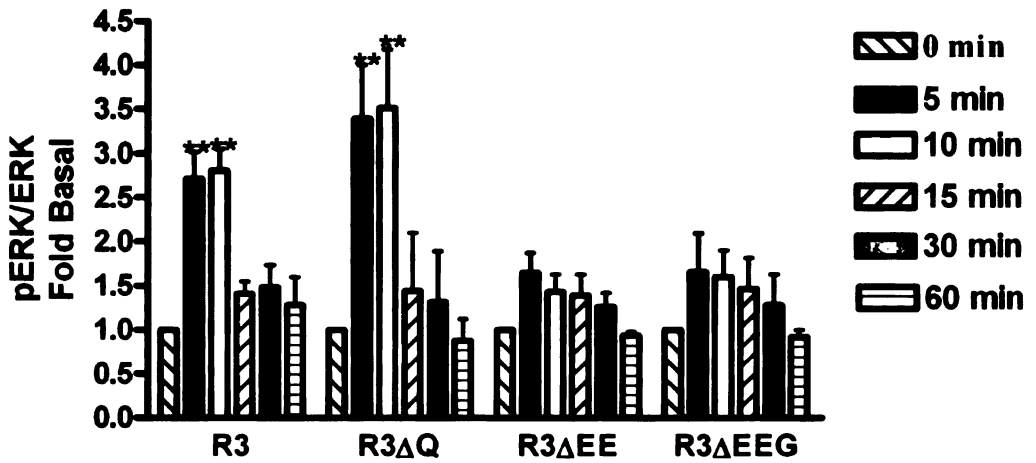

Figure 20. Effect of R3 ERKD-Domain mutation on membrane-associated ERK phosphorylation following FGF-2 treatment. NRK cells were transfected with 5ug of pCMVTag2-R3, R3ΔEE, R3ΔEEG, or R3ΔQ DNA. Control samples were transfected with pCMV vector. 24 hours following transfection, cells were serum-starved overnight and ERK phosphorylation time courses were performed by treating the cells with 5ng/mLFGF-2 for 0 (basal), 5, 10, 15, 30 and 60 minutes. Membrane fractions were prepared as described previously. Protein concentration was determined by the Bradford assay. For each time point, 40ug membrane fraction protein was separated on a 10% SDS-polyacrylamide gel. Western blotting was performed with anti-pERK antibody (Santa Cruz) to assess ERK phosphorylation status. Bands were visualized using chemiluminescence (Pierce Supersignal West Pico) on XO-Mat film. Blots were stripped by immersion in a 95°C solution of.5% SDS/.1XSSC and then re-probed for ERK-2 (Santa Cruz). Graph represents pERK/ERK ratios, **$p \leq 0.001$ (R3, R3ΔQ 5 and 10 min time points vs. their respective 0 min-basal time points); n=5.

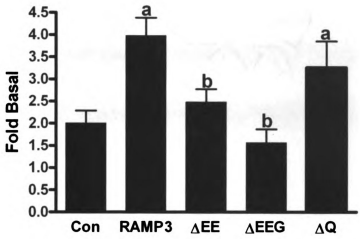

Figure 21. The role of R3 ERK-DD in FGF-2-stimulated proliferation of NRK. Site-directed mutagenesis was performed using a pair of complementary oligonucleotides (Michigan State University Macromolecular Structure Facility) containing the appropriate point mutations in the sequence of the R3 ERK DD. The mutated DNA sequences were confirmed by automated sequencing (Michigan State University Genomic Technology Support Facility). NRK cells were transfected with 5ug of pCMVTag2-R3, R3ΔEE, R3ΔEEG, or R3ΔQ DNA Control samples were transfected with pCMV vector. 24 hours later, the cells were plated on 24-well tissue culture plates, and the following day the cells were serum-starved overnight. NRKs were then treated for 16 hours with 5ng/mL FGF-2. NRK proliferation was assessed using ^{3}H thymidine incorporation. $^{a}p \leq 0.05$ (R3 and R3ΔQ vs. Control), $^{b}p \leq 0.05$ (R3 vs. R3ΔEE and R3ΔEEG); $n \geq 4$.

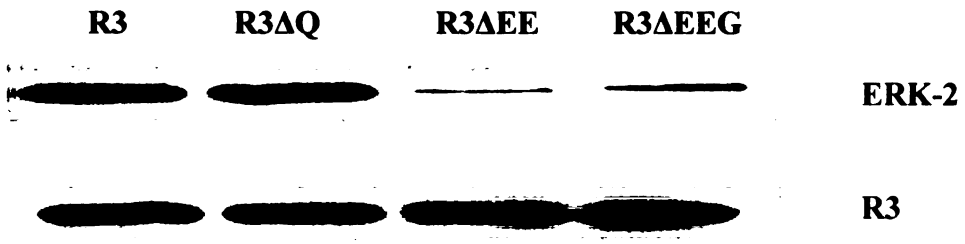

Figure 22. GST Overlay with R3 mutations. Site-directed mutagenesis was performed to produce the appropriate point mutations in the sequence of the R3 ERK DD. The mutated DNA sequences were confirmed by automated sequencing (Michigan State University Genomic Technology Support Facility). 10uG of R3, R3ΔQ, R3ΔEE, and R3ΔEEG GST fusion proteins were resolved on a 10%SDS-polyacrylamide gel and transferred to a PVDF membrane. Filters were blocked then incubated overnight at 4 degrees in a solution containing either 25nM purified inactive or active ERK. The following day the blots were washed and probed with antibodies to ERK-2, washed, and incubated with a horseradish peroxidase-conjugated secondary antibody to detect R3:ERK interaction. Blots were stripped and re-probed for R3. Blot is representative of 4 overlay experiments.

4.4 Discussion

PTKR activation of MAPK is probably the most extensively investigated mechanism of mesangial cell proliferation. However, both FGF-2 [199-202] and PDGF-ββ [203-205] can induce a proliferative response in certain cell types by activating phospholipase C-γ, resulting in increased intracellular Ca^{+2}. The specific MEK inhibitors, U0126 and PD98059, were utilized to assess the contribution of ERK in RMCs. U0126 is a chemically synthesized organic compound that inhibits both active and inactive MEK1/2, while PD098059 inhibits activation of inactive MEK 1/2 by binding to inactive MEK to prevent its activation. In RMC, MEK inhibition almost totally inhibited PDGF-ββ induced proliferation, and it significantly decreased the FGF-2 induced proliferation of NRK. In NRK, approximately 12% of the proliferative response was not blocked by MEK inhibition. This small amount may be due to a non-ERK mediated response, such as activation of PLC-γ.

RMCs endogenously express both R2 and R3, however; only R3 expression is upregulated following PDGF-ββ treatment. A previous study from our laboratory focused on the consequences of R3 upregulation on AM-mediated (anti-proliferative) responses [124]. However, the non-AM associated effects of increased RMC R3 expression were not addressed. Given the recent reports identifying novel RAMP receptor and protein interaction partners [97, 102, 105, 106], it seemed plausible that R3 might play an alternative role in PDGF- ββ mediated cellular responses. Studies were undertaken to identify and characterize such roles.

PDGF-ββ is a potent mitogen for RMC, and deregulated PDGF-ββ-induced RMC growth known to play a role in a variety of glomerular diseases. PDGF-ββ treatment of cultured RMC results in a dose-dependent increase in proliferation, with 50ng/mL PDGF-ββ treatment resulting in a maximal proliferative response [124]. Initial experiments employed to identify R3's role in PDGF-ββ-induced proliferation employed Invitrogen's "dicer" technology. In these experiments, R3 knockdown completely inhibited the proliferative effects of 50ng/mL PDGF-ββ treatment. Dicer generates short, double-stranded interfering RNA for an entire gene of interest. This technology has been utilized successfully for specific gene knockdown with certain short gene products, and the inhibition of RMC proliferation was not observed with R2 or lac-Z knockdown. However, dicer can result in some non-specific effects. Specific double-stranded RNA oligonucleotides knockdown confirmed the R3 effects on proliferation.

Since RAMPs are class I transmembrane proteins, crude membrane preparations were utilized to assess the role of R3 in PDGF-ββ mediated actions. PDGF- ββ treatment resulted in quick (5 minute) peak activation of membrane-associated ERK that steadily decreased to control levels in 20 minutes. Consistent with the RMC proliferation data, gene-specific knockdown of R3, but not R2, resulted in a decrease of membrane-associated ERK activation. While the peak (5minute) ERK activation trended towards, but did not reach statistical significance, maximal membrane-associated ERK activation was decreased in both the 10 and 15-minute time points.

To further validate the effects of R3 knockdown on proliferation, R3 DNA was transfected into NRK cells. Rat interstitial fibroblasts (NRK) express CRLR and R2, but not R3 [206]. AM is anti-proliferative in NRK, however, as in the case of RMC, non-

AM mediated RAMP effects have not been studied. Since FGF-2 is a well-characterized fibroblast mitogen, a FGF-2 dose-response curve to assess proliferation was performed in NRK. Maximal proliferation was observed following 5ng/mL FGF-2 treatment. Consistent with the RMC data suggesting a role for R3 in PDGF-ββ induced proliferation, the introduction of R3 in NRK resulted in a significant increase in both basal and 5ng/mL FGF-2 treatment compared to vector-transfected cells. R3's effect on serum-starved basal proliferation may be a result of culturing the newly transfected cells with serum for one day after plating them on 24-well plates prior to serum-starving them the following evening. These cells had ample exposure to numerous growth factors within the serum that, together with R3, may have affected their rate of proliferation. It may also be possible that the introduction of R3 into these cells independently results in an increased cell-turnover rate. Although the mechanism is unclear, introducing R3 into a cell line that does not normally express it resulted in a robust basal and FGF-2 stimulated proliferation.

To characterize R3 involvement in NRK MAPK activation, membrane-associated ERK activation was assessed. First, a time course for NRK membrane-associated ERK activation following FGF-2 treatment was established. Like the quick (5 minute peak and decrease back to basal at 15 minutes) membrane-associated ERK activation observed in RMC following PDGF-ββ treatment, the FGF-2 response in NRK peaked at 5 minutes and returned back to basal levels by 10 minutes. Although the introduction of R3 into NRK did not effect the level of ERK activation at 5 minutes it did result in a significant increase in membrane associated ERK activation at the 10-minute time point compared to vector transfected control. This membrane-associated ERK activation in the R3

transfected cells was sustained, but not statistically significant at the 15 and 30-minute time points. By utilizing both R3 knockdown and introduction it is clear that R3 influences membrane-associated ERK activation in RMC and NRK.

The N-terminal amino acid sequence of R3 harbors a putative ERK D-Domain. Mutating one or both of the basic arginine residues of the putative ERKDD to acidic glutamic acids did not affect *in vitro* binding of GST fusion proteins to either inactive or active (phosphorylated) ERK protein. The sequential addition of a hydrophobic, helix-breaking praline to an uncharged, polar glycine residue mutation resulted in a slight, but significant decrease in ERK:R3 binding. Mutating the downstream hydrophobic amino acid leucine to glutamine also had no effect on ERK:R3 interaction.

In NRK a significant amount of FGF-2 induced proliferation is mediated through ERK cascade activation. R3-GST fusion protein overlays demonstrated that R3 could physically interact with both active and inactive ERK protein. In addition, R3 expression resulted in an increased ERK activation and proliferation of NRK. It seems plausible that the D-Domain of R3 might mediate membrane-associated ERK activity.

Although R3 membrane expression was assessed in NRK, mutating the R3 D-Domain may result in a decreased membrane expression of the corresponding mutated proteins. R3 ERK D-Domain mutant expression in the NRK membrane fraction was verified, and the effects of mutating key amino acid s within the ERK D-Domain were measured. Transfecting NRK with R3 resulted in increased membrane-associated ERK activity, mutating the extreme N-terminal D-Domain residues from basic, positively charged, hydrophilic arginines to acidic, negative charged, hydrophilic glutamates (R3EE) resulted in decreased ERK activation levels that were similar to control (pCMV)

levels. Mutating the adjacent neutral, helix breaking amino acid proline to a neutral glycine (R3EEG) residue did not significantly decrease ERK activation from control levels. Mutating the downstream hydrophobic amino acid leucine to glutamine did not significantly decrease ERK activity levels from R3 transfected levels.

While R3 introduction into a cell line (NRK) that does not endogenously express it resulted in a robust proliferative response to FGF-2, but the biological responses following specific ERK D-Domain mutation would provide a much better assessment of R3's role in ERK-cascade activation. To this end, proliferation of NRK following mutant R3 transfection and subsequent FGF-2 treatment correlated well with the membrane-associated ERK activity. Transfecting NRK with the R3EE mutant did not significantly alter FGF-2 stimulated proliferation from control (vector) transfected levels, but it was significantly lower than the R3 response. Introducing a R3EEG mutant resulted in a small, but insignificant decrease from control, and a significant decrease in proliferation compared to the R3Q mutation. Proliferation following R3Q mutant introduction was not statistically different from R3.

The findings reported thus far suggest that the ERK D-Domain of R3 might play an important role as a mediator of ERK cascade activation and the subsequent proliferative response following PDGF-ββ treatment in RMC and FGF-2 treatment in NRK. This D-Domain is located in the extreme N-terminus of the class I transmembrane protein, R3. How then, is this integral membrane protein able to interact and mediate the activity of a cytosolic protein such as ERK?

5. Identification of the subcellular site(s) of R3:ERK interaction

5.1 Introduction

All signal transduction cascades transmit signals from the cell surface into the cytoplasm and nucleus to elicit a cellular response. These cascades contain multiple components, and classical cascades act by a sequential series of phosphorylation steps. Since MAP kinases phosphorylate very similar motifs (consensus sequence Ser/Thr-Pro (S/TP)), and several potential substrates contain this motif, it is important to provide specificity to direct individual kinases towards the correct substrates. Multiple mechanisms exist for generating signaling specificity within these cascades to ensure specific cellular responses. One important mechanism for ensuring signaling specificity involves targeting MAPKs to their substrates within distinct cellular compartments. Compartmentalized signaling is a relatively new paradigm in signal transduction. Most work thus far has focused on the roles of scaffolding proteins that chaperone and tether MAPK components together in close proximity in specific cellular locales.

Kermorgant et al. have recently demonstrated that traffic to endosomes is essential for hepatocyte growth factor (HGF/c-Met) to trigger an ERK response [171]. In addition, normal endocytic trafficking of EGFR is important for the full activation of MAPK. Inhibition of clathrin-mediated endocytosis by dominant-negative dynamin in EGF- activated cells revealed that internalization of EGFR is needed for maximal MAPK activation [172]. Burke et al. have also reported that the EGF receptor (EGFR) activates its targets Ras, Raf, and MAPKK (MEK) at the plasma membrane, but endocytosis had to occur to activate ERK [167, 173]. Like EGF, nerve growth factor (NGF) activation of

TrkA receptors results in internalization of phosphorylated TrkA via endocytosis. Howe et al. demonstrated that upon NGF stimulation, PC12 derived endosomes contained phosphorylated TrkA, Shc, Raf, ERK, as well as activated Ras [174]. Since it is believed that the R3:CRLR dimer is maintained during translocation to the cell surface, receptor activation, internalization and degradation, it is plausible that R3:ERK interaction also occurs at the endosomal membrane.

Cell surface receptors such as tyrosine kinases, (RTK) and G protein-coupled receptors transmit activation signals to the Raf/MEK/ERK cascade through different isoforms (H-Ras, N-Ras, and K-Ras 4B/4A) of the small GTPase protein Ras [135, 136]. Activation of only 5% of Ras molecules is sufficient to induce full activation of ERK1/2 [137]. Compartmentalized signaling may also help explain how a single regulatory molecule such as Ras can control such a plethora of cellular responses such as cell proliferation, differentiation, transformation, and apoptosis. Ras proteins must associate with the cytosolic leaflet of cellular membranes to be fully activated [138, 139]. Recently, it was demonstrated that the information required for accurate membrane localization is contained within the CAAX region [181], which also dictates how Ras proteins traffic to their destinations. Whereas H- and N-Ras traffic to the PM along the secretory pathway through the ER then Golgi complex, K-Ras4B is directly routed from the ER to the plasma membrane [178, 182]. The presence of H-Ras in ER/golgi subcellular locations seems not to be a transient event associated with the transport and/or recycling of H-Ras proteins to and from the PM; instead, a pool of H-Ras appears to permanently reside in these organelles. These observations have led investigators to ask whether ER/golgi associated H-Ras undergoes GTP-GDP exchange and subsequent

MAPK pathway signaling. Using live cell imaging utilizing a probe consisting of Raf-1's Ras binding domain fused to green fluorescent protein (RBD-GFP), Chiu et al. demonstrated that following EGF stimulation activated Ras is present at the plasma membrane, ER and the Golgi [183]. The studies describing the kinetics/mechanisms of Ras activation within these subcellular compartments have expanded our understanding regarding the complexities of Ras:ERK activation. They allow us to consider how other membrane-associated proteins, such as R3, could influence ERK signaling in locales other than the PM. (Figure 23)

Most secreted, and many membrane proteins contain cleavable N-terminal signal sequences that coordinate their targeting to and translation across the ER [207, 208]. Signal sequences are usually located at the extreme N-terminus of these proteins and are typically 20-30 amino acids in length. Not surprisingly, all three RAMP isoforms contain signal peptide sequences at their N-termini. R3's putative ERK D-Domain is located within its signal peptide region.

Traditionally, signal sequences were thought to be simple, interchangeable domains that played a somewhat passive role in protein processing. Although all signal sequences share a recognizable three-domain structure consisting of a basic "N" domain, followed by a 7-13 residue hydrophobic "H" domain, terminating with a slightly polar "C" domain [209], overall, prokaryotic, as well as eukaryotic signal sequences lack any significant homology.[207]. Recently, several broad-ranging studies, assessing a variety of functions and experimental systems, have disputed the "passive" signal sequence paradigm. Indeed, the diversity of signal sequences within membrane and secretory

proteins can effect their targeting pathways, translocon interaction, cleavage, and post-cleavage processing.

The sequence is first recognized by the signal sequence recognition particle (SRP). SRP interacts with the ribosome-nascent chain in the ribosome, slows translation, and targets the chain to the SRP receptor located on the ER membrane. Following GTP hydrolysis, the ribosome engages with the translocon. SRP is then released from the complex, and translation resumes. The amino acid residues within the hydrophobic region of the signal sequence have been shown to orchestrate the interaction with Sec61 and the efficiency, and thus kinetics, of the translocation and translation process [210]. Signal sequences are usually released from the precursor protein by signal peptidase (SP) during passage of the growing polypeptide chain through the ER membrane, but the details/kinetics of this step are not well characterized. For example, while the signal peptide sequences of most precursor proteins are cleaved rapidly (ass soon as the C-region enters the ER lumen), the signal sequences of HIV-1 and feline immunodeficiency virus are cleaved very slowly (very late in their protein maturation process) [211, 212]. Signal peptides are thought to span the ER membrane at their hydrophobic region, with the N terminus facing the cytosol and the C terminus exposed toward the ER lumen [213-216]. Following liberation by SP, many, but not all, of these peptides are processed further by signal peptide peptidase (SPP) within the ER membrane, resulting in fragments that are released into the cytosol [217]. Cleavage by SPP is mediated by helix-breaking residues, such as proline(s) located in the membrane spanning region of the peptide [216].(Figure 24)

Conventionally, it was assumed that signal peptides were degraded rapidly following cleavage by SPP, and therefore had no other cellular function. However, SPP is found in the genomes of plants and animals, but not in fungi or bacteria, both of which process proteins with signal sequence, suggesting the possibility of additional roles. Recent studies have also demonstrated that liberated peptides can have additional cellular functions. One such example is SPP cleavage of Fas ligand (FasL). FasL binding to Fas receptor triggers the apoptosis that plays a pivotal role in the maintenance of immune system homeostasis. SPP cleavage liberates a small, unstable peptide fragment. This fragment translocates to the nucleus and is capable of inhibiting gene transcription [218]. Another example indicating a post-targeting function of SPP- liberated peptides is observed in the generation of human lymphocyte antigen (HLA)-E epitopes in humans. HLA-E epitopes are derived from major histocompatability complex (MHC) class I molecules. During biosynthesis of MHC class I molecules, the signal sequence is first cleaved by SP, then SPP, and a nine-residue N-terminal fragment is released into the cytosol, loaded onto the HLA-E molecule, and transported to the cell surface for presentation to natural killer cells. HLA-E expression on the cell surface of presenting cells results in a decreased natural killer response [215] In addition, liberated signal peptides have been shown to interact with cytosolic signal transduction molecules. Site-specific photo-crosslinking studies have followed the fate of the signal sequence of preprolactin in a cell-free system. The preprolactin SP cleaved signal sequence is processed by SPP and an N-terminal fragment is released into the cytosol. This signal peptide fragment was found to interact efficiently with Ca^{+2}/calmodulin [219, 220]. Similar to preprolactin, a signal peptide fragment of the HIV-1 envelope protein p-gp160

is cleaved by SPP, released into the cytosol, and subsequently binds to calmodulin through interactions within its signal peptide [221]. A cytosolic form of the ER chaperone calreticulin was found to arise by an aborted translocation mechanism dependent on its signal sequence. In this study, in addition to its well-established ER functions, a portion of calreticulin influenced glucocorticoid receptor-mediated gene activation in the cytosol.[222]. Taken together, these studies suggest bioactive roles for liberated signal peptides in transcriptional regulation, cell surface presentation, and interaction with various cytosolic cell-signaling mediators.

Although the signal peptide of R3 contains a putative SP cleavage site at amino acid 23, no study to date has determined if it is indeed cleaved. We hypothesized that if the signal peptide is cleaved, R3:ERK membrane interaction occurs at the ER. If, it is not cleaved during protein processing, R3:ERK membrane interaction may occur in another subcellular compartment. The purpose of this study is to determine if the signal sequence of R3 is cleaved at the ER, and to identify the subcellular location of R3;ERK interaction.

5.2. Materials and Methods

5.2.1. Materials

NRK and HEK 293T cells were obtained from ATCC. DMEM, penicillin/streptomycin, and fetal bovine serum were purchased from Invitrogen (Carlsbad, CA). Adrenomedullin was purchased from Bachem Bioscience, Inc. (King of Prussia, PA). cAMP level was measured using the Biotrak cAMP Enzyme Immunoassay System from Amersham Biosciences (Piscataway, NJ). Fugene 6 transfection reagent was obtained from Roche (Nutley,NJ). Anti EEA, Calnexin, and gm230 antibodies were from BD Biosciences (San Jose, CA). Anti-R3 and anti-pERK antibodies were from Santa

Cruz Biotechnology (Santa Cruz, CA). Chemiluminescence reagents were from Pierce (Rockford, IL). pCMVTag2 vector and DH5α competent cells were from Stratagene (La Jolla, CA). Anti-Flag antibody and optiprep reagent was purchased from Sigma Aldrich (St.Louis,MO). All other reagents were of the highest quality available.

5.2.2. Cell Culture

HEK 293 cells were maintained in Dulbecco's modified Eagle's medium low glucose medium containing 10% fetal bovine serum, and 1% penicillin-streptomycin. NRK were cultured using Dulbecco's modified Eagle's medium supplemented with 4 mM L-glutamine, 1.5 g/L sodium bicarbonate and 4.5 g/L glucose, 5% bovine calf serum, 5% Non-Essential Amino Acids, and 1% Penicillin/Strepomycin.

5.2.3. R3 Cloning and Expression

Full length cDNA of human R3 was cloned into a pCMV-Tag2(flag) vector using the restriction cut sites EcoR1/Xho1 as described previously. 5ug pCMV-Tag2R3 was transfected into HEK 293 and NRK cells using Fugene 6 as per manufacturer's directions.

5.2.4. Desensitization Assays

HEK 293 cells were transiently transfected with CRLR and either PCDNAR3 or Tag2(flag)R3 DNA using Fugene 6 as per manufacturer's directions. 48 h after transfection, HEK293 were seeded on a 24-well plate until reaching 75-80% confluency and then incubated in serum-free medium overnight before the experiment. Cells were pretreated with or without 10 nM AM in Dulbecco's modified Eagle's medium containing 0.2% bovine serum albumin for one hour. After agonist exposure, cells were washed three times with Dulbecco's phosphate-buffered saline. Cells were then re-challenged with AM

(100 nM) for 10 min at 37 °C. and frozen at -80°C for cAMP accumulation assays.. Determination of cAMP level was measured using the Biotrak cAMP enzyme immunoassay system according to the manufacturer's instructions. cAMP levels in RMCs were calculated using a standard curve ranging from 10 to 10^4 fmol of cAMP. Each experiment was done in triplicate and repeated at least three times. Data is expressed as the percentage of maximal response, percentage of forskolin.

5.2.5. Optiprep Protocol for the subcellular fractionation of plasma membrane, endosomes, golgi, and ER

HEK 293 cells were transfected with 5ug pCMVTag2R3 using Fugene 6 as per manufacturer's directions. 24 hours later, the cells were plated on 150mm tissue culture plates. The following day, the cells were serum-starved overnight. Cells were treated for 10 minutes with 50ng/mL PDGF-ββ then snap frozen at -80°C. The Optiprep protocol was adapted from Puglielli [223]. Briefly, cells were scraped in a small volume of buffer containing .25M sucrose, 140mM NaCl, 1mM EDTA, 20mM Tris-HCl, 1mM PMSF, 0.2mM sodium orthovaadate, 100nM NaF, 5ug/mL leupeptin, and 10ug/mL aprotinin. and homogenized using 20 strokes in a Dounce homogenizer. The homogenates were then spun at 800g for 5 minutes at 4°C to pellet debris and the nuclear pellet. The PNS was used for subsequent centrifugation. A continuous 8-34% iodixanol gradient was prepared in 13 mL tubes using a gradient mixer. 1mL of the PNS was carefully loaded onto the gradient and samples were spun at 4°C for 18 hours at 100,000g in a Sorvall ultracentrifuge. .35mL fractions were carefully removed from the meniscus, precipitated with cold 10% trichloroacetic acid, spun, and washed with cold acetone. Fractions were resuspended in 4X protein loading dye. Proteins were separated by electrophoresis

through a 4-20% SDS- polyacrylamide gel. Western blotting was performed with anti-pERK, anti-R3, anti-Flag, anti-EEA, anti gm-230 and anti-calnexin antibodies. Bands were visualized using chemiluminescence (Pierce Supersignal West Pico) on XO-Mat film.

5.2.6. Confocal Microscopy

HEK 293 cells were cultured on coverslips then permeablized with 0.1% v/v Triton X-100 in PBS and blocked overnight in 0.1% v/v Triton X-100 in PBS + 10% goat serum. Samples were incubated in primary antibody (mouse anti EEA, Calnexin, or gm230 at 1:200), or rabbit/mouse anti-Flag (at 1:300), or rabbit anti pERK (at 1:300) in blocking buffer for 2h at room temperature. Appropriate secondary antibodies were applied for 1h at room temperature (anti-rabbit Cy3 at 1:400, anti mouse Alexa 488 at 1:500). Coverslips were mounted in Shandon mounting medium. Cells were visualized on an Olympus laser confocal microscope. Images presented are representative single optical sections from at least 20 fields imaged from at least three experiments.

5.2.7. Co-Immunoprecipitation experiments

HEK293 were transfected with pCMVTag2R3 (or vector control) as described above and serum-starved overnight. The following day, cells were treated for 15 minutes with 50ng/mL PDGF-ββ and snap-frozen. Cells were lysed in a buffer containing 50mM HEPES, 150mMNaCl, 1.5mM $MgCl_2$, 1mM EGTA, 10% glycerol, and 1% Nonidet P-40 and spun for 15 minutes at 4°C at 1200xG. Supernatants were then spun at 4°C for 1 hour at 100,000xG to obtain cytosolic and membrane fractions. Cytosolic fractions were concentrated by spinning through a 5,000MWCO filter to a volume of 600ul. Pellets were re-suspended in a volume of 600ul lysis buffer. Both cytosolic and membrane fractions

were pre-cleared by the addition of washed protein A sepharose beads and subsequent rocking at 4°C for 1 hour. The protein A sepharose was pelleted by centrifugation at 14,000xG for 1 minute. Supernatants were divided in half; and either 1ug polyclonal anti-Flag antibody or polyclonal anti-ERK antibody was added to the tubes. These samples were rocked for 1.5 hours at 4°C, and then 40ul washed protein A sephaorse was added to each tube. The cell extract/antibody/protein A sepharose samples were rocked at 4°C for 2 hours, spun, and washed three times in lysis buffer. Samples were eluted in SDS loading buffer and resolved on a 10% SDS-polyacrylamide gel and transferred to a nitrocellulose membrane. Blots were probed with monoclonal anti-pERK or rabbit polyclonal R3 antibodies.

5.2.8. Statistics

Data are presented as mean ± S.E.M. Multiple group comparisons were made using analysis of variance (ANOVA), followed by Bonferoni's multiple comparison between treatments. Two treatment comparisons were compared using Student's t-test method. Statistical significance was set at $P<0.05$.

5.3. Results

5.3.1. Desensitization Assays following N-terminal Flag addition

In order to establish whether or not the putative signal peptide sequence of R3 is indeed cleaved during protein processing, full-length human R3 cDNA was cloned into a pCMVTag2 vector containing a flag tag at the N-terminus of the multiple cloning site. Studies were undertaken to access any alterations in AM signaling that may arise due to addition of the N-terminal flag tag by comparing the normal desensitization process in PCDNAR3/PCDNACRLR and pCMVTag2R3/PCDNACRLR transfected HEK 293

cells. For these assays, transfected cells are exposed to 10nM AM (pretreat) for one hour, washed, then re-challenged with 100nM AM for 15 minutes. cAMP levels were measured to assess desensitization of the AM-1R. No significant difference was observed between PCDNAR3 and Tag2R3 transfected HEK 293 cells, indicating that the receptor is able to desensitize normally following AM exposure (Figure 25).

5.3.2. Confocal Microscopy to detect Co-localization of R3 in pCMVTag2R3 transfected HEK293

For these experiments, EEA, gm230, and calnexin were used to identify endosomal, golgi, and ER compartments, respectively. Confocal microscopy experiments in pCMVTag2R3-transfected HEK293 cells demonstrated the colocalization of Flag with calnexin at the ER, but not golgi (gm230), or endosomal (EEA) compartments (Figure 26).

5.3.3. Subcellular fractionation to identify R3 signal peptide cleavage

For these studies, the N-terminal flag epitope tag of pCMVTag2R3 was utilized to monitor the signal peptide fate of R3. Anti-flag antibody, as well as an antibody that recognizes the C-terminal region of R3, were utilized to identify the cellular location of N- and C-termini. A continuous 8-34% iodixanol gradient was used to separate plasma membrane/endosomes, golgi, and ER membranes. Antibodies to EEA, gm230, and calnexin were used to identify endosomal, golgi, and ER membrane compartments. The N-terminal flag tag was observed only in ER membrane fractions, while an antibody detecting the C-terminus of R3 demonstrated that it localized to ER, golgi, and plasma membrane/endosomal compartments. In serum-starved conditions, pERK was not detected in any membrane compartment (Figure 27).

5.3.4. Subcellular fractionation to identify pERK locale following PDGF-ββ stimulation in HEK293

First, the presence of PDGF-βR in HEK293 cells was confirmed (Figure 28 upper panel). HEK 293 cells were transfected with pCMVTag2R3 to identify the cellular locations of N- and C-terminal R3 and pERK, and lysate were fractionated using a continuous 8-34% iodixanol gradient following PDGF-ββ stimulation. pERK localized to ER and plasma membrane/endosomal fractions. R3 was detected in ER, golgi, and plasma membrane/endosomal fractions under PDGF-ββ–stimulated conditions, and the Flag epitope localized in ER membrane fractions (Figure 28 lower panel).

5.3.5. Confocal Microscopy identifying colocalization of Flag epitope and pERK in HEK293 cells following PDGF-ββtreatment

For these experiments, a rabbit anti-Flag antibody and a mouse anti-calnexin antibody were used to identify the presence or absence of R3 at the ER compartment. Confocal microscopy demonstrated the colocalization of Flag with calnexin at the ER following PDGF-ββ treatment (Figure 29).

5.3.6. Co-Immunoprecipitation of R3 and pERK

Antibody immunoprecipitation of both membrane (100,000Gpellet) and cytosolic (100,000G supernatant) fractions of pCMVTag2R3 transfected HEK 293 cells using polyclonal anti-Flag antibody demonstrated co-immunoprecipitation of activated ERK under serum-starved and PDGF-ββ treated conditions. The Flag antibody co-immunoprecipitation of activated ERK following PDGF-ββ treatment was significantly increased in both cytosolic and membrane fractions. Co-immunoprecipitation of R3 with the Flag antibody occurred only in the membrane fractions of both serum-starved and PDGF-ββ treated samples. Polyclonal ERK-2 antibody co-immunoprecipitation of

activated ERK occurred in both membrane and cytosolic fractions, but was significantly increased in cytosolic fractions following PDGF-ββ treatment. Ploy clonal ERK antibody co-immunoprecipitation of R3 occurred only in the membrane fraction following PDGF-ββ treatment (Figure30).

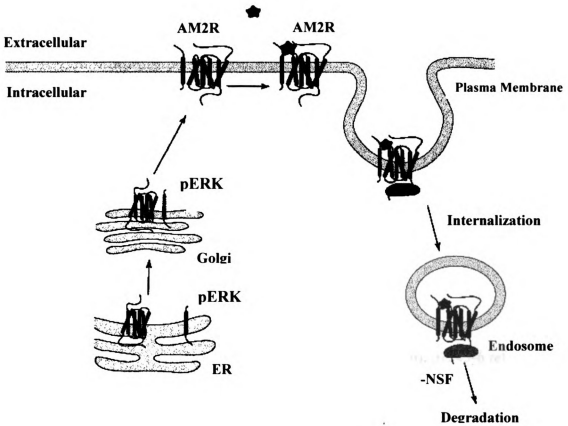

Adapted from: **TIBS 31**(11): 631-38 ref [104]

Figure 23. Potential Subcellular locations for R3:ERK interaction. Potential R3:ERK membrane interaction sites include the ER, golgi, PM, and endosomes.

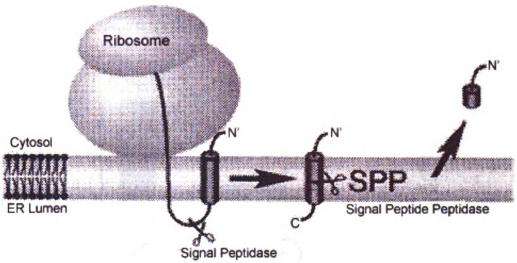

Adapted from **Biochemical Society Transactions 31**(6): p1243-6 ref [224]

Figure 24. Signal peptide cleavage and processing. A newly synthesized protein containing a signal peptide is targeted to the ER membrane by the ribosome and i N' translocated into the ER lumen. For most secretory and transmembrane proteins, signal peptidase then cleaves the signal peptide from the precursor protein. The amino acid residues within the signal sequence determine the exact timing and efficiency of signal peptidase activity. The signal peptide spans the ER membrane with the N-terminus facing the cytosol and the C-terminus within the ER lumen. For some, but not all proteins, signal peptide peptidase then cleaves he signal peptide within its hydrophobic region (shown as a barrel shape) to release the signal peptide into the cytoplasm. The liberated peptide can then undergo degradation, or participate in other cellular functions. These functions include cytosolic Ca^{+2}/calmodulin binding and glucocorticoid receptor-mediated gene activation, as well as cytosolic/nuclear shuttling.

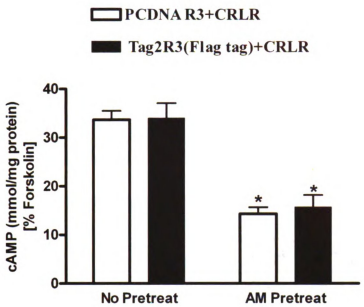

Figure 25. Comparison of PCDNAR3 and pCMVTag2R3(Flag-tag) transient transfection on AM1R desensitization. HEK 293 cells were transiently transfected with CRLR and either PCDNAR3 or Tag2(flag)R3 DNA using Fugene 6 as per manufacturer's directions. Cells were plated on 24-well plates, serum starved overnight, then treated for one hour with 10nM AM (pretreat). Cells were then washed repeatedly and assayed for cAMP accumulation to assess receptor desensitization by being re-challenged with 100nM AM for 15 minutes then snap frozen. cAMP levels were measured using the Biotrak cAMP enzyme immunoassay system (Amersham Biosciences) according to manufacturer's instructions. Cellular cAMP levels in the transfected HEK293 cells were calculated from a standard curve ranging from 10 to 10^4 fmol of cAMP. Each cAMP measurement was done in triplicate. Data is expressed as percent maximal response, % forskolin. *$p \leq 0.05$; n=3. No significant difference was observed between PCDNAR3 and Tag2(Flag)R3 transfected HEK 293 cells.

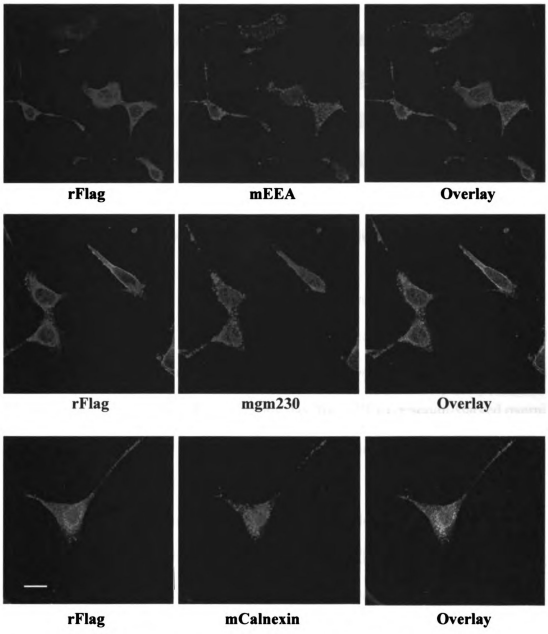

Figure 26. Confocal Microscopy identifying subcellular location of Flag epitope expression in HEK293 cells. Tag2(flag)R3 DNA transfection and confocal microscopy were performed as described in Methods. Images shown are representative of at least 20 fields imaged from at least three experiments. Bar scales on all images represent 20μm.

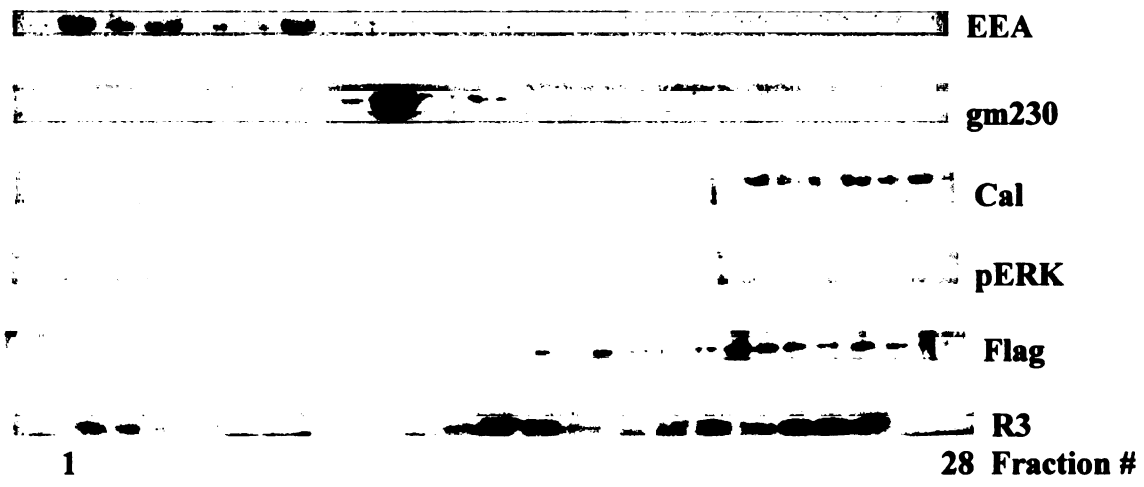

Figure 27. Optiprep Protocol for the subcellular fractionation of plasma membrane, endosomes, golgi, and ER. HEK 293 cells were transfected with 5ug pCMVTag2R3 using Fugene 6 as per manufacturer's directions. 24 hours later, the cells were plated on 150mm tissue culture plates. The following day, the cells were serum-starved overnight. The Optiprep protocol was adapted from Puglielli [223]. The PNS was used for Optiprep centrifugation. A continuous 8-34% iodixanol gradient was prepared in 13 mL tubes using a gradient mixer. 1mL of the PNS was carefully loaded onto the gradient and samples were spun at 4°C for 18 hours at 100,000xG. .35mL fractions were carefully removed from the meniscus, precipitated with trichloroacetic acid and washed with acetone. Proteins were separated by electrophoresis through a polyacrylamide gel. Western blotting was performed with anti-pERK, anti-R3, anti-Flag, anti-EEA, anti gm-230 and anti-calnexin antibodies. EEA antibody was used as an endosomal marker, gm 230 as a golgi marker, and Calnexin as an ER marker. Blot is representative of 4 experiments.

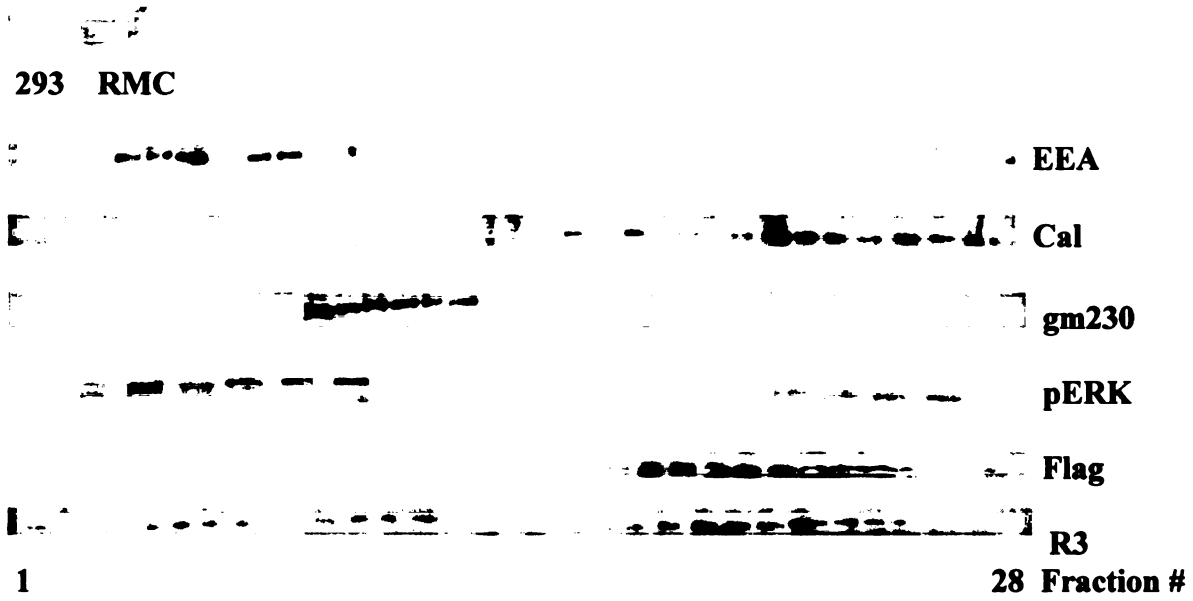

Figure 28 Upper Panel. Western blot for PDGFβR expression in HEK293 cells. Lower Panel. Subcellular fractionation using Optiprep gradient following PDGF-ββ treatment. HEK 293 cells were transfected with 5ug pCMVTag2(Flag)R3 using Fugene 6 as per manufacturer's directions. 24 hours later, the cells were plated on 150mm tissue culture plates. The following day, the cells were serum-starved overnight. Cells were treated for 10 minutes with 50ng/mL PDGF-ββ then snap frozen at -80°C. The Optiprep protocol was adapted from Puglielli [223] as described above. Western blotting was performed with anti-pERK, anti-R3, anti-Flag, anti-EEA, anti gm-230 and anti-calnexin antibodies. Blot is representative of 4 experiments.

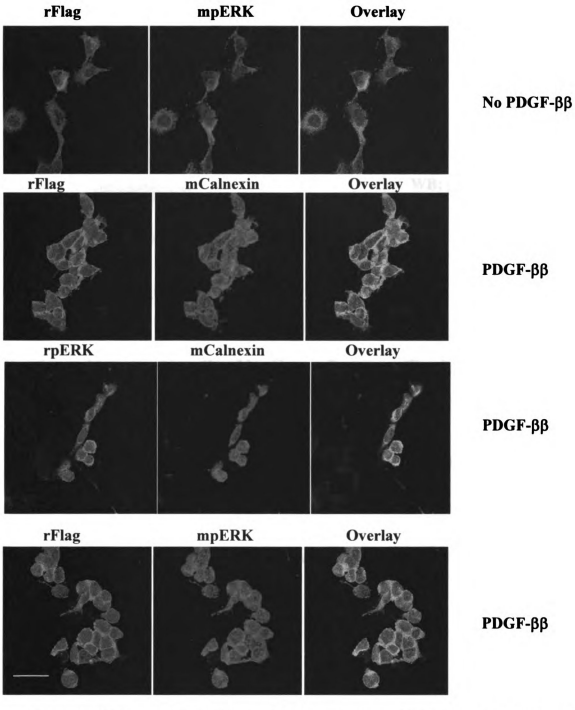

Figure 29. Confocal Microscopy identifying colocalization of Flag epitope and pERK in HEK293 cells following PDGF-ββ treatment, Confocal microscopy was performed as described in Methods. Images shown are representative of at least 20 fields imaged from at least three experiments. Bar scales on all images represent 50μm.

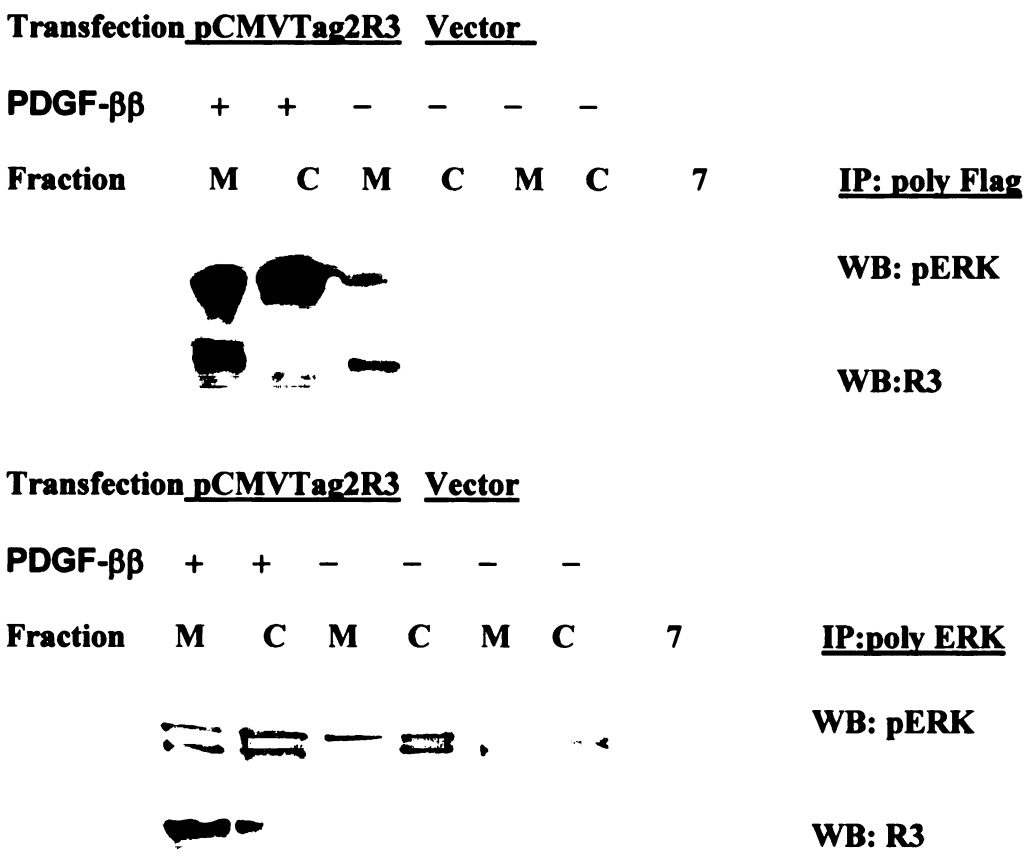

Figure 30. Co-immunoprecipitation of R3 and pERK. Co-immunoprecipitation experiments were performed as described in Materials and Methods. P=pellet from 100,000G spin, S=supernatant from 100,000G spin. Vector=pCMV transfected, Lane7=IgG + Protein A Sepharaose negative control. Blots are one representative of three experiments.

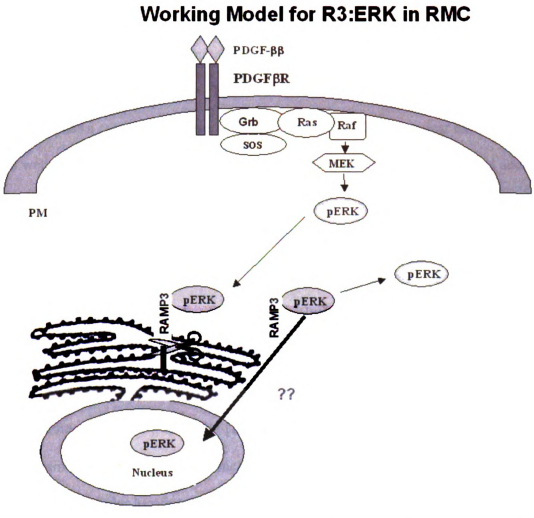

Figure 31. Working model depicting N-terminal R3:pERK cellular location. Following PDGF-ββ stimulation results in autophosphorylation of the PDGF-βR, and the recruitment of Grb/SOS. Ras switches to it's GTP-bound state, resulting in raf activation. Raf then phosphorylates MEK, which in turn phosphorylates ERK. A portion of the activated ERK then travels to the ER where it binds to the ERKD-Domain of R3, which is located within its signal peptide. This signal peptide is cleaved by SP, then SPP, and the peptide is released into the cytoplasm. The activated ERK may be released from the signal peptide (or remain attached), and translocate to the nucleus, or the cytoplasm to phosphorylate specific nuclear/cytosolic substrates.

5.4. Discussion

In mammals, approximately one third of all proteins reside in, or transition through the secretory pathway. The ER chaperone calreticulum (CRT) was first identified as a cytosolic integrin binding protein [225, 226], a nuclear export factor [227], as well a p21 translation regulator [228]. In each of these studies, functional and physical interactions have been demonstrated in the cytosol. Another ER resident protein, glucosidase II β subunit, was originally described as a cytosolic protein kinase C target [229] that modulates calcium homeostasis by binding to the cytosolic tail of the TRP5 channel [230]. Recently, it has been shown to interact with Grb3 [231], serving a shuttle between the cytosol and nucleus. Some class I transmembrane signal peptides display novel subcellular localizations. They include transforming growth factor-β [232], cytochrome p450 [233], and Slit3 [234] (all mitochondrial), as well as IL-15 [235] and cathepsin L [236] (both cytoplasmic). Many studies have incidentally observed unexpected cellular locations for signal sequence-containing proteins presumably intended for the secretory pathway. Levine, et al. suggested that for many secretory pathway proteins, a biologically significant portion of the total protein can have access to the cytosol [237]. Clearly, many signal peptide-containing proteins, or portions of them, exhibit physiological functions other than their documented ER roles. In each instance, the diversity within the signal peptide sequences of these proteins dictated the efficiency of SP/SPP cleavage, as well as the final fate of the peptide and/or protein.

To that end, the results of this study demonstrate that the signal peptide is indeed cleaved from mature R3 at the ER, as indicated by confocal microscopy identifying colocalization of the N-terminal Flag epitope and the C-terminal portion of R3 at the ER,

but not at other subcellular compartments. Data from the subcellular fractionation studies suggest that under serum-arrested conditions, a portion of R3's N-terminus remains in an ER fraction, as indicated by Flag epitope detection in this compartment. In addition, while no membrane-associated pERK was detected under serum-arrested conditions, a small portion of pERK was detected at the ER membrane following PDGF-ββ treatment. Confocal microscopy indicated that the Flag epitope colocalized with pERK at the ER. Co-immunoprecipitation experiments identified interaction between R3 and pERK in a supernatant fraction from a 100,000G spin, which probably represents a cytosolic cellular fraction. This interaction was increased following PDGF-ββ treatment. R3 was detected only in the 100,000G pellet fraction (representing membrane) when co-immunoprecipitated with the N-terminal Flag epitope. Further experiments are warranted to determine the fate of R3's signal peptide. Taken together, these results suggest a novel role for R3 in ERK-mediated proliferation in NRK and RMC (Figure 31).

6. The effects of FGF-2 treatment on membrane R3 expression in RMC

6.1. Introduction

Several laboratories have published RAMP gene expression profiles for many cell lines and tissues. Many studies have reported variable RAMP gene expression in diverse disease models, physiological states, and following certain drug treatments. R3 expression was specifically upregulated in several growth-associated cell culture and disease models. This upregulation did not correlate with an increase in AM1R components, namely CRLR and R2.

RMC express all components of the AM signaling system; R1, R2, R3, and CRLR. Published reports from our laboratory have demonstrated specific membrane-associated R3 upregulation in RMC following PDGF-ββ treatment. The physiological consequences of R3 upregulation were described in the context of the AM signaling system. The AM-independent cellular effects of increased R3 expression were not investigated. The focus of the present studies has focused on R3-mediated cellular actions outside the usual paradigm of the AM system.

PDGF-ββ and FGF-2 are important regulators of mesangial cell proliferation and matrix deposition following glomerular injury. Experiments within this document have demonstrated that the FGF-2-induced proliferation observed in RMC is primarily ERK-mediated. Furthermore, R3 introduction into the R3-deficient cell line, NRK, increased membrane-associated ERK activation and subsequently also increased proliferation. Does FGF-2 treatment of RMC also preferentially increase R3 expression? Studies were undertaken to assess the effect of FGF-2 treatment on membrane-associated R3 expression in RMC.

6.2. Materials and Methods

6.2.1. Materials

RMC were obtained from ATCC. RPMI1640, penicillin/streptomycin, and fetal bovine serum were purchased from Invitrogen (Carlsbad, CA). FGF-2 was obtained from Oncogene (Cambridge, MA). R2 and R3 antibodies were purchased from Santa Cruz Biotechnology (Santa Cruz, CA) and chemiluminescence reagents from Pierce (Rockford, IL). SDS-polyacrylamide gels were from Bio-Rad Laboratories (Hercules, CA). All other reagents were of the highest quality available.

6.2.2. Cell Culture

RMC were maintained in RMPI 1640 media containing 15% FBS and 1% penicillin-streptomycin.

6.2.3. Membrane expression of R3 following FGF-2 treatment in RMC

RMC were plated on 150mm tissue culture dishes, then serum-starved overnight. The following day the cells were treated with 0, 1, 5, and 10ng/mL FGF-2 for 24 hours. The media was removed and the plates were snap-frozen. The cells were then scraped from the plates in homogenization buffer (10mMHepes, 0.15MnaCl, 1mM EDTA, 1mM PMSF, 0.2mM sodium orthovanadate, 100nM NaF, 5ug/mL leupeptin, and 10ug/mL aprotinin). This lysate was dounce-homogenized for 20 strokes. The homogenates were centrifuged at 1300xg for 20 minutes at 4°C to pellet nuclear and cell debris. The supernatant was centrifuged at 100,000xg at 4°C for 1 hour to isolate the membrane fraction. Protein concentration was determined by the Bradford assay. For each time point, 40ug membrane fraction protein was separated on a 10% SDS-polyacrylamide gel. Western blotting was performed with anti-R2 or R3 antibody (Santa Cruz) to assess

RAMP protein levels. Bands were visualized using chemiluminescence (Pierce Supersignal West Pico) on XO-Mat film. Blots were stripped and re-probed for actin for protein normalization.

6.2.4. Statistics

Data are presented as mean ± S.E.M. Multiple group comparisons were made using analysis of variance (ANOVA), followed by Bonferoni's multiple comparison between treatments. Two treatment comparisons were compared using Student's t-test method. Statistical significance was set at $P<0.05$.

6.3. Results

6.3.1. Membrane expression of R3 following FGF-2 treatment in RMC

24-hour FGF-2 treatment of RMC resulted in a concentration-dependent increase in membrane-associated R3 expression (Figure 32). Membrane-associated R3 expression increased (2.8±. 33 fold basal) following 24-hour 5ng/mL FGF-2 treatment (Figure 33). Membrane-associated R2 expression was not statistically different from basal levels following 24-hour 5ng/mL FGF-2 treatment.

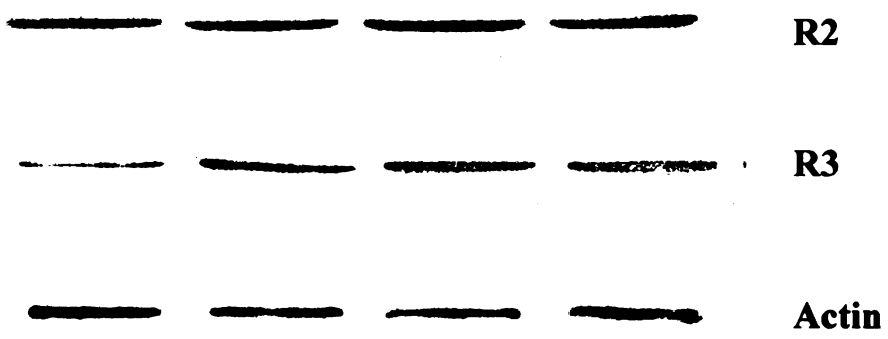

Figure 32. RAMP membrane expression in RMC following FGF-2 treatment.

RMC were plated on 150mm tissue culture dishes, serum-starved, and treated with 0,1,5, and 10ng/mL FGF-2 for 24 hours. Membrane fractions were prepared as described in Methods. Western blotting was performed with anti R2 antibody. Blots were stripped and re-probed for R3 and actin. Blots are representative of four experiments.

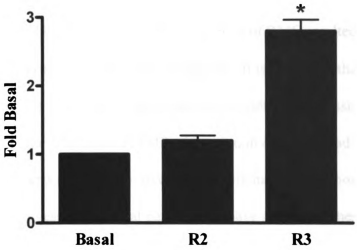

Figure 33. Membrane RAMP expression in RMC following 5ng/mLFGF-2 treatment. Graph represents RAMP/Actin ratios of the experiments described in Figure XX following 5ng/mL FGF-2 treatment. *$p \leq 0.05$; n=4.

6.4. Discussion

Like PDGF-ββ, FGF-2 treatment of RMC resulted in a specific up-regulation of R3 in a cellular membrane component. It is intriguing that two potent mesangial cell mitogens significantly increased R3, but not R2, expression. Clearly, ample evidence exists for differential RAMP expression in cell lines, and in animal disease models. Since AM exerts anti-proliferative responses in many cells, most of these studies, especially those investigating renal pathologies, have associated these RAMP increases with AM-mediated, anti-proliferative responses. The results observed herein suggest that the specific upregulation of R3 may play a noteworthy role in non-AM mediated cellular responses.

7. Summary and Conclusions

7.1. Specific aims, major hypotheses, and results of the study

The major aim of this study was to investigate the role of AM-independent R3 actions in ERK-mediated proliferation. It was hypothesized that R3 is a critical regulator of renal mesangial cell proliferation following stimulation by PDGFββ, by direct interaction with the MAPK cascade. Hence, as summarized below, the following specific aims were addressed and hypotheses relating to these aims were tested:

Specific Aim #1: In RMC, PDGFββ-induced activation of the ERK signal transduction cascade and subsequent proliferation requires R3.

Hypothesis 1: A significant portion of the PDGFββ-induced proliferative response in RMC occurs through activation of ERK.

Hypothesis 2: The amino acid sequence of R3 contains a punitive ERK-Docking domain that may allow for direct R3:ERK physical interaction.

Hypothesis 3: R3 is involved in ERK-mediated RMC proliferation following PDGFββ treatment.

Hypothesis 4: R3 mediates PDGFββ-induced RMC proliferation by modulating ERK activation.

Results:

a. The PDGF-ββ-induced proliferation of RMC is almost exclusively ERK-mediated. Similar findings were observed for FGF-2-induced proliferation of NRK.
b. A putative ERK D-Domain was identified using *Scansite* database software.
c. GST-tagged R2 protein does not interact with neither inactive nor active forms of ERK-2 protein *in vitro*. GST-R3 showed a robust interaction with both inactive and active forms of purified ERK-2 protein.

d. Using two separate approaches, R3 knockdown completely abolished PDGF-ββ-induced proliferation in RMC.

e. Introducing R3 into a cell line that normally does not express it, NRK, resulted in a significantly increased basal and FGF-2-induced proliferative response.

f. R3 knockdown resulted in a decreased membrane-associated ERK activation in RMC. Introducing R3 into NRK significantly increased membrane-associated ERK activation following FGF-2 treatment.

g. R3 does not mediate cytosolic ERK activation in RMC.

Specific Aim #2: To identify the subcellular location of R3:ERK interaction.

Hypothesis 1: R3 interacts with ERK at a cellular membrane component.

Hypothesis 2: R3:ERK interaction occurs at an ERK D-Domain located within R3's N-terminal signal sequence. This sequence is cleaved at the ER during R3 synthesis, suggesting that R3:ERK interaction occurs in this subcellular compartment.

Results:

a. R3 and pERK colocalized at the ER in HEK293 cells following PDGF-ββ.treatment.

b. R3's N-terminal signal sequence is cleaved at the ER.

Specific Aim #3: To determine the specific amino acid requirement of the R3 ERKDD in PDGFββ-induced ERK activation and subsequent proliferation.

Hypothesis 1: Mutating specific amino acid residues within the R3 ERK D-Domain will result in decreased R3:ERK protein binding *in vitro*.

Hypothesis 2: Mutating specific amino acid residues within the R3 ERK D-Domain will decrease membrane-associated ERK activation following FGF-2 treatment in NRK:

Hypothesis 3: The ERK D-Domain mutations that result in decreased membrane-associated ERK activation will also result in a decreased FGF-2 proliferative response in NRK following FGF-2 treatment.

Results:

a. The extreme N-terminal arginine (positions7 and 8) residues, as well as the adjacent praline (position 9) residue, of R3's D-Domain are necessary for R3:ERK protein interaction *in vitro*.
b. The7/8 arginines, and the adjacent proline residue of the ERK D-Domain mediate ERK membrane-associated activation in NRK following FGF-2 treatment. These residues also mediate the subsequent FGF-2-induced proliferative response in NRK.
c. The downstream D-Domain leucine (at position 11) does not mediate *in vitro* R3:ERK protein interaction, membrane-associated ERK activation, or NRK proliferation following FGF-2 treatment.

Specific Aim #4: To assess the effects of FGF-2 treatment on R3 expression.

Specific Hypothesis: FGF-2 treatment of RMC will result in an increased expression of R3.

Results:

a. FGF-2 treatment of RMC results in a dose-dependent increase in R3 expression in a membrane fraction.

b. 5ng/mL FGF-2 treatment of RMC increases basal R3 expression 2.8 fold..

7.2. Limitations of the study

1. The primary limitation of this study was the use of cell culture systems exclusively to demonstrate the role of R3 in ERK-mediated proliferation. Clearly, cell culture systems were warranted for investigating detailed molecular mechanisms. However, mesangial cells *in vivo* are in a dynamic environment, in which endocrine/paracrine factors, as well as cell:cell interactions within the glomerulus, ultimately contribute to their cellular responses.
2. All of the experiments in this study were performed using rat mesangial and kidney fibroblasts, or human embryonic kidney cells. Although these cells have been used extensively in the study of renal disease, the results obtained may not necessarily reflect the responses and regulatory mechanisms in human cells. The cell lines were chosen because the AM signaling system has been well characterized in these cells, they are easily cultured and manipulated, resulting in highly reproducible responses.

3. ERK activation, and the resulting proliferative response were elicited by the exogenous administration of PDGF-ββ and FGF-2. While concentrations used were clearly within previously published ranges, it is difficult to assess the concentrations that mesangial cells and renal fibroblasts are exposed to *in vivo*.
4. Although this preliminary study clearly demonstrates a role for R3 in ERK-mediated proliferation, more work is warranted to unravel the mechanisms involved in activated ERK translocation to the nucleus following its interaction with R3 at the ER. To date, most studies describing signal peptide release into the cytoplasm utilize complex, cell-free *in vitro* reticulocyte methodologies. Future studies employing these systems could potentially provide additional mechanistic information regardingR3:ERK interaction at the ER as well as signal peptide fate.

7.3. Positive outcomes of the study

AM, the ligand for R3:CRLR, is known to exhibit potent anti-proliferative and anti-migratory effects in RMC. However, prior to these studies, the extent of non-AM mediated RAMP involvement in the anti-proliferative process has not been thoroughly investigated. R3 expression has been shown to be upregulated in several growth-related animal and cell culture models, even when CRLR (and R2) levels remain unchanged, or even decrease. For example, in RMC, PDGF-β treatment results in an increased R3 (but not R2) protein expression, and subsequent increases AM-mediated adenylate cyclase activity result in an anti-proliferative response. But, in all published results, AM-independent R3-mediated effects on proliferation were not investigated. Are all R3 effects on proliferation AM-mediated?

R2 and R3 exhibit great diversity within their amino acid sequences (they are only 30% homologous), yet both elicit an identical cellular response following agonist exposure. Recent studies from our lab have demonstrated the importance of R3's unique C-terminal PDZ domain in post-endocytic trafficking of the R3:CRLR complex. In addition, several recent studies have shown promiscuity in RAMP interactions. For example, even though in a recent RAMP binding study, when co-expressed with RAMPS, 6 out of 10 class B receptors demonstrated RAMP interaction [105] Recently published results suggest RAMPs may also modulate GPCR coupling efficiency through diverse cell signaling pathways. Unlike the interaction of RAMPs with CRLR, VPAC1R is expressed at the plasma membrane independently of RAMP presence. The classic coupling pathway associated with VPAC1R is a significant accumulation of cAMP with little PI hydrolysis. However, the VPAC1R:R2 heterodimer exhibits enhanced phosphoinositide (PI) hydrolysis with no significant change in cAMP stimulation. So, although R2 was not necessary to shuttle the VPAC1R to the plasma membrane, it's interaction with this receptor altered the conventional signaling response. The scope of RAMP-mediated GPCR regulation was further expanded by studies identifying a class C calcium-sensing receptor, (CaSR), interaction with RAMPs [106]. In a paradigm similar to CRLR, recombinant CaSR expressed in COS7 cells does not translocate to the plasma membrane unless R1 or R3 (but not R2) is also co-expressed. In the same study, R3 was shown to mediate both the glycosylation and trafficking of CaSR from the ER to Golgi. In the absence of R3, CaSR was retained in an intracellular compartment that confocal microscopy identified to be the ER. Clearly, all of these studies suggest that RAMPs

participate in many diverse cellular functions, well beyond their classical AM-associated roles.

This study was the first to describe a novel, AM-independent role for R3 in ERK-mediated proliferation. While ERK involvement in the proliferation of many cell types has been extensively studied, other cell signaling cascades can contribute significantly to this process. This study demonstrated that both PDGF-ββ (in RMC) and FGF-2 (in NRK) exert mitogenic actions primarily through ERK activation.

The extreme N-terminus of R3, but not R2, contains a putative ERK D-Domain that is very similar to the ERKD-Domains of MEK1 and 2. We hypothesized that R3 had the potential to mediate ERK activity by interacting with ERK through its D-Domain. By utilizing both R3 overexpression and knockdown methodologies, this study demonstrated that R3 is a critical mediator of membrane-associated ERK activity. Specifically, using RMC, we employed two separate technologies to knockdown endogenous R3 prior to PDGF-ββ stimulation. Both of these approaches resulted in significantly decreased PDGF-ββ stimulated growth. To confirm these results, R3 was introduced into a cell line that does not endogenously express it (NRK). R3 introduction into these cells resulted in an increased proliferation in both basal and FGF-2-stimulated conditions.

Published reports have indicated the importance of basic arginine residues in MEK:ERK interaction. These residues are located at the extreme N-terminus of the ERK D-Domain. These residues were also found to be important in R3 modulation of membrane-associated ERK activity and proliferation following FGF-2 treatment of NRK. A helix-breaking proline residue located just downstream of the arginines has also been reported to be necessary for MEK:ERK interaction. This was not observed for R3:ERK

interaction, membrane-associated ERK activation, or proliferation in NRK following FGF-2 treatment.

As with almost all class I transmembrane proteins, the amino acid sequence of R3 contains a signal peptide that targets them ER and orchestrates their protein processing there. Many, but not all, signal peptides are cleaved by SP at the ER. They can then be processed further within the ER membrane by SPP, resulting in the release of the peptide into the cytosol. The actual mechanisms and kinetics involved in protein processing have been thoroughly investigated for only a few transmembrane proteins. Even less is understood regarding signal peptide release/fate in the cytoplasm. Initially, it was assumed that signal peptides were degraded rapidly following cleavage by SPP, and therefore had no other cellular function. However, recent studies have demonstrated that liberated peptides can have additional cellular functions. One notable study demonstrating novel signal peptide functions includes MHC class I molecules [215], whose signal peptide interacts with the HLA-E molecule and transports it to the cell surface. Other signal peptides, including those of preprolactin and HIV-1p-gp160, have been reported to modulate cytosolic $Ca^{+2/}$calmodulin signaling [219-221, 224]. In addition, it has been demonstrated that a small percentage of calreticulin's signal peptide pool influences glucocorticoid receptor-mediated gene activation in the cytosol.[222]. Thus, bioactive roles for liberated signal peptides have been demonstrated for transcriptional regulation, cell surface presentation, and interaction with various cytosolic cell-signaling mediators.

Both confocal microscopy and differential centrifugation were employed to establish the subcellular localization of R3:ERK interaction. First, confocal microscopy

revealed that the N-terminus of R3 is present only at the ER, while an antibody recognizing the C-terminal region of R3 is observed at both the ER and plasma membrane. This data suggests that the signal peptide of R3 is indeed cleaved from mature R3 protein during synthesis. Secondly, differential centrifugation demonstrated that the N-terminal region of R3, as well as activated ERK, were both present in an ER membrane fraction following PDGF-ββ treatment of pCMVTag2-R3 transfected HEK 293 cells. Confocal microscopy indicated their colocalization at the ER, but not golgi or endosomes.

This thesis has identified a novel role for R3 in mediating ERK activity and proliferation at a unique subcellular membrane compartment. Given the fact that, in several models of progressive glomerular disease, loss of coordinated mesangial cell proliferation, phenotypic changes and increased growth factor expression precede up-regulation of genes for ECM and mesangial expansion. A better understanding of the mechanisms involved in R3:ERK mediated mesangial proliferation may allow us to develop novel anti-proliferative strategies for the treatment of glomerular disease.

7.4. Future studies

1. As discussed previously in this thesis, the use of animal models, such as R3 knockout mice, would greatly advance or understanding of the physiological role R3 plays in proliferation. Caron, et al. recently generated R3 knockout mice. They reported that mice lacking R3 exhibited a normal phenotype, other than decreased body weight [238]. It would be interesting to induce glomerulonephritis (by injection of the anti-mesangial cell antibody Thy1.1) in these animals. In control mice, an acute phase of complement-dependent mesangial cell lysis, followed by

a phase of deregulated mesangial cell proliferation and altered matrix deposition would ensue [14]. Would similar mesangial cell effects be observed in R3 knockout mice?

2. AM is known exhibit anti-proliferative effects in several cell types, including mesangial cells, fibroblasts, and vascular smooth muscle cells. Conversely, in keratinocytes, epithelial cells, and endothelial cells, AM exhibits robust proliferative effects. Interestingly, in bone AM promotes osteoblast growth both *in vitro* and *in vivo* [239, 240]. It is intriguing that, although the physiologic consequences were not investigated, PTH treatment of primary mouse osteoblast cells results in the specific upregulation of R3 [131]. Using both cell clines and animal models, AM has been demonstrated to be proliferative in several types of carcinomas including breast, endometrial ovarian, melanoma, prostate, and glioblastomas. Interestingly, administration of the uterine mitogens estrogen or phytoestrogen to rats preferentially increased uterine R3 expression levels, and actually significantly deceased CRLR levels [114, 127]. Hewitt et al. [241] recently found that R3, with a 43-fold increase, was one of the most potently induced genes in the uterus of wild-type mice treated with estrogen. Other studies have shown that regulatory region of the R3 gene contains an estrogen response element [127].

   Although RAMP expression, (and the physiological consequences of altered RAMP expression) have not been extensively studied in cancer, some noteworthy findings have recently been published. Dysregulation of the Wnt/ beta-catenin signal transduction pathway has been extensively implicated in the pathogenesis

of mammary gland and colon tumors. Gene expression microarray analysis of mouse mammary epithelial cells inducibly expressing a constitutively active mutant of beta-catenin identified R3 as one of a handful of target genes of this pathway [242]. In addition, R3 is expressed in the prostate cancer cell line, DU145 [123], and in prostate carcinoma biopsies the levels of R3 were significantly elevated (compared to prostate hyperplasia biopsies) while expression levels of R2 were unchanged in these samples [123]. R3 knockdown experiments (unpublished data) from our laboratory have suggested that R3 mediates EGF-stimulated proliferation of DU145 cells. Is it plausible that in growth-associated pathologies, altered cellular levels of R3 can influence certain cell types to preferentially proliferate, while not affecting others? Clearly, RAMP expression profiles, with characterization of the ensuing physiological consequences of altered expression, are needed to address these questions.

REFERENCES

1. Schlondorff, D., *Roles of the mesangium in glomerular function.* Kidney Int, 1996. **49**(6): p. 1583-5.

2. Schlondorff, D., *The glomerular mesangial cell: an expanding role for a specialized pericyte.* Faseb J, 1987. **1**(4): p. 272-81.

3. Jefferson, J. and R. Johnson, *Experimental mesangial proliferative glomerulonephritis.* J Nephrol, 1999. **12**(5): p. 297-307.

4. Thomas, G.J., et al., *Rat mesangial cells in vitro synthesize a spectrum of proteoglycan species including those of the basement membrane and interstitium.* Kidney Int, 1995. **48**(4): p. 1278-89.

5. Haas, C., et al., *Regulatory mechanism in glomerular mesangial cell proliferation.* J Nephrol, 1999. **12**(6): p. 405-415.

6. Pabst, R. and R. Sterzel, *Cell renewal of glomerular cell types in normal rats.* Kidney Int, 1983. **24**(5): p. 626-31.

7. Floege, J., et al., *Glomerular cell proliferation and PDGF expression precede glomerulosclerosis in the remnant kidney model.* Kidney Int, 1992. **41**(2): p. 297-309.

8. Couser, W., *Pathogenesis of glomerular damage in glomerulonephritis.* Nephrol Dial Transplant, 1998. **13**(Suppl 1): p. 10-15.

9. Rifai, A., et al., *Experimental IgA nephropathy.* J Exp Med, 1979. **150**(5): p. 1161-73.

10. Stad, R., et al., *An acute model for IgA-mediated glomerular inflammation in rats induced by monoclonal polymeric rat IgA antibodies.* Clin Exp Immunol, 1993. **92**(3): p. 514-21.

11. Wakuai, H., et al., *Anti-histone autoantibodies in ddYY mice, an animal model for spontaneous IgA nephritis.* Clin Immunol Immunopathol, 1989. **52**(2): p. 248-56.

12. Cattell, V. and J. Bradfield, *Focal mesangial proliferative glomerulonephritis in the rat caused by habu snake venom.* Am J Pathol, 1977. **87**(3): p. 511-24.

13. Yan, D., W. Rumbeiha, and J. Pestka, *Experimental murine IgA nephropathy following passive administation of vomitoxin-induced IgA monoclonal antibodies.* Food Chem Toxicol, 1998. **36**(12): p. 1095-106.

14. Floege, J., et al., *Mitogenic effect of platelet-derived growth factor in human glomerular mesangial cells: Modulation and/or suppression by inflammatory cytokines.* Clin Exp Immunol, 1991. **86**: p. 334-41.

15. Alpers, C., et al., *Enhanced expression of "muscle specific" actin in glomerulonephritis.* Kidney Int, 1992. **41**(5): p. 1134-42.

16. Liu, J., et al., *Growth-promoting effect of platelet-derived growth factor on rat cardiac myocytes.* Regul Pept, 2005. **127**(1-3): p. 11-8.

17. Leveen, P., et al., *Mice deficient for PDGF B show renal, cardiovascular, and hematological abnormalities.* Genes Dev, 1994. **8**(16): p. 1875-87.

18. Soriano, P., *Abnormal kidney development and hematological disorders in PDGF beta-receptor mutant mice.* Genes Dev, 1994. **8**(16): p. 1888-96.

19. Lindahl, P., et al., *Pericyte loss and microaneurysm formation in PDGF-B-deficient mice.* Science, 1997. **277**(5323): p. 242-5.

20. Robson, M.C., et al., *Platelet-derived growth factor BB for the treatment of chronic pressure ulcers.* Lancet, 1992. **339**(8784): p. 23-5.

21. Rodt, S.A., et al., *A novel physiological function for platelet-derived growth factor-BB in rat dermis.* J Physiol, 1996. **495 (Pt 1)**: p. 193-200.

22. Ross, R., E.W. Raines, and D.F. Bowen-Pope, *The biology of platelet-derived growth factor.* Cell, 1986. **46**(2): p. 155-69.

23. Ross, R., *The pathogenesis of atherosclerosis: a perspective for the 1990s.* Nature, 1993. **362**(6423): p. 801-9.

24. Heldin, C.H., *Structural and functional studies on platelet-derived growth factor.* Embo J, 1992. **11**(12): p. 4251-9.

25. Oefner, C., et al., *Crystal structure of human platelet-derived growth factor BB.* Embo J, 1992. **11**(11): p. 3921-6.

26. Muller, Y.A., et al., *Vascular endothelial growth factor: crystal structure and functional mapping of the kinase domain receptor binding site.* Proc Natl Acad Sci U S A, 1997. **94**(14): p. 7192-7.

27. Murray-Rust, J., et al., *Topological similarities in TGF-beta 2, PDGF-BB and NGF define a superfamily of polypeptide growth factors.* Structure, 1993. **1**(2): p. 153-9.

28. Duan, D.S., et al., *A functional soluble extracellular region of the platelet-derived growth factor (PDGF) beta-receptor antagonizes PDGF-stimulated responses.* J Biol Chem, 1991. **266**(1): p. 413-8.

29. Fretto, L.J., et al., *Mechanism of platelet-derived growth factor (PDGF) AA, AB, and BB binding to alpha and beta PDGF receptor.* J Biol Chem, 1993. **268**(5): p. 3625-31.

30. Herren, B., et al., *Dimerization of extracellular domains of platelet-derived growth factor receptors. A revised model of receptor-ligand interaction.* J Biol Chem, 1993. **268**(20): p. 15088-95.

31. Bishayee, S., et al., *Ligand-induced dimerization of the platelet-derived growth factor receptor. Monomer-dimer interconversion occurs independent of receptor phosphorylation.* J Biol Chem, 1989. **264**(20): p. 11699-705.

32. Heldin, C.H., et al., *Dimerization of B-type platelet-derived growth factor receptors occurs after ligand binding and is closely associated with receptor kinase activation.* J Biol Chem, 1989. **264**(15): p. 8905-12.

33. Kanakaraj, P., et al., *Ligand-induced interaction between alpha- and beta-type platelet-derived growth factor (PDGF) receptors: role of receptor heterodimers in kinase activation.* Biochemistry, 1991. **30**(7): p. 1761-7.

34. Wiesmann, C., et al., *Crystal structure at 1.7 A resolution of VEGF in complex with domain 2 of the Flt-1 receptor.* Cell, 1997. **91**(5): p. 695-704.

35. Yu, J.C., et al., *Structural coincidence of alpha PDGFR epitopes binding to platelet-derived growth factor-AA and a potent neutralizing monoclonal antibody.* J Biol Chem, 1994. **269**(14): p. 10668-74.

36. Heidaran, M.A., et al., *Chimeric alpha- and beta-platelet-derived growth factor (PDGF) receptors define three immunoglobulin-like domains of the alpha-PDGF receptor that determine PDGF-AA binding specificity.* J Biol Chem, 1990. **265**(31): p. 18741-4.

37. Claesson-Welsh, L., et al., *cDNA cloning and expression of the human A-type platelet-derived growth factor (PDGF) receptor establishes structural similarity to the B-type PDGF receptor.* Proc Natl Acad Sci U S A, 1989. **86**(13): p. 4917-21.

38. Matsui, T., et al., *Isolation of a novel receptor cDNA establishes the existence of two PDGF receptor genes.* Science, 1989. **243**(4892): p. 800-4.

39. Yarden, Y., et al., *Structure of the receptor for platelet-derived growth factor helps define a family of closely related growth factor receptors.* Nature, 1986. **323**(6085): p. 226-32.

40. Shulman, T., et al., *An antibody reactive with domain 4 of the platelet-derived growth factor beta receptor allows BB binding while inhibiting proliferation by impairing receptor dimerization.* J Biol Chem, 1997. **272**(28): p. 17400-4.

41. Omura, T., C.H. Heldin, and A. Ostman, *Immunoglobulin-like domain 4-mediated receptor-receptor interactions contribute to platelet-derived growth factor-induced receptor dimerization.* J Biol Chem, 1997. **272**(19): p. 12676-82.

42. Lokker, N.A., et al., *Functional importance of platelet-derived growth factor (PDGF) receptor extracellular immunoglobulin-like domains. Identification of PDGF binding site and neutralizing monoclonal antibodies.* J Biol Chem, 1997. **272**(52): p. 33037-44.

43. Kelly, J.D., et al., *Platelet-derived growth factor (PDGF) stimulates PDGF receptor subunit dimerization and intersubunit trans-phosphorylation.* J Biol Chem, 1991. **266**(14): p. 8987-92.

44. Daniel, T.O. and D.A. Kumjian, *Platelet-derived growth factor in renal development and disease.* Semin Nephrol, 1993. **13**(1): p. 87-95.

45. Shultz, P., et al., *Mesangial cells express PDGF mRNAs and proliferate in response to PDGF.* Am J Pathol, 1988. **255**(4 pt. 2): p. F674-84.

46. Silver, B., F. Jaffer, and H. Abboud, *Platelet-derived growth factor synthesis in mesangial cells: induction by multiple peptide mitogens.* Proc Natl Acad Sci USA, 1988. **86**: p. 1056-60.

47. Doi, T., et al., *Receptor-specific increase in extracellular matrix production in mouse mesangial cells by advanced glycosilation end products is mediated via platelet-derived growth factor.* Proc Natl Acad Sci USA, 1992. **89**: p. 2873-77.

48. Abboud, H., *Nephrology forum: growth factors in glomerulonephritis.* Kidney Int, 1993. **43**: p. 252-67.

49. Johnson, R., et al., *Role of platelet-derived growth factor in glomerular disease.* J. Am. Soc. Nephrol, 1993. **4**: p. 119-28.

50. Silver, B., F. Jaffer, and H. Abboud, *Platelet-derived growth factor synthesis in mesangial cells: induction by multiple peptide mitogens.* Proc Natl Acad Sci USA, 1989. **86**: p. 1056-1060.

51. Haas, C.S., et al., *Regulatory mechanism in glomerular mesangial cell proliferation.* J Nephrol, 1999. **12**(6): p. 405-15.

52. Iida, H., et al., *Platelet-derived growth factor (PDGF) and PDGF receptor are induced in mesangial proliferative nephritis in the rat.* Proc Natl Acad Sci USA, 1991. **88**(15): p. 6560-4.

53. Johnson, R., et al., *Inhibition of mesangial cell proliferation and matrix expansion in glomerulonephritis in the rat by antibody to platelet-derived growth factor.* J Exp Med, 1992. **175**(5): p. 1413-6.

54. Yoshimura, A., et al., *Demonstration of PDGF B-chain mRNA in glomeruli in mesangial proliferative nephritis by in situ hybridization.* Kidney Int, 1991. **40**: p. 470.

55. Gesualdo, L., et al., *Platelet-derived growth factor (PDGF) expression in mesangial proliferative glomerulophritis.* Lab Invest, 1991. **65**: p. 160.

56. Floege, J., et al., *Novel approach to specific growth factor inhibition in vivo: antagonism of platelet-derived growth factor in glomerulonephritis by aptamers.* Am J Pathol, 1999. **154**(1): p. 169-79.

57. Gesualdo, L., et al., *Trapidil inhibits human mesangial cell proliferation: Effect on PDGF beta-receptor binding and expression.* Kidney Int, 1994. **46**: p. 1002-09.

58. Hillis, G., L. Duthie, and A. MacLeod, *Dipyridamole inhibits human mesangial cell proliferation.* Nephron, 1998. **78**: p. 172-78.

59. Haraguchi, M., et al., *Anti-angiogenic compound (TNP-470) inhibits mesangial cell proliferation in vitro and vivo.* Kidney Int, 1997. **51**: p. 1838-46.

60. Gilbert, R., et al., *PDGF signal transduction inhibition ameliorates experimental mesangial proliferative glomerulonephritis.* Kidney Int, 2001. **59**: p. 1324-32.

61. Bikfalvi, A., et al., *Biological roles of fibroblast growth factor-2.* Endocr Rev, 1997. **18**(1): p. 26-45.

62. Nugent, M.A. and R.V. Iozzo, *Fibroblast growth factor-2.* Int J Biochem Cell Biol, 2000. **32**(2): p. 115-20.

63. Conrad, H.E., *Heparin-binding proteins.* 1998, San Diego: Academic Press.

64. Iozzo, R.V., *Matrix proteoglycans: from molecular design to cellular function.* Annu Rev Biochem, 1998. **67**: p. 609-52.

65. Folkman, J., et al., *A heparin-binding angiogenic protein--basic fibroblast growth factor--is stored within basement membrane.* Am J Pathol, 1988. **130**(2): p. 393-400.

66. Sperinde, G.V. and M.A. Nugent, *Heparan sulfate proteoglycans control intracellular processing of bFGF in vascular smooth muscle cells.* Biochemistry, 1998. **37**(38): p. 13153-64.

67. Kan, M., et al., *An essential heparin-binding domain in the fibroblast growth factor receptor kinase.* Science, 1993. **259**(5103): p. 1918-21.

68. Yayon, A., et al., *Cell surface, heparin-like molecules are required for binding of basic fibroblast growth factor to its high affinity receptor.* Cell, 1991. **64**(4): p. 841-8.

69. Mohammadi, M., et al., *A tyrosine-phosphorylated carboxy-terminal peptide of the fibroblast growth factor receptor (Flg) is a binding site for the SH2 domain of phospholipase C-gamma 1.* Mol Cell Biol, 1991. **11**(10): p. 5068-78.

70. Ong, S.H., et al., *FRS2 proteins recruit intracellular signaling pathways by binding to diverse targets on fibroblast growth factor and nerve growth factor receptors.* Mol Cell Biol, 2000. **20**(3): p. 979-89.

71. Dhalluin, C., et al., *Structural basis of SNT PTB domain interactions with distinct neurotrophic receptors.* Mol Cell, 2000. **6**(4): p. 921-9.

72. Kouhara, H., et al., *A lipid-anchored Grb2-binding protein that links FGF-receptor activation to the Ras/MAPK signaling pathway.* Cell, 1997. **89**(5): p. 693-702.

73. Lax, I., et al., *The docking protein FRS2alpha controls a MAP kinase-mediated negative feedback mechanism for signaling by FGF receptors.* Mol Cell, 2002. **10**(4): p. 709-19.

74. Floege, J., et al., *Rat glomerular mesangial cells synthesize basic fibroblast growth factor.* J Clin Invest, 1992. **90**(6): p. 2362-9.

75. Rapraeger, A., A. Krufka, and B. Olwin, *Requirement of heparan sulfate for bFGF-mediated fibroblast growth and myoblast differentiation.* Science, 1991. **252**(5013): p. 1705-08.

76. Klein, D., et al., *Proteoglycans synthesized by human glomerular mesangial cells in culture.* J Biol Chem, 1990. **265**(16): p. 9533-43.

77. Izevbigie, E., J. Gutkind, and P. Ray, *Angiotensin II and Basic Fibroblast Growth Factor Mitogenic Pathways in Human Fetal Mesangial Cells.* Pediatric Research, 2000. **47**(5): p. 614-621.

78. Kunz, D., et al., *Platlet-derived growth factor and fibroblast growth factor differntially regulate IL-1b and cAMP-induced nitric oxide synthase expression in rat renal mesangial cells.* J Clin Invest, 1997. **100**(11): p. 2800-09.

79. Savill, J., et al., *Glomerular mesangial cells and inflammatory macrophages ingest neutrophils undergoing apoptosis.* Kidney Int, 1992. **90**(6): p. 924-36.

80. Fraser, N.J., et al., *The amino terminus of receptor activity modifying proteins is a critical determinant of glycosylation state and ligand binding of calcitonin receptor-like receptor.* Mol Pharmacol, 1999. **55**(6): p. 1054-9.

81. Morfis, M., A. Christopoulos, and P.M. Sexton, *RAMPs: 5 years on, where to now?* Trends Pharmacol Sci, 2003. **24**(11): p. 596-601.

82. Hilairet, S., et al., *Protein-protein interaction and not glycosylation determines the binding selectivity of heterodimers between the calcitonin receptor-like receptor and the receptor activity-modifying proteins.* J Biol Chem, 2001. **276**(31): p. 29575-81.

83. Kuwasako, K., et al., *Visualization of the calcitonin receptor-like receptor and its receptor activity-modifying proteins during internalization and recycling.* J Biol Chem, 2000. **275**(38): p. 29602-9.

84. Hay, D.L. and D.M. Smith, *Knockouts and transgenics confirm the importance of adrenomedullin in the vasculature.* Trends Pharmacol Sci, 2001. **22**(2): p. 57-9.

85. Nagae, T., et al., *Rat receptor-activity-modifying proteins (RAMPs) for adrenomedullin/CGRP receptor: cloning and upregulation in obstructive nephropathy.* Biochem Biophys Res Commun, 2000. **270**(1): p. 89-93.

86. Husmann, K., et al., *Mouse receptor-activity-modifying proteins 1, -2 and -3: amino acid sequence, expression and function.* Mol Cell Endocrinol, 2000. **162**(1-2): p. 35-43.

87. McLatchie, L., et al., *RAMPs regulate the transport and ligand specificity of the calcitonin-receptor-like receptor.* Nature, 1998. **393**: p. 333-339.

88. Flahaut, M., et al., *N-Glycosylation and conserved cysteine residues in RAMP3 play a critical role for the functional expression of CRLR/RAMP3 adrenomedullin receptor.* Biochemistry, 2003. **42**(34): p. 10333-41.

89. Muff, R., W. Born, and J.A. Fischer, *Adrenomedullin and related peptides: receptors and accessory proteins.* Peptides, 2001. **22**(11): p. 1765-72.

90. Flahaut, M., B.C. Rossier, and D. Firsov, *Respective roles of calcitonin receptor-like receptor (CRLR) and receptor activity-modifying proteins (RAMP) in cell surface expression of CRLR/RAMP heterodimeric receptors.* J Biol Chem, 2002. **277**(17): p. 14731-7.

91. Fitzsimmons, T.J., X. Zhao, and S.A. Wank, *The extracellular domain of receptor activity-modifying protein 1 is sufficient for calcitonin receptor-like receptor function.* J Biol Chem, 2003. **278**(16): p. 14313-20.

92. Kuwasako, K., et al., *Functions of the cytoplasmic tails of the human receptor activity-modifying protein components of calcitonin gene-related peptide and adrenomedullin receptors.* J Biol Chem, 2006. **281**(11): p. 7205-13.

93. Hall, R.A., et al., *A C-terminal motif found in the beta2-adrenergic receptor, P2Y1 receptor and cystic fibrosis transmembrane conductance regulator determines binding to the Na+/H+ exchanger regulatory factor family of PDZ proteins.* Proc Natl Acad Sci U S A, 1998. **95**(15): p. 8496-501.

94. Bomberger, J.M., et al., *Novel function for receptor activity-modifying proteins (RAMPs) in post-endocytic receptor trafficking.* J Biol Chem, 2005. **280**(10): p. 9297-307.

95. Cong, M., et al., *Binding of the beta2 adrenergic receptor to N-ethylmaleimide-sensitive factor regulates receptor recycling.* J Biol Chem, 2001. **276**(48): p. 45145-52.

96. Song, I., et al., *Interaction of the N-ethylmaleimide-sensitive factor with AMPA receptors.* Neuron, 1998. **21**(2): p. 393-400.

97. Bomberger, J., et al., *Novel function for receptor activity-modifying proteins (RAMPs) in post-endocytic receptor trafficking.* J Biol Chem, 2005. **280**(10): p. 9297-307.

98. Weinman, E.J., et al., *The association of NHERF adaptor proteins with g protein-coupled receptors and receptor tyrosine kinases.* Annu Rev Physiol, 2006. **68**: p. 491-505.

99. Li, J.G., C. Chen, and L.Y. Liu-Chen, *Ezrin-radixin-moesin-binding phosphoprotein-50/Na+/H+ exchanger regulatory factor (EBP50/NHERF) blocks U50,488H-induced down-regulation of the human kappa opioid receptor by enhancing its recycling rate.* J Biol Chem, 2002. **277**(30): p. 27545-52.

100. Hall, R.A., et al., *The beta2-adrenergic receptor interacts with the Na+/H+-exchanger regulatory factor to control Na+/H+ exchange.* Nature, 1998. **392**(6676): p. 626-30.

101. Sneddon, W.B., et al., *Activation-independent parathyroid hormone receptor internalization is regulated by NHERF1 (EBP50).* J Biol Chem, 2003. **278**(44): p. 43787-96.

102. Bomberger, J., et al., *Receptor Activity-modifying Protein (RAMP) Isoform-specific Regulation of Adrenomedullin Receptor Trafficking by NHERF-1.* J Biol Chem, 2005. **280**(25): p. 23926-35.

103. Hall, J.M. and D.M. Smith, *Calcitonin gene-related peptide--a new concept in receptor-ligand specificity?* Trends Pharmacol Sci, 1998. **19**(8): p. 303-5.

104. Parameswaran, N. and W.S. Spielman, *RAMPs: The past, present and future.* Trends Biochem Sci, 2006. **31**(11): p. 631-8.

105. Christopoulos, A., et al., *Novel receptor partners and function of receptor activity-modifying proteins.* J Biol Chem, 2003. **278**(5): p. 3293-7.

106. Bouschet, T., S. Martin, and J.M. Henley, *Receptor-activity-modifying proteins are required for forward trafficking of the calcium-sensing receptor to the plasma membrane.* J Cell Sci, 2005. **118**(Pt 20): p. 4709-20.

107. Ono, Y., et al., *Decreased gene expression of adrenomedullin receptor in mouse lungs during sepsis.* Biochem Biophys Res Commun, 2000. **271**(1): p. 197-202.

108. Ueda, T., et al., *Expression of receptor-activity modifying protein (RAMP) mRNAs in the mouse brain.* Brain Res Mol Brain Res, 2001. **93**(1): p. 36-45.

109. Sexton, P.M., et al., *Receptor activity modifying proteins.* Cell Signal, 2001. **13**(2): p. 73-83.

110. Nagae, T., et al., *Rat receptor-activity modifying proteins (RAMPs) for adrenomedullin/CGRP receptor: cloning and upregulation in obstructive nephropathy.* Biochem Biophys Res Commun, 2000. **270**: p. 89-93.

111. Hwang, I.S., et al., *The gene expression of adrenomedullin, calcitonin-receptor-like receptor and receptor activity modifying proteins (RAMPs) in CCl4-induced rat liver cirrhosis.* Regul Pept, 2006. **135**(1-2): p. 69-77.

112. Ishii, A., et al., *Expression of calcitonin receptor in rat mammary gland during lactation.* Endocr J, 2006. **53**(3): p. 317-24.

113. Thota, C. and C. Yallampalli, *Progesterone upregulates calcitonin gene-related peptide and adrenomedullin receptor components and cyclic adenosine 3'5'-monophosphate generation in Eker rat uterine smooth muscle cell line.* Biol Reprod, 2005. **72**(2): p. 416-22.

114. Ikeda, K., et al., *Estrogen and phytoestrogen regulate the mRNA expression of adrenomedullin and adrenomedullin receptor components in the rat uterus.* Mol Cell Endocrinol, 2004. **223**(1-2): p. 27-34.

115. Thota, C., et al., *Changes in the expression of calcitonin receptor-like receptor, receptor activity-modifying protein (RAMP) 1, RAMP2, and RAMP3 in rat uterus during pregnancy, labor, and by steroid hormone treatments.* Biol Reprod, 2003. **69**(4): p. 1432-7.

116. Nishikimi, T., et al., *Ventricular adrenomedullin system in the transition from LVH to heart failure in rats.* Hypertension, 2003. **41**(3): p. 512-8.

117. Udawela, M., D.L. Hay, and P.M. Sexton, *The receptor activity modifying protein family of G protein coupled receptor accessory proteins.* Semin Cell Dev Biol, 2004. **15**(3): p. 299-308.

118. Cueille, C., et al., *Increased myocardial expression of RAMP1 and RAMP3 in rats with chronic heart failure.* Biochem Biophys Res Commun, 2002. **294**(2): p. 340-6.

119. Nishikimi, T., et al., *Role of increased circulating and renal adrenomedullin in rats with malignant hypertension.* Am J Physiol Regul Integr Comp Physiol, 2001. **281**(6): p. R2079-87.

120. Tadokoro, K., et al., *Altered gene expression of adrenomedullin and its receptor system and molecular forms of tissue adrenomedullin in left ventricular hypertrophy induced by malignant hypertension.* Regul Pept, 2003. **112**(1-3): p. 71-8.

121. Qing, X., J. Svaren, and I.M. Keith, *mRNA expression of novel CGRP1 receptors and their activity-modifying proteins in hypoxic rat lung.* Am J Physiol Lung Cell Mol Physiol, 2001. **280**(3): p. L547-54.

122. Dackor, R. and K. Caron, *Mice heterozygous for adrenomedullin exhibit a more extreme inflammatory response to endotoxin-induced septic shock.* Peptides, 2007.

123. Mazzocchi, G., et al., *Adrenomedullin (AM) and AM receptor type 2 expression is up-regulated in prostate carcinomas (PC), and AM stimulates in vitro growth of a PC-derived cell line by enhancing proliferation and decreasing apoptosis rates.* Int J Oncol, 2004. **25**(6): p. 1781-7.

124. Nowak, W., et al., *Novel regulation of adrenomedullin receptor by PDGF: role of receptor activity modifying protein-3.* Am J Pysiol Cell Physiol, 2002. **282**: p. C1322-1331.

125. Phelps, E., et al., *Parathyroid Hormone Induces Receptor Activity Modifying Protein-3 (RAMP3) Expression Primarily Via 3',5'-Cyclic Adenosine Monophosphate Signaling in Osteoblasts.* Calcif Tissue Int, 2005.

126. Carraro, G., et al., *Differential expression of adrenomedullin and its receptors in newborn and adult rat thymus.* Int J Mol Med, 2002. **10**(6): p. 767-71.

127. Watanabe, H., et al., *The estrogen-responsive adrenomedullin and receptor-modifying protein 3 gene identified by DNA microarray analysis are directly regulated by estrogen receptor.* J Mol Endocrinol, 2006. **36**(1): p. 81-9.

128. Nishikimi, T., et al., *Response of adrenomedullin system to cytokine in cardiac fibroblasts-role of adrenomedullin as an antifibrotic factor.* Cardiovasc Res, 2005. **66**(1): p. 104-13.

129. Yoshihara, F., et al., *Upregulation of intracardiac adrenomedullin and its receptor system in rats with volume overload-induced cardiac hypertrophy.* Regul Pept, 2005. **127**(1-3): p. 239-44.

130. Mishima, K., et al., *Angiotensin II modulates gene expression of adrenomedullin receptor components in rat cardiomyocytes.* Life Sci, 2003. **73**(13): p. 1629-35.

131. Phelps, E., et al., *Parathyroid hormone induces receptor activity modifying protein-3 (RAMP3) expression primarily via 3',5'-cyclic adenosine monophosphate signaling in osteoblasts.* Calcif Tissue Int, 2005. **77**(2): p. 96-103.

132. Sebolt-Leopold, J., *Development of anticancer drugs targeting the MAP kinase pathway.* Oncogene, 2000. **19**: p. 6594-6599.

133. Kim, S. and H. Iwao, *Stress and vascular responses: mitogen-activated protein kinases and activator protein-1 as promising therapeutic targets of vascular remodeling.* J Pharmacol Sci., 2003. **91**(3): p. 177-81.

134. Lewis, T.S., P.S. Shapiro, and N.G. Ahn, *Signal transduction through MAP kinase cascades.* Adv Cancer Res, 1998. **74**: p. 49-139.

135. Wood, K.W., et al., *ras mediates nerve growth factor receptor modulation of three signal-transducing protein kinases: MAP kinase, Raf-1, and RSK.* Cell, 1992. **68**(6): p. 1041-50.

136. Campbell, S.L., et al., *Increasing complexity of Ras signaling.* Oncogene, 1998. **17**(11 Reviews): p. 1395-413.

137. Hallberg, B., S.I. Rayter, and J. Downward, *Interaction of Ras and Raf in intact mammalian cells upon extracellular stimulation.* J Biol Chem, 1994. **269**(6): p. 3913-6.

138. Bivona, T.G. and M.R. Philips, *Ras pathway signaling on endomembranes.* Curr Opin Cell Biol, 2003. **15**(2): p. 136-42.

139. Quatela, S.E. and M.R. Philips, *Ras signaling on the Golgi.* Curr Opin Cell Biol, 2006. **18**(2): p. 162-7.

140. Clarke, S., et al., *Posttranslational modification of the Ha-ras oncogene protein: evidence for a third class of protein carboxyl methyltransferases.* Proc Natl Acad Sci U S A, 1988. **85**(13): p. 4643-7.

141. Geyer, M. and A. Wittinghofer, *GEFs, GAPs, GDIs and effectors: taking a closer (3D) look at the regulation of Ras-related GTP-binding proteins.* Curr Opin Struct Biol, 1997. **7**(6): p. 786-92.

142. Chong, H., H.G. Vikis, and K.L. Guan, *Mechanisms of regulating the Raf kinase family.* Cell Signal, 2003. **15**(5): p. 463-9.

143. Mercer, K.E. and C.A. Pritchard, *Raf proteins and cancer: B-Raf is identified as a mutational target.* Biochim Biophys Acta, 2003. **1653**(1): p. 25-40.

144. Downward, J., *Targeting RAS signalling pathways in cancer therapy.* Nat Rev Cancer, 2003. **3**(1): p. 11-22.

145. Whitmarsh, A.J. and R.J. Davis, *Structural organization of MAP-kinase signaling modules by scaffold proteins in yeast and mammals.* Trends Biochem Sci, 1998. **23**(12): p. 481-5.

146. Peyssonnaux, C. and A. Eychene, *The Raf/MEK/ERK pathway: new concepts of activation.* Biol Cell, 2001. **93**(1-2): p. 53-62.

147. Schaeffer, H.J., et al., *MP1: a MEK binding partner that enhances enzymatic activation of the MAP kinase cascade.* Science, 1998. **281**(5383): p. 1668-71.

148. Wunderlich, W., et al., *A novel 14-kilodalton protein interacts with the mitogen-activated protein kinase scaffold mp1 on a late endosomal/lysosomal compartment.* J Cell Biol, 2001. **152**(4): p. 765-76.

149. Sundaram, M. and M. Han, *The C. elegans ksr-1 gene encodes a novel Raf-related kinase involved in Ras-mediated signal transduction.* Cell, 1995. **83**(6): p. 889-901.

150. Yu, W., et al., *Regulation of the MAP kinase pathway by mammalian Ksr through direct interaction with MEK and ERK.* Curr Biol, 1998. **8**(1): p. 56-64.

151. Cacace, A.M., et al., *Identification of constitutive and ras-inducible phosphorylation sites of KSR: implications for 14-3-3 binding, mitogen-activated protein kinase binding, and KSR overexpression.* Mol Cell Biol, 1999. **19**(1): p. 229-40.

152. Stewart, S., et al., *Kinase suppressor of Ras forms a multiprotein signaling complex and modulates MEK localization.* Mol Cell Biol, 1999. **19**(8): p. 5523-34.

153. Yeung, K., et al., *Suppression of Raf-1 kinase activity and MAP kinase signalling by RKIP.* Nature, 1999. **401**(6749): p. 173-7.

154. Karin, M., *The regulation of AP-1 activity by mitogen-activated protein kinases.* J Biol Chem, 1995. **270**(28): p. 16483-6.

155. Hibi, M., et al., *Identification of an oncoprotein- and UV-responsive protein kinase that binds and potentiates the c-Jun activation domain.* Genes Dev, 1993. **7**(11): p. 2135-48.

156. Dai, T., et al., *Stress-activated protein kinases bind directly to the delta domain of c-Jun in resting cells: implications for repression of c-Jun function.* Oncogene, 1995. **10**(5): p. 849-55.

157. Kallunki, T., et al., *c-Jun can recruit JNK to phosphorylate dimerization partners via specific docking interactions.* Cell, 1996. **87**(5): p. 929-39.

158. Whitmarsh, A.J., et al., *A mammalian scaffold complex that selectively mediates MAP kinase activation.* Science, 1998. **281**(5383): p. 1671-4.

159. Dickens, M., et al., *A cytoplasmic inhibitor of the JNK signal transduction pathway.* Science, 1997. **277**(5326): p. 693-6.

160. Enslen, H. and R.J. Davis, *Regulation of MAP kinases by docking domains.* Biology of theCell, 2001. **93**: p. 5-14.

161. Tanoue, T., et al., *A conserved docking motif in MAP kinases common to substrates, activators and regulators.* Nat Cell Biol, 2000. **2**(2): p. 110-6.

162. Yang, S.H., A. Galanis, and A.D. Sharrocks, *Targeting of p38 mitogen-activated protein kinases to MEF2 transcription factors.* Mol Cell Biol, 1999. **19**(6): p. 4028-38.

163. Yang, S.H., et al., *Differential targeting of MAP kinases to the ETS-domain transcription factor Elk-1.* Embo J, 1998. **17**(6): p. 1740-9.

164. Sharrocks, A., S. Yang, and A. Galanis, *Docking domains and substrate-specificity determination for MAP kinases.* TIBS, 2000. **25**: p. 448-453.

165. Bardwell, L. and J. Thorner, *A conserved motif at the amino termini of MEKs might mediate high-affinity interaction with the cognate MAPKs.* Trends Biochem Sci, 1996. **21**(10): p. 373-4.

166. Muller, J., et al., *C-TAK1 regulates Ras signaling by phosphorylating the MAPK scaffold, KSR1.* Mol Cell, 2001. **8**(5): p. 983-93.

167. Burke, P., K. Schooler, and H.S. Wiley, *Regulation of epidermal growth factor receptor signaling by endocytosis and intracellular trafficking.* Mol Biol Cell, 2001. **12**(6): p. 1897-910.

168. Daaka, Y., et al., *Essential role for G protein-coupled receptor endocytosis in the activation of mitogen-activated protein kinase.* J Biol Chem, 1998. **273**(2): p. 685-8.

169. Jiang, X. and A. Sorkin, *Coordinated traffic of Grb2 and Ras during epidermal growth factor receptor endocytosis visualized in living cells.* Mol Biol Cell, 2002. **13**(5): p. 1522-35.

170. McPherson, P.S., B.K. Kay, and N.K. Hussain, *Signaling on the endocytic pathway.* Traffic, 2001. **2**(6): p. 375-84.

171. Kermorgant, S., D. Zicha, and P.J. Parker, *PKC controls HGF-dependent c-Met traffic, signalling and cell migration.* Embo J, 2004. **23**(19): p. 3721-34.

172. Kranenburg, O., I. Verlaan, and W.H. Moolenaar, *Dynamin is required for the activation of mitogen-activated protein (MAP) kinase by MAP kinase kinase.* J Biol Chem, 1999. **274**(50): p. 35301-4.

173. Wang, Y., et al., *Endosomal signaling of epidermal growth factor receptor stimulates signal transduction pathways leading to cell survival.* Mol Cell Biol, 2002. **22**(20): p. 7279-90.

174. Howe, C.L., et al., *NGF signaling from clathrin-coated vesicles: evidence that signaling endosomes serve as a platform for the Ras-MAPK pathway.* Neuron, 2001. **32**(5): p. 801-14.

175. Teis, D., W. Wunderlich, and L.A. Huber, *Localization of the MP1-MAPK scaffold complex to endosomes is mediated by p14 and required for signal transduction.* Dev Cell, 2002. **3**(6): p. 803-14.

176. Vomastek, T., et al., *Modular construction of a signaling scaffold: MORG1 interacts with components of the ERK cascade and links ERK signaling to specific agonists.* Proc Natl Acad Sci U S A, 2004. **101**(18): p. 6981-6.

177. Luttrell, L.M., et al., *Activation and targeting of extracellular signal-regulated kinases by beta-arrestin scaffolds.* Proc Natl Acad Sci U S A, 2001. **98**(5): p. 2449-54.

178. Choy, E., et al., *Endomembrane trafficking of ras: the CAAX motif targets proteins to the ER and Golgi.* Cell, 1999. **98**(1): p. 69-80.

179. Dai, Q., et al., *Mammalian prenylcysteine carboxyl methyltransferase is in the endoplasmic reticulum.* J Biol Chem, 1998. **273**(24): p. 15030-4.

180. Schmidt, W.K., et al., *Endoplasmic reticulum membrane localization of Rce1p and Ste24p, yeast proteases involved in carboxyl-terminal CAAX protein processing and amino-terminal a-factor cleavage.* Proc Natl Acad Sci U S A, 1998. **95**(19): p. 11175-80.

181. Jaumot, M., et al., *The linker domain of the Ha-Ras hypervariable region regulates interactions with exchange factors, Raf-1 and phosphoinositide 3-kinase.* J Biol Chem, 2002. **277**(1): p. 272-8.

182. Apolloni, A., et al., *H-ras but not K-ras traffics to the plasma membrane through the exocytic pathway.* Mol Cell Biol, 2000. **20**(7): p. 2475-87.

183. Chiu, V.K., et al., *Ras signalling on the endoplasmic reticulum and the Golgi.* Nat Cell Biol, 2002. **4**(5): p. 343-50.

184. Rocks, O., et al., *An acylation cycle regulates localization and activity of palmitoylated Ras isoforms.* Science, 2005. **307**(5716): p. 1746-52.

185. Goodwin, J.S., et al., *Depalmitoylated Ras traffics to and from the Golgi complex via a nonvesicular pathway.* J Cell Biol, 2005. **170**(2): p. 261-72.

186. Fivaz, M. and T. Meyer, *Reversible intracellular translocation of KRas but not HRas in hippocampal neurons regulated by Ca2+/calmodulin.* J Cell Biol, 2005. **170**(3): p. 429-41.

187. Furthauer, M., et al., *Sef is a feedback-induced antagonist of Ras/MAPK-mediated FGF signalling.* Nat Cell Biol, 2002. **4**(2): p. 170-4.

188. Torii, S., et al., *Sef is a spatial regulator for Ras/MAP kinase signaling.* Dev Cell, 2004. **7**(1): p. 33-44.

189. Bivona, T.G., et al., *Phospholipase Cgamma activates Ras on the Golgi apparatus by means of RasGRP1.* Nature, 2003. **424**(6949): p. 694-8.

190. Arozarena, I., et al., *Activation of H-Ras in the endoplasmic reticulum by the RasGRF family guanine nucleotide exchange factors.* Mol Cell Biol, 2004. **24**(4): p. 1516-30.

191. Sobering, A.K., et al., *A novel Ras inhibitor, Eri1, engages yeast Ras at the endoplasmic reticulum.* Mol Cell Biol, 2003. **23**(14): p. 4983-90.

192. Caloca, M.J., J.L. Zugaza, and X.R. Bustelo, *Exchange factors of the RasGRP family mediate Ras activation in the Golgi.* J Biol Chem, 2003. **278**(35): p. 33465-73.

193. Papadaki, P., et al., *Two ras pathways in fission yeast are differentially regulated by two ras guanine nucleotide exchange factors.* Mol Cell Biol, 2002. **22**(13): p. 4598-606.

194. Kamitani, S., et al., *The RAMP2/CRLR complex is a functional adrenomedullin receptor in human endothelial and vascular smooth muscle cells.* FEBS Lett, 1999. **448**(1): p. 111-4.

195. Schulein, R., et al., *A dileucine sequence and an upstream glutamate residue in the intracellular carboxyl terminus of the vasopressin V2 receptor are essential for cell surface transport in COS.M6 cells.* Mol Pharmacol, 1998. **54**(3): p. 525-35.

196. Hilairet, S., et al., *Agonist-promoted internalization of a ternary complex between calcitonin receptor-like receptor, receptor activity-modifying protein 1 (RAMP1), and beta-arrestin.* J Biol Chem, 2001. **276**(45): p. 42182-90.

197. Parameswaran, N., et al., *Desensitization and resensitization of adrenomedullin-sensitive receptor in rat mesangial cells.* Eur J Pharmacol, 2000. **407**(3): p. 205-10.

198. Obenauer, J.C., L.C. Cantley, and M.B. Yaffe, *Scansite 2.0: Proteome-wide prediction of cell signaling interactions using short sequence motifs.* Nucleic Acids Res, 2003. **31**(13): p. 3635-41.

199. Oh, D.Y., et al., *Phospholipase D1 activation through Src and Ras is involved in basic fibroblast growth factor-induced neurite outgrowth of H19-7 cells.* J Cell Biochem, 2007. **101**(1): p. 221-34.

200. Webber, C.A., et al., *Multiple signaling pathways regulate FGF-2-induced retinal ganglion cell neurite extension and growth cone guidance.* Mol Cell Neurosci, 2005. **30**(1): p. 37-47.

201. Bartunek, P., et al., *bFGF signaling and v-Myb cooperate in sustained growth of primitive erythroid progenitors.* Oncogene, 2002. **21**(3): p. 400-10.

202. Tappia, P.S., et al., *Fibroblast growth factor-2 stimulates phospholipase Cbeta in adult cardiomyocytes.* Biochem Cell Biol, 1999. **77**(6): p. 569-75.

203. Egan, C.G., et al., *PDGF-induced signaling in proliferating and differentiated vascular smooth muscle: effects of altered intracellular Ca2+ regulation.* Cardiovasc Res, 2005. **67**(2): p. 308-16.

204. Liu, B., et al., *The role of phospholipase C and phosphatidylinositol 3-kinase in vascular smooth muscle cell migration and proliferation.* J Surg Res, 2004. **120**(2): p. 256-65.

205. Noh, D.Y., S.H. Shin, and S.G. Rhee, *Phosphoinositide-specific phospholipase C and mitogenic signaling.* Biochim Biophys Acta, 1995. **1242**(2): p. 99-113.

206. Parameswaran, N., et al., *Regulation of adrenomedullin signaling in kidney interstitial fibroblasts.* Cell Physiol Biochem, 2003. **13**(6): p. 391-400.

207. Hegde, R.S. and H.D. Bernstein, *The surprising complexity of signal sequences.* Trends Biochem Sci, 2006. **31**(10): p. 563-71.

208. Johnson, A.E. and M.A. van Waes, *The translocon: a dynamic gateway at the ER membrane.* Annu Rev Cell Dev Biol, 1999. **15**: p. 799-842.

209. von Heijne, G., *Signal sequences. The limits of variation.* J Mol Biol, 1985. **184**(1): p. 99-105.

210. Plath, K., et al., *Signal sequence recognition in posttranslational protein transport across the yeast ER membrane.* Cell, 1998. **94**(6): p. 795-807.

211. Verschoor, E.J., et al., *Post-translational processing of the feline immunodeficiency virus envelope precursor protein.* Virology, 1993. **193**(1): p. 433-8.

212. Li, Y., et al., *The HIV-1 Env protein signal sequence retards its cleavage and down-regulates the glycoprotein folding.* Virology, 2000. **272**(2): p. 417-28.

213. Weihofen, A., et al., *Release of signal peptide fragments into the cytosol requires cleavage in the transmembrane region by a protease activity that is specifically blocked by a novel cysteine protease inhibitor.* J Biol Chem, 2000. **275**(40): p. 30951-6.

214. Goder, V. and M. Spiess, *Molecular mechanism of signal sequence orientation in the endoplasmic reticulum.* Embo J, 2003. **22**(14): p. 3645-53.

215. Lemberg, M.K., et al., *Intramembrane proteolysis of signal peptides: an essential step in the generation of HLA-E epitopes.* J Immunol, 2001. **167**(11): p. 6441-6.

216. Lemberg, M.K. and B. Martoglio, *Requirements for signal peptide peptidase-catalyzed intramembrane proteolysis.* Mol Cell, 2002. **10**(4): p. 735-44.

217. Lyko, F., et al., *Signal sequence processing in rough microsomes.* J Biol Chem, 1995. **270**(34): p. 19873-8.

218. Kirkin, V., et al., *The Fas ligand intracellular domain is released by ADAM10 and SPPL2a cleavage in T-cells.* Cell Death Differ, 2007. **14**(9): p. 1678-87.

219. Weihofen, A., et al., *Identification of signal peptide peptidase, a presenilin-type aspartic protease.* Science, 2002. **296**(5576): p. 2215-8.

220. Martoglio, B. and B. Dobberstein, *Snapshots of membrane-translocating proteins.* Trends Cell Biol, 1996. **6**(4): p. 142-7.

221. Martoglio, B., R. Graf, and B. Dobberstein, *Signal peptide fragments of preprolactin and HIV-1 p-gp160 interact with calmodulin.* Embo J, 1997. **16**(22): p. 6636-45.

222. Shaffer, K.L., et al., *Regulation of protein compartmentalization expands the diversity of protein function.* Dev Cell, 2005. **9**(4): p. 545-54.

223. Puglielli, L., et al., *Acyl-coenzyme A: cholesterol acyltransferase modulates the generation of the amyloid beta-peptide.* Nat Cell Biol, 2001. **3**(10): p. 905-12.

224. Martoglio, B., *Intramembrane proteolysis and post-targeting functions of signal peptides.* Biochem Soc Trans, 2003. **31**(Pt 6): p. 1243-7.

225. Coppolino, M.G., et al., *Calreticulin is essential for integrin-mediated calcium signalling and cell adhesion.* Nature, 1997. **386**(6627): p. 843-7.

226. Leung-Hagesteijn, C.Y., et al., *Cell attachment to extracellular matrix substrates is inhibited upon downregulation of expression of calreticulin, an intracellular integrin alpha-subunit-binding protein.* J Cell Sci, 1994. **107 (Pt 3)**: p. 589-600.

227. Holaska, J.M., et al., *Calreticulin Is a receptor for nuclear export.* J Cell Biol, 2001. **152**(1): p. 127-40.

228. Iakova, P., et al., *Competition of CUGBP1 and calreticulin for the regulation of p21 translation determines cell fate.* Embo J, 2004. **23**(2): p. 406-17.

229. Sakai, K., et al., *Isolation of cDNAs encoding a substrate for protein kinase C: nucleotide sequence and chromosomal mapping of the gene for a human 80K protein.* Genomics, 1989. **5**(2): p. 309-15.

230. Gkika, D., et al., *80K-H as a new Ca2+ sensor regulating the activity of the epithelial Ca2+ channel transient receptor potential cation channel V5 (TRPV5).* J Biol Chem, 2004. **279**(25): p. 26351-7.

231. Goh, K.C., et al., *Identification of p90, a prominent tyrosine-phosphorylated protein in fibroblast growth factor-stimulated cells, as 80K-H.* J Biol Chem, 1996. **271**(10): p. 5832-8.

232. Heine, U.I., et al., *Localization of transforming growth factor-beta 1 in mitochondria of murine heart and liver.* Cell Regul, 1991. **2**(6): p. 467-77.

233. Addya, S., et al., *Targeting of NH2-terminal-processed microsomal protein to mitochondria: a novel pathway for the biogenesis of hepatic mitochondrial P450MT2.* J Cell Biol, 1997. **139**(3): p. 589-99.

234. Little, M.H., et al., *Dual trafficking of Slit3 to mitochondria and cell surface demonstrates novel localization for Slit protein.* Am J Physiol Cell Physiol, 2001. **281**(2): p. C486-95.

235. Kurys, G., et al., *The long signal peptide isoform and its alternative processing direct the intracellular trafficking of interleukin-15.* J Biol Chem, 2000. **275**(39): p. 30653-9.

236. Goulet, B., et al., *A cathepsin L isoform that is devoid of a signal peptide localizes to the nucleus in S phase and processes the CDP/Cux transcription factor.* Mol Cell, 2004. **14**(2): p. 207-19.

237. Levine, C.G., et al., *The efficiency of protein compartmentalization into the secretory pathway.* Mol Biol Cell, 2005. **16**(1): p. 279-91.

238. Dackor, R., et al., *Receptor activity-modifying proteins 2 and 3 have distinct physiological functions from embryogenesis to old age.* J Biol Chem, 2007. **282**(25): p. 18094-9.

239. Cornish, J., et al., *Adrenomedullin is a potent stimulator of osteoblastic activity in vitro and in vivo.* Am J Physiol, 1997. **273**(6 Pt 1): p. E1113-20.

240. Cornish, J., et al., *Systemic administration of adrenomedullin(27-52) increases bone volume and strength in male mice.* J Endocrinol, 2001. **170**(1): p. 251-7.

241. Hewitt, S.C., et al., *Global uterine genomics in vivo: microarray evaluation of the estrogen receptor alpha-growth factor cross-talk mechanism.* Mol Endocrinol, 2005. **19**(3): p. 657-68.

242. Kenny, P.A., T. Enver, and A. Ashworth, *Receptor and secreted targets of Wnt-1/beta-catenin signalling in mouse mammary epithelial cells.* BMC Cancer, 2005. **5**: p. 3.